Doctoral Dissertation (Censored)

博士論文（要約）

Identification of two functionally different domains in the seed region of siRNA guide strand and development of a new siRNA design procedure for therapeutic application

（siRNAガイド鎖seed領域の2つの機能ドメインの同定と
核酸医薬品開発に向けた新規配列設計法の構築）

A Dissertation Submitted for the Degree of Doctor of Philosophy
December 2020

令和2年12月博士（理学）申請

Department of Biological Sciences, Graduate School of Science,
The University of Tokyo

東京大学大学院理学系研究科生物科学専攻

Kobayashi Yoshiaki

小林 芳明

Abstract

In RNA interference (RNAi), a small interfering RNA (siRNA) is loaded onto Argonaute (AGO) protein, and the siRNA guide strand base pairs with a target mRNA with perfect sequence complementarity to repress its expression through cleavage of mRNA by AGO protein. On the other hand, siRNA often exhibits off-target effect which represses the expression of unintended mRNAs with partial sequence complementarities in the seed region (2–8 nucleotides from the 5′ end) of the guide strand.

Previously, we reported that off-target effect is avoided by the introduction of 2′-O-methyl (2′-OMe) modifications in the seed region, since they induce steric hindrance in the duplex formation on the AGO protein without affecting the RNAi activity. In this study, the detailed mechanism to avoid off-target effect was examined by systematic introduction of 2′-OMe modifications in the seed region. As a result, it was revealed that seed region is composed of two functionally different regions. The modifications at positions 2–5 induced steric hindrance in formation of duplex between siRNA guide strand and off-target mRNA on the AGO protein, resulted in the reduction of off-target effect. On the other hand, the modifications at positions 6–8, especially that at position 7, contributed to form stable base-pairing with target or off-target mRNAs, leading to their repression.

Recently three siRNAs were approved as nucleic acid drugs by Food and Drug Administration (FDA). However, all of them repress the expression of target genes without distinguishing wild type gene from its mutated ones. Thus, siRNA which can specifically repress the mutated gene has not been developed yet. In this thesis, I succeeded in the development of siRNA which can distinguish single nucleotide differences. I revealed that mismatches at positions 5 or 6 in addition to 11 in base-pairing between siRNA guide strand and target mRNAs are effective for distinguishing the single nucleotide differences. This is the first way in the world for developing single nucleotide variant-distinguishable (SNVD)-siRNA as a nucleic acid drug.

Table of contents

Abbreviation List

A	adenosine
AGO1	Argonaute 1
AGO2	Argonaute 2
AGO3	Argonaute 3
AGO4	Argonaute 4
AHP	acute hepatic porphyria
ALAS1	5′-aminolevulinate synthase 1
BRAF	v-Raf murine sarcoma viral oncogene homolog B
C	cytidine
cDNA	complementary DNA
CLTC	clathrin heavy chain
CM	complete-matched
COSMIC	catalogue of somatic mutations in cancer
DICER	dsRNA cleavage enzyme
DMEM	Dulbecco′s Modified Eagle′s Medium
DNA	deoxyribonucleic acid
dsRNA	double-stranded RNA
EGFR	epidermal growth factor receptor
FDA	Food and Drug Administration
G	guanosine
GAPDH	glyceraldehyde-3-phosphate dehydrogenase
GRK4	G protein-coupled receptor kinase 4
HAO1	hydroxyacid oxidase 1
hATTR	hereditary transthyretin amyloidosis
Helix-7	α-helix 7
HRP	Horseradish peroxidase
IC_{50}	half maximal inhibitory concentration
IDH1	isocitrate dehydrogenase 1
IgG	immunoglobulin G
IP	immunoprecipitation
KRAS	kirsten rat sarcoma virus

L1	linker 1
L2	linker 2
Luc	luciferase
mRNA	messenger RNA
MID	middle
miRNA	microRNA
MTPN	myotrophin
N	N-terminal
NRAS	neuroblastoma ras viral oncogene homolog
Oct4	transcription factor encoded by the Pou5f1
PAZ	Piwi–Argonaute–Zwille
PBS	Phosphate-buffered saline
PCR	polymerase chain reaction
PH1	primary hyperoxaluria type1
PIWI	P-element induced wimpy testes
PVDF	PolyVinylidene DiFluoride
qRT-PCR	quantitative RT-PCR
RNA	ribonucleic acids
RNAi	RNA interference
RPMI1640	Roswell Park Memorial Institute medium 1640
RT	reverse transcription
SDS-PAGE	sodium dodecyl sulfate-polyacrylamide gel electrophoresis
siRNA	small interfering RNA
SM	seed-matched
SNVD-siRNA	single nucleotide variant distinguishable-siRNA
SURF4	surfeit 4
TBST	Tris Buffered Saline with Tween
TNRC6A	trinucleotide repeat containing 6A
TTR	transthyretin
U	uridine
UTR	untranslated region
VAPA	vesicle-associated membrane protein-associated protein A
VIM	vimentin

wt	wild-type
2′-OMe	2′-O-methyl

Chapter 1 Introduction

1.1 Biogenesis and function of siRNA

RNA interference (RNAi) is a post-transcriptional gene silencing phenomenon triggered by small interfering RNA (siRNA) (Fire *et al*. 1998). siRNA is 21-nucleotide (nt)-long double-stranded RNA (dsRNA) with 2-nt 3′overhangs generated by processing via dsRNA cleavage enzyme, Dicer (Zamore *et al*. 2000, Bernstein *et al*. 2001, Elbashir *et al*. 2001, Ketting *et al*. 2001) (Figure 1). It is loaded onto Argonaute2 (AGO2) protein, which is a core protein of the RNA-induced silencing complex (RISC) (Hammond *et al*. 2001, Doi *et al*. 2003, Liu *et al*. 2004, Meister *et al*. 2004, Rivas *et al*. 2005). The loaded duplex is unwound into single-stranded RNAs: one of them (guide strand) remains on AGO2 while the other (passenger strand) is degraded (Matranga *et al*. 2005, Rand *et al*. 2005, Kawamata *et al*. 2009, Yoda *et al*. 2010). The guide strand recognizes the target mRNA with perfect sequence complementarity and the target mRNA is cleaved by AGO2, resulting in the repression of the expression of target gene (Liu *et al*. 2004, Meister *et al*. 2004, Rivas *et al*. 2005).

As a mode of action different from RNAi, siRNA represses mRNAs with partial and not completely complementary sequences through the mechanism similar to that of microRNA (miRNA)-mediated RNA silencing. This phenomenon is known as off-target effect. Partial complementary sequences with siRNA seed region are observed in the 3′UTRs of off-target transcripts (Jackson *et al*. 2003, Scacheri *et al*. 2004, Lewis *et al*. 2005, Lim *et al*. 2005, Lin *et al*. 2005, Birmingham *et al*. 2006, Jackson *et al*. 2006, Grimson *et al*. 2007) (Figure 1).

1.2 Target RNA cleavage activities by AGO family proteins are essential for RNA silencing and mammalian development

The cleavage activity of target RNA by AGO has been demonstrated to play an important role in viral defense system or protection of the genome from transposable elements in many eukaryotic organisms (Ding *et al*. 2007, Chung *et al*. 2008, Czech *et al*. 2008, Ghildiyal *et al*. 2008, Kawamura *et al*. 2008, Maillard *et al*. 2013). In mammals, there are four paralogs of AGO family proteins (AGO1, AGO2, AGO3, AGO4). It has been thought that AGO2 is only AGO protein capable of catalyzing siRNA-directed cleavage of target RNAs (Liu *et al*. 2004, Meister *et al*. 2004). However, AGO3 is revealed to be catalytically activated by different lengths of guide RNA (Park *et al*. 2020), in consistent with the fact that AGO2 and AGO3 share the same catalytic tetrad (DEDH, Asp–Glu–Asp–His) (Nakanishi *et al*. 2012). Furthermore, AGO2-deficient mice are embryonic lethal (Liu *et al*. 2004), and knock-in mice with a slicer-deficient AGO2 are dead in a short period after birth (Cheloufi *et al*. 2010, Cifuentes

et al. 2010). These results indicate that the cleavage activity appears to be necessary in mammalian development.

1.3 Effective siRNA sequence in mammalian cells

siRNA-mediated cleavage mechanism is proven to be a powerful tool for exogenous gene manipulation (Elbashir *et al*. 2001). However, since the effective siRNAs are limited in mammalian cells, identification of functional siRNA sequence conditions were essential for effective mammalian RNAi. It was revealed that siRNAs, satisfying the following four sequence conditions simultaneously, are functional in our laboratory (Ui-Tei *et al*. 2004) (Figure 2): (i) A/U at the 5′-termini of the siRNA guide strand, (ii) G/C at the 5′-termini of the passenger strand, (iii) more than four nts of AU in the 5′-7-nts of the guide strand, and (iv) less than 9 nts GC stretch. The siRNAs that satisfy all four rules are assigned as Class I siRNA. Among them, siRNA with more than 5 A/U in 5′-7-nts of the guide strand is designated as Class Ia and that with 4 A/U is Class Ib. In contrast, siRNAs which is not satisfied any rules are classified into Class III, and those not classified into neither Class I nor III are designated as Class II. The importance of these criteria of Class I siRNA sequence have been confirmed by a number of studies. The asymmetry in the thermodynamic stabilities of both siRNA termini is essential for determining the unwinding direction of siRNA duplex into single-stranded RNAs (Noland *et al*. 2011, Betancur *et al*. 2012, Noland *et al*. 2013). Furthermore, a 5′-end nucleotide of the single-stranded RNA is anchored in the binding pocket in the MID domain of the AGO protein. The binding affinity of A or U at the 5′-end is preferentially anchored at the 30-fold higher affinity than that of G or C (Frank *et al*. 2010). Thus, an RNA strand with the unstable 5′-termini can act as a functional guide RNA.

1.4 Domain structure of AGO family proteins and interaction of AGO with siRNA guide strand

All of four AGO family proteins are composed of common two lobes formed by four globular and two linker domains. The N-terminal lobe consists of the N and PAZ (Piwi–Argonaute–Zwille) domains, while the C-terminal lobe consists of the MID (middle) and PIWI (P-element induced wimpy testes) domains. The two lobes are connected by the L1 and L2 linker domains and form the central cleft that accommodate the duplex between guide and target RNAs (Wang *et al*. 2008a, 2008b, Elkyam *et al*. 2012, Nakanishi *et al*. 2012, Schirle and MacRae 2012). The guide RNA interacts amino acids in all domains of AGO, but almost all interactions are through the RNA sugar-phosphate backbone (Wang *et al*. 2008a and 2008b, Elkyam *et al*. 2012, Schirle and MacRae 2012). The 5′-phosphate, which is

important for initial loading of siRNA, is embedded in a hydrophilic pocket at the interface of the MID and PIWI domains. Then, the 5′ end nucleotide of the guide strand is also embedded by interactions with the MID domain. So, the 5′ end nucleotide does not contribute to base-pairing with complementary target RNAs (Lewis *et al*. 2005, Ma *et al*. 2005, Parker *et al*. 2005). Furthermore, the functional siRNA sequence in mammalian cells is revealed to be preferable to be A or U at the 5′-end of the guide strand (Khvorova *et al*. 2003, Schwarz *et al*. 2003, Ui-Tei *et al*. 2004). This preference considered to be contributed by a nucleotide selectivity of loop in the AGO MID domain (Frank *et al*. 2010 and 2012). This loop serves as the only identified sequence-specific interaction between AGO and guide RNA.

1.5 Seed region of guide RNA on human AGO2

The importance of siRNA seed region has been revealed by structural studies. The backbone phosphates in the seed nucleotides of guide strand RNA are ordered on a quasi-helical structure on the surface of human AGO2 PIWI domain to serve as the entry or nucleation site for mRNA in helical conformation (Elkyam *et al*. 2012, Shirle and Macrae 2012, Shirle *et al*. 2014). Of these nucleotides, nucleotides 2–6 are pre-organized in A-form helix for base-pairing with target mRNAs. Between nucleotides 6 and 7, α-helix (helix-7) structure is inserted through hydrophobic residue (M364 and I365 in human AGO2) (Schirle and MacRae 2012, Faehnle *et al*. 2013, Nakanishi 2013, Klum *et al*. 2018). Then, its base stacking is interrupted by a kink. Once base-pairing beyond nucleotide 5 with target RNA, helix-7 shifts about 4Å and releases the kink (Schirle *et al*. 2014). Subsequently, helix-7 undergoes docking into the minor groove of seed-target duplex. This docking acts as molecular wedge that preventing from base-pairing mismatches or G:U wobble with seed-paired target RNA (Klum *et al*. 2018). Of pre-organized nucleotides 2–6, only nucleotides 2–4 are exposed to the solvent prior to base-pairing with target RNA (Schirle *et al*. 2014). According to biochemical analysis for base-pairing between guide RNA and seed-paired target RNA, it is revealed that mismatches in positions 2–4 of guide RNA is far more sensitive than those in positions 5–6 (Chandradoss *et al*. 2015).

1.6 Effects of chemical modifications in siRNA seed region

In addition to RNAi effect, siRNA also induces off-target effect, repressing unintended mRNAs with complementary sequences mainly with siRNA seed region. Such seed-dependent off-target effect is highly correlated with the thermodynamic stability in the duplex formed between the seed region of the siRNA guide strand and its target mRNAs (Ui-Tei *et al*. 2008a). The main factors that affect the thermodynamic stability of RNA duplex are hydrogen bonds and stacking interactions. The

thermodynamic stability of base-pairing is sequence-dependent, and the higher the seed–target stability, the higher the off-target effect. Thus, to avoid the off-target effect, it is necessary to select the siRNA whose seed-sequence shows thermodynamically low stability. However, this selection procedure decreases the number of selectable siRNAs to 2.1% (Naito *et al*. 2009).

Recently, I and my collaborators investigated whether or not chemical modifications are effective for avoiding off-target effect (Iribe *et al*. 2017). DNA modifications in siRNA seed region decreased off-target activities, since thermodynamic stability of base-pairing of DNA-RNA duplex is weaker than that of RNA-RNA duplex. This result is also in consistent with the previous report of our laboratory (Ui-Tei *et al*. 2008b). Although 2′-O-methyl (2′-OMe) modification contributes to high base-pairing stability, the modification significantly reduced off-target activity without decreasing RNAi activity. The computational simulation revealed that introduction of 2′-OMe into nucleotide at position 3 in the siRNA guide strand reduced off-target effect by inducing steric hindrance in duplex formation without affecting interaction with AGO protein (Iribe *et al*. 2017). These results suggest that base-pairing in the non-seed region may compensate for the steric hindrance in the seed region.

1.7 Nucleic acid drug

Nucleic acid drug is therapeutically applicable DNA or RNA which can operate gene information. Representative nucleic acid drugs are classified into three types: aptamer, antisense oligonucleotide, and siRNA. Since nucleic acid drugs have higher specificity, it is expected to target genes which are impossible to target by the conventional low molecular and/or antibody drugs. However, most of all approved nucleic acid drugs are targeting genes, which are responsible for hereditary diseases or diseases caused by viral infection. Thus, there is no approved nucleic acid drugs targeting oncogene.

1.8 Importance of siRNAs for knocking down genes with single nucleotide mutations

Recently three siRNAs were approved as nucleic acid drugs by Food and Drug Administration (FDA) (Adams *et al*. 2018, Balwani *et al*. 2020, https://clinicaltrials.gov/ct2/show/NCT03681184). The target of first siRNA drug (patisiran) was *transthyretin* (TTR) gene, which is responsible for hereditary transthyretin amyloidosis (hATTR) (Adams *et al*. 2018). hATTR amyloidosis is a rare, autosomal dominantly inherited disease caused by mutations in the *TTR* gene. A mutated form of TTR protein is produced by the liver, and accumulates as amyloid deposits at multiple sites, leading in many cases autonomic neuropathy and/or cardiomyopathy. The second siRNA drug is givosiran (Balwani *et al*. 2020), which targets *5′-aminolevulinate synthase 1* (ALAS1) gene, and it is developed for the treatment of acute hepatic porphyria (AHP). AHP is a family of rare, serious genetic disorder of liver

heme synthesis. The third approved siRNA was lumasiran (https://clinicaltrials.gov/ct2/show/NCT03681184), which can knock down *hydroxyacid oxidase* 1 (HAO1) gene and is developed for children and adult primary hyperoxaluria type 1 (PH1). PH1 is a rare disorder characterized by hepatic oxalate overproduction. Lumasiran is used to decrease the urinary oxalate level. All of these siRNAs efficiently repress their target genes, respectively, regardless the mutations in these genes.

Mutations in many oncogenes cause dysregulation of downstream processes, leading uncontrolled cell growth. It is known that the presence of *kirsten rat sarcoma virus* (*KRAS*) proto-oncogene mutation has been associated with aggressive tumor behavior such as accelerated tumor growth (Pylayeva-Gupta *et al*. 2011, Simanshu *et al*. 2016), early formation of distant metastasis (Cejas *et al*. 2009, Tie *et al*. 2011), and resistance to anti-epidermal growth factor receptor (EGFR)-based regimens (Panitumumab and Cetuximab) in metastatic colorectal cancer patients (Lièvre *et al*. 2006). On the other hand, *KRAS*-deficient mice are embryonic lethal (Koera *et al*. 1997). Therefore, in order to develop the siRNA against *KRAS* mutations, it is necessary to knock down the mutated gene alone without affecting the expression of wild-type gene for therapeutic application.

1.9 The purpose of this work

Our previous report revealed that 2′-OMe modifications in the seed region inhibit off-target effect through steric hindrance without affecting RNAi effect (Iribe *et al*. 2017). However, it was not clear whether all of the nucleotides in the siRNA seed region contribute to the steric hindrance and the reduction of off-target effect or the only limited nucleotides can contribute to such steric hindrance. In this study, I firstly investigated the effects of sequential introduction of 2′-OMe modifications into the siRNA guide strand on RNAi and off-target effects.

siRNA design procedure, I next tried to the development of a new siRNA design algorithm. Then, I succeeded in the development of siRNA which can specifically repress the gene with single nucleotide mutation by distinguishing from its wild type one.

Chapter 2 Identification of two functionally different domains in the seed region of siRNA guide strand

2.1 Introduction

In RNAi pathway, siRNA functions to suppress the expression of its target mRNA with perfect sequence complementarity. In the mechanism different from RNAi, siRNA also represses unintended mRNAs with complementary sequences mainly with siRNA seed region. Such seed-dependent off-target effect is known to be highly correlated with the thermodynamic stability in the duplex formed between the seed region of the siRNA guide strand and its target mRNAs (Ui-Tei *et al*. 2008a). Therefore, the thermodynamic stability of base-pairing is sequence-dependent, and the higher seed-target stability accounts for the higher off-target effect. Thus, to avoid the off-target effect, it is necessary to select the siRNA whose seed-sequence is thermodynamically low stability. However, this decreased the number of selectable siRNAs to 2.1% (Naito *et al*. 2009). Our previous report revealed that siRNA with 2′-OMe modifications in the seed region decreases off-target effect (Iribe *et al*. 2017). The result of computational simulation revealed that introduction of 2′-OMe into nucleotide at position 3 in the siRNA guide strand reduced off-target effect by inducing steric hindrance in duplex formation between the guide strand and mRNA on the AGO protein without affecting the RNAi activity (Iribe *et al*. 2017). However, it was not clear whether other nucleotide contributes to the reduction of off-target effect or not. Here I investigated positional effect of the seed region by introducing 2′-OMe modifications sequentially in the guide strand.

2.2 Materials and Methods

Cell culture

Human HeLa cells derived from cervical cancer were cultured in Dulbecco's Modified Eagle's Medium (FUJIFILM Wako, Osaka, Japan) containing 10% fetal bovine serum (BioWest, Nuaille´, France) at 37°C with 5% CO_2.

Chemical synthesis of siRNA duplexes

RNA oligonucleotides corresponding to the guide and passenger strands of each siRNA were chemically synthesized (Gene Design, Osaka, Japan) and subsequently annealed to form endogenous siRNA duplexes. All siRNA sequences used in this study were summarized in Table 1.

Construction of complete- and seed-matched luciferase reporters

All of the reporter plasmids used in this study were derived from psiCHECK-1 (Promega, Madison, WI, USA). Oligonucleotides with a complete-matched (CM) sequence were synthesized for each siRNA guide strand and passenger strand. On the other hand, oligonucleotides with three tandem repeats of seed-matched (SM) sequence were synthesized for each one. All oligonucleotides for the construction of CM and SM reporters were synthesized with Xhol/EcoRI sticky ends and inserted into the corresponding restriction enzyme sites within 3´ UTR region of *Renilla luciferase* (luc) gene in psiCHECK-1; their sequences are listed in Tables 2 and 3. PsiCHECK-CM and SM reporter constructs were then used to test the silencing efficacy of the corresponding siRNAs.

RNA silencing activity measured by dual luciferase reporter assay

RNA silencing activity was measured using a luciferase reporter assay. A HeLa cell suspension (1.0×10^5 cells/mL) was inoculated into a well of 24-well culture plates 1 day before transfection. Cells were simultaneously transfected with 0.0005, 0.005, 0.05, 0.5, 5 nM of each siRNA, 0.1 μg of pGL3-Control vector or pGL4.13 vector (Promega), both of which are encoding the firefly *luciferase* gene, and 0.01 μg of each psiCHECK construct by using Lipofectamine 2000 reagent (Thermo Fisher Scientific, Waltham, MA, USA). An siRNA called siGY441, which did not target any CM- and SM-reporter constructs, were used as an internal control. The transfected cells were lysed with 1×passive lysis buffer (Promega) 24 h after transfection. Luciferase activity was measured using the Dual-Luciferase Reporter Assay System (Promega) and GloMax Discover Microplate Reader (Promega), and the *Renilla* luciferase activity normalized by firefly luciferase activity (*Renilla* luciferase activity / firefly

luciferase activity) was calculated.

The half maximal inhibitory concentrations (IC_{50}s) of siRNAs were estimated using the following linear model.

IC_{50}=10^(LOG_{10}(A/B)*(50-C)/(D-C)+LOG_{10}(B))

A: Concentration when inhibitory efficiency is lower than 50%

B: Concentration when inhibitory efficiency is higher than 50%

C: Inhibitory efficiency in B

D: Inhibitory efficiency in A

The IC_{50}s are listed in Tables 4 and 5.

Microarray analysis

A HeLa cell suspension (0.5×10^5 cells/mL) was inoculated into a well of 24-well culture plates 1 day before transfection. Cells were transfected with 100 nM of each siRNA by using Lipofectamine 2000. At 24 h post-transfection, cells were harvested from three wells per one sample. Total RNA was purified using FastGene RNA Premium Kit (NIPPON Genetics, Tokyo, Japan) and the quality of the total RNA was confirmed using a NanoDrop 2000 spectrophotometer (Thermo Fisher Scientific) and a Bioanalyzer (Agilent Technologies, Santa Clara, CA, USA). cDNA and Cy3-labeled RNA were synthesized using the Quick Amp Labeling kit for One Color (Agilent Technologies). Cy3-labeled RNAs were fragmented using the Gene Expression Hybridization Kit (Agilent Technologies) and hybridized to a SurePrint G3 Human GE Microarray (version 3, 8×60 K) (Agilent Technologies) at 65ºC for 17 h. After being washed, the microarray slide was scanned by a DNA Microarray Scanner (Agilent Technologies) and the signals were quantified by Feature Extraction 10.5.1.1 software (Agilent Technologies). RNA from mock-transfected cells treated with the transfection reagent in the absence of siRNA was used as a control, and the distributions of the signal intensities of transcripts were normalized across all samples by quantile normalization (Bolstad *et al*. 2005). Results were shown in MA plots and cumulative accumulations.

Quantitative RT-PCR (qRT-PCR)

A HeLa cell suspension (1.0×10^5 cells/mL) was inoculated into a well of 24-well culture plates 1 day before transfection. Cells were transfected with 0.05, 0.5, 5, 50, 100 nM of siRNA by using Lipofectamine 2000. At 24 h post-transfection, cells were harvested from two wells per one sample. Total RNA was purified using FastGene RNA Premium Kit (NIPPON Genetics). RNA from siGY441-transfected cells was used as a control. Aliquot of total RNA (1 μg) was reverse-transcribed using

High-Capacity cDNA Reverse Transcription Kits (Applied Biosystems, Foster City, CA, USA). The mixture of synthesized cDNA, gene-specific primer sets, and KAPA SYBR Fast qPCR Kit (NIPPON Genetics) was subjected to PCR reaction. The levels of PCR products were monitored with StepOnePlus Real-Time PCR system (Applied Biosystems) and analyzed by the ΔΔCt method. The expression level of each sample was first normalized to the amount of glyceraldehyde-3-phosphate dehydrogenase (GAPDH) and then to the siGY441-transfection control. Used primer sets are listed in Table 6. The IC_{50}s are listed in Table 7.

Computational prediction of the structure of modified RNA

The Cartesian coordinates of the crystal structure (PDB ID: 4W5O) were used as initial geometry for 5′-AUU-3′ RNAs in positions 6–8 from the 5′ end of the guide RNA loaded on the AGO protein. Met364, Ile365, Lys709, and His753 of the AGO protein were taken into account in the calculations, in which the main chains of these amino acids were replaced by methyl groups at the atoms bonded to Cα. For 5′-AUU-3′ RNA, I introduced 2′-OMe modifications of all combinations at positions 6–8. Full geometry optimization was with the Cα atoms of Lys709 and His753 being fixed at the theoretical level of ωB97X-D/6-31G(d). The energies are listed in Appendix together with all Cartesian coordinates. The Gaussian 09 program package (Frisch *et al*. 2005) was used for all calculations. The simulations were carried out at the Center for Quantum Life Sciences and the Research Center for Computational Science, Okazaki National Research Institutes.

Immunoprecipitation by anti-AGO2 antibody

A HeLa cell suspension was plated into a 9-cm dish (1.0×10^6 cells/dish) 1 day before transfection. Cells were simultaneously transfected with 20 nM of each siRNA and 1 μg of psiCHECK-SM reporter construct using Lipofectamine 2000. Cells were harvested from four dishes per one sample, washed with PBS and lysed in cold lysis buffer (20 mM Tris-HCl [pH 7.5], 4 mM MgCl2, 10 mM KCl, 0.5 mM DTT, 140 mM NaCl, 1 mM Na3VO4, 10 mM NaF, 0.5% NP-40, complete protease inhibitor and 0.03 units RNase inhibitor) 24 h following transfection. For immunoprecipitation, 50 μl of Dynabeads Protein G (Thermo Fisher Scientific) were conjugated with 2.5 μg of mouse anti-AGO2 antibody (FUJIFILM Wako) or 2.5 μg of mouse IgG (Santa Cruz Biotechnology, Dallas, TX, USA) as a negative control by rotation at 4 ºC for overnight. The cell lysates were then added to antibody-bound Dynabeads Protein G and rotated at 4 ºC for 2 h. The beads were washed three times with wash buffer (lysis buffer containing 300 mM NaCl) and twice with lysis buffer. To elute the bound proteins with RNA, 100 μl of 2 × SDS-PAGE sample buffer (4% (wt/vol) SDS, 0.1 M Tris–HCl (pH 6.8), 12%

(vol/vol) β-mercaptoethanol, 20% (wt/vol) glycerol and 0.01% (wt/vol) bromophenol blue) was added and the beads were heated at 70 ºC for 10 min. Dynabeads were removed by using DynaMag (Thermo Fisher Scientific). Half of the eluted supernatant was subjected to western blot, and the remaining was subjected to RNA extract.

Western blot

The eluate of the immunoprecipitate was separated by SDS-PAGE and transferred to the immobilon-P PVDF membrane (Merck Millipore, Burlington, MA, USA) using the Mini Trans-Blot Cell (Bio-Rad, Hercules, CA, USA). The membranes were blocked for 1 h at room temperature in TBST (20 mM Tris–HCl [pH 7.5], 150 mM NaCl and 0.1% Tween) supplemented with 5% Difco skim milk (FUJIFILM Wako). Blocked membranes were incubated with each of the following primary antibodies at 4 ºC overnight in TBST + 5% skim milk or Can Get Signal immunoreaction enhancer solution (TOYOBO, Osaka, Japan): anti-AGO2 at 1:500 dilution (FUJIFILM Wako), anti-TNRC6A at 1:1500 (Bethyl Laboratories, Montgomery, TX, USA), anti-alpha tubulin at 1:2000 (Abcam, Cambridge, UK), or anti-*Renilla* luciferase at 1:1000 (MBL, Aichi, Japan). After incubation with primary antibody, the membranes were washed for 10 min at room temperature with TBST three times and then incubated for 1 h at room temperature with HRP-conjugated anti-mouse IgG (GE Healthcare, Chicago, IL, USA) at 1:3000 dilution or anti-rabbit IgG (GE Healthcare) at 1:3000 dilution in TBST. After being washed three times for 10 min in TBST at room temperature, the membrane was incubated with ECL Prime Western Blotting Detection Reagent (GE Healthcare), and signals were detected by FUSION (VILBER, Collégien, France).

Quantification of siRNAs loaded onto AGO2

ISOGEN (Nippon Gene, Tokyo, Japan) was added to the eluate of the immunoprecipitation by anti-AGO2 antibody or mouse IgG. It was also added to 10% of the cell lysates as input samples. RNA extraction was performed according to the manufacturer's protocol. An aliquot of RNA (80 ng) was reverse transcribed using the stem-loop primer specific for each strand of siRNA with High-Capacity cDNA Reverse Transcription Kits. A mixture of synthesized cDNA, siRNA-specific forward primer, and loop-specific reverse primer was subjected to PCR amplification using the KAPA SYBR Fast qPCR Kit. The levels of PCR products were monitored using the StepOnePlus Real-Time PCR System, and the copy numbers of each sample were calculated using the absolute quantification method. To prepare the standard curve for each sample, each synthesized siRNA (0.00005–5 ng) was similarly reverse transcribed. Each copy number from the immunoprecipitate was normalized to that in the input

fraction. The primer sets are listed in Table 6.

Calculation of siRNA thermodynamics

Tm values were calculated for all possible regions in siRNA duplex of previously reported 26 siRNAs (Ui-Tei *et al*. 2008a), by means of the nearest-neighbor model (Panjkovich *et al*. 2005). Tm values were calculated as follows.

ΔH: Sum of nearest neighbor enthalpy changes (kcal mol^{-1})

A: Helix initiation constant (-10.8 cal $mol^{-1}K^{-1}$)

ΔS: Sum of nearest neighbor entropy changes (kcal $mol^{-1}K^{-1}$)

R: Gas constant (1.987 cal $deg^{-1}mol^{-1}$)

Ct: Total molecular concentration (100 μM)

$[Na^+]$: Sodium ion concentration (100 mM)

Enthalpy and entropy values (Xia *et al*. 1998) were used for the calculation of Tm values.

Determining the responsible regions through repeated random sampling

Correlation heatmaps were generated in RStudio (ver. 3.4.0) to visualize the correlations between previously reported relative luciferase activities for the off-target effects of 26 siRNAs (Ui-Tei *et al*. 2008a) and their Tm values across all possible siRNA duplex regions. A repeated sampling process was adopted to determine the statistically significant start and end positions of each responsible region. In each sampling cycle, 13 of 26 siRNAs were randomly sampled (10,400,600 possible combinations in total). The sampling process was repeated 1000 times. Among the selected samples, start (x) and end (y) positions of the top-ranked or top 10 regions with positive or negative correlations with luciferase activity were recorded. Furthermore, the siRNA samples (n = 26) were randomly divided into training data (n = 13) and validation data (n = 13) (10,400,600 possible combinations in total) for a total of 1000 replications. In the training or validation data, correlations for each identified responsible region were randomly calculated and compared using Student's *t*-test.

2.3 Results

Effects of sequential 2′-OMe modifications in the seed region of the siRNA guide strand on RNAi and off-target activities

In our previous report, introduction of 2′-OMe into the siRNA seed region (positions 2–8) reduced off-target activity without affecting RNAi activity (Iribe *et al*. 2017). To investigate the position-dependent effects of 2′-OMe modifications in the siRNA seed region in more detail, RNAi and seed-dependent off-target activities of siRNAs were investigated using luciferase reporter assays (Figure 3). I used two types of reporter plasmids for the guide strand, psiCHECK-gCM and psiCHECK-gSM, with completely matched and three tandem-repeated seed-matched sequences of the siRNA guide strand, respectively, in the 3′ UTR of the *Renilla luciferase* gene. Each of these plasmids was transfected into human HeLa cells with pGL3-Control, which expresses firefly luciferase as a control, and each siRNA at different concentrations. The siRNAs against human *vimentin* (siVIM-270) and *clathrin heavy chain* (siCLTC-2416) were used for the reporter assays. The siVIM-270 is a Class Ia siRNA, whereas siCLTC-2416 is a Class Ib siRNA (Figure 2), and the number following each siRNA name indicates the nucleotide position in each target gene corresponding to the 3′ end of each siRNA guide strand, and the nucleotide positions with 2′-OMe modifications were further added. The 2′-OMe-modified nucleotides were sequentially increased from position 2 to position 11 in siVIM-270 and to position 8 in siCLTC-2416, and their modified positions are shown in magenta. RNAi activities of both siVIM-270 and siCLTC-2416 were similar and obviously high, even when 2′-OMe was introduced into any position in their seed regions (IC_{50}s were 11–46 and 4–18 pM, respectively), although the activities of siVIM-270_2-5 and siCLTC-2416_2-5 decreased slightly (Figure 4A, B, Table 4). The off-target activities of unmodified siVIM-270 were clearly observed and gradually decreased along with the increase in 2′-OMe-modified nucleotides from positions 2 to 5, then reached a plateau and increased slightly after position 5. The off-target activities of unmodified siCLTC-2416 were also obvious and decreased with the increase of 2′-OMe-modified nucleotides up to position 5, and then increased from positions 6 to 8 (Figure 4A, B, Table 4). These results suggest that the nucleotides at positions 2–5 and 6–8 may have distinct functions in off-target activities.

RNAi and seed-dependent off-target activities of the passenger strands of the Class I siRNAs, siVIM-270 and siCLTC-2416, were also investigated. I used psiCHECK-pCM and psiCHECK-pSM reporter plasmids with completely matched and three tandem-repeated seed-matched sequences of the siRNA passenger strand, respectively, in the 3′ UTR region of the *Renilla* luciferase gene (Figure 5A). These plasmids were used for reporter assays. RNAi activities of the passenger strand of siVIM-270

increased along with increasing 2′-OMe modifications up to position 5 in the guide strand (Figure 5B, Table 5). However, when the number of 2′-OMe modifications was increased further, RNAi activities gradually decreased, and were almost lost in siRNAs with 2′-OMe modifications at positions 2–9 on the guide strand. The off-target activities of the passenger strand of siVIM-270 were weak, and they were not altered by the 2′-OMe modifications (Figure 5B, Table5). Similar results were observed for siCLTC-2416 (Figure 5C, Table 5). RNAi activities of the passenger strand of siCLTC-2416 increased along with increasing 2′-OMe modifications up to position 5 in the guide strand and gradually decreased when the number of 2′-OMe modifications was increased further (Figure 5C, Table 5). The off-target activities of the siCLTC-2416 passenger strand were weak, and they were not altered by the modifications (Figure 5C, Table 5).

These results clearly indicate that the off-target activity of the guide strand was decreased by 2′-OMe modifications at positions 2–5, and the RNAi activities of the passenger strand increased concurrently. Because an RNA strand with weak stability at the 5′ end is easily unwound from its 5′ end and loaded onto AGO (Ui-Tei *et al*. 2004, Noland *et al*. 2013), the increase in 2′-OMe modifications, which increase base-pairing stability, from the 5′ end of the guide strand might have made it difficult to unwind from the 5′ end. This might have been reflected in the decrease in the amount of guide strands loaded onto the AGO protein as well as the increase in the amount of passenger strands. This might have been the reason why RNAi activities of siRNA guide strands with 2′-OMe modifications at positions 2–5 were slightly decreased compared to those of the unmodified siRNAs (Figure 4).

Functionally different effects of 2′-OMe modifications at positions 2–5 and 6–8 in siRNA seed region on RNAi and off-target activities

To investigate the functional differences of nucleotides at positions 2–5 and 6–8, the RNAi and off-target activities of siRNAs with 2′-OMe modifications at either position were compared in detail using siVIM-270 (Class Ia), siOCT-797 (Class Ia), siCLTC-2416 (Class Ib), siVIM-333 (Class II), siGRK4-189 (Class II), and siVIM-491 (Class III).

The RNAi and off-target activities of unmodified Class Ia siVIM-270 were clearly observed, and the IC_{50} of its RNAi activity was 11 pM, whereas that of its off-target activity was 39 pM (Figure 6A, Table 4). The RNAi activity of siVIM-270_2-5 was only slightly reduced (IC_{50} = 46 pM) and no significant difference was observed at 5 nM siRNA compared to the unmodified siVIM-270 (Student′s *t*-test, $p = 0.31$), but its off-target activity was significantly eliminated ($IC_{50} = \infty$) (Student′s *t*-test, $p = 0.0001$) (Figure 6A, Table 4). RNAi activities of siVIM-270_6-8 (IC_{50} = 17 pM) and siVIM-270_7-8

(IC_{50} = 18 pM) were similar to those of unmodified siVIM-270, and the IC_{50} of their off-target activities were 38 and 51 pM, respectively (Table 4). Next, siVIM-270_2-8 exhibited intermediate RNAi and off-target activity levels (IC_{50} = 21 pM for RNAi activity, IC_{50} = ∞ for off-target activity), and its off-target activity was between those of siVIM-270_2-5 and siVIM-270_6-8/siVIM-270_7-8: its off-target activity was increased but not significant compared to siVIM-270_2-5 (Student´s *t*-test, $p = 0.07$) and significantly decreased compared to siVIM-270_6-8/siVIM-270_7-8 (Student´s *t*-test, *p* values = 0.0001) (Figure 6A, Table 4). Similar results were observed for another Class Ia siRNA, siOCT-797, which targets the Oct4 transcription factor encoded by the *Pou5f1* gene (Figure 6B, Table 4). Unmodified siOCT-797 exhibited strong RNAi activity (IC_{50} = 2 pM) and weak off-target activity (IC_{50} = 348 pM). Significant changes in the RNAi activities of siOCT-797 and its modified forms were not observed, and their IC_{50} were in the range of 2–8 pM. The off-target activities of siOCT-797_2-5 and siOCT-797_2-8 were significantly decreased compared to that of unmodified siOCT-797 (Student´s *t*-test, $p = 0.002$ and 0.008, respectively), but the off-target activities of siOCT-797_6-8 and siOCT-797_7-8 were similar or only slightly decreased compared to that of unmodified siOCT-797. The RNAi activity of Class Ib siCLTC-2416_2-5 (IC_{50} = 18 pM) was also slightly reduced compared to that of unmodified siCLTC-2416 (IC_{50} = 4 pM), but its off-target activity was significantly reduced compared to that of unmodified siCLTC-2416 (Student´s *t*-test, $p = 1.7 \times 10^{-6}$) (Figure 6C, Table 4). The RNAi (IC_{50} = 2 pM) and off-target (IC_{50} = 265 pM) activity levels of siCLTC-2416_7-8 were both similar to those of unmodified siCLTC-2416. As with siVIM-270, siCLTC-2416_2-8 exhibited intermediate RNAi (IC_{50} = 17 pM) and off-target (IC_{50} = 335 pM) activities, falling between siCLTC-2416_2-5 and siCLTC-2416_7-8: its off-target activity was significantly increased compared to siCLTC-2416_2-5 (Student´s *t*-test, $p = 8.6 \times 10^{-6}$) but no significant reduction was not observed compared to siCLTC-2416_7-8 (Student´s *t*-test, $p = 0.12$). The off-target activity of siCLTC-2416_6-8 (IC_{50} = 1819 pM) was weak compared to that of siCLTC-2416_7-8 (IC_{50} = 265 pM) (Table 4). An siRNA guide strand with 2´-OMe modifications at positions 2–5 is difficult to unwind from its 5´-end, but the unwinding from the 5´-end of the passenger strand may be easier (Figure 5). This may result in a decrease in the amount of guide strands loaded onto the AGO protein and an increase in the amount of passenger strands. Subsequently, the RNAi activity of the passenger strand would also increase. However, the passenger strands of siVIM-270 and siCLTC-2416 with 2´-OMe modifications at positions 6–8 and 7–8, respectively, exhibited significantly reduced RNAi activities compared to unmodified siRNAs (Student´s *t*-test, $p = 0.0002 – 0.002$) (Figure 7), indicating that siRNA guide strands with 2´-OMe modifications at positions 6–8 and 7–8 are more easily loaded onto the AGO protein. As shown in our previous study (Iribe *et al*. 2017), 2´-OMe modifications at the seed region

induce steric hindrance of duplex formation on the AGO protein. However, the results of three Class I siRNAs (siVIM-270, siOCT-797, and siCLTC-2416) in this study revealed that the region that inhibits off-target effects from 2′-OMe modifications is limited to positions 2–5. In contrast to the off-target effect, 2′-OMe modifications at positions 2–5 have little effect on RNAi activity, indicating that the nucleotide base-pairings between positions 6–21 and target mRNAs are sufficient to compensate for the steric hindrance caused by 2′-OMe modifications at positions 2–5. The 2′-OMe modifications at positions 6–8 or 7–8 had no inhibitory effects on RNAi, and off-target effects were also unaffected except for siOct-797. Although the off-target activity of siVIM-270_6-8 was similar to that of siVIM-270_7-8 (Figure 6A, Table 4), the off-target activity of siCLTC-2416_6-8 was weak compared to that of siCLTC-2416_7-8 (Figure 6B, Table 4), suggesting that the functions of the nucleotides at positions 5 and 6 are slightly different depending on the siRNA sequence.

Furthermore, I also investigated the effects of 2′-OMe modifications in Class II and III siRNAs. The siRNA against *G protein-coupled receptor kinase 4* (*GRK4*) (siGRK4-189) and siVIM-333 are Class II siRNAs (Figure 6D, E), whereas siVIM-491 is a Class III siRNA (Figure 6F). The RNAi activity of unmodified siGRK4-189 (IC_{50} = 16 pM) was similar to that of siGRK4-189_6-8 (IC_{50} = 20 pM), but RNAi activity was significantly eliminated in siGRK4-189_2-5 (IC_{50} = ∞) compared to that of unmodified siGRK4-189 (Student′s *t*-test, $p = 0.002$), and siGRK4-189_2-8 exhibited intermediate activity (IC_{50} = 170 pM) (Figure 6D, Table 4). The results for siVIM-333 were similar to those of siGRK4-189. The RNAi activity of unmodified siVIM-333 was clearly observed (IC_{50} = 24 pM), whereas that of siVIM-333_2-5 was eliminated (IC_{50} = ∞) (Figure 6E, Table 4). However, siVIM-333_6-8 exhibited similar or higher RNAi activity (IC_{50} = 18 pM) compared to unmodified siVIM-333, and siVIM-333_2-8 exhibited intermediate activity (IC_{50} = 219 pM). The off-target activity exhibited by siGRK4-189 (IC_{50} = 72 pM) was significantly diminished in siGRK4-189_2-5 (IC_{50} = ∞) (Student′s *t*-test, $p = 0.0003$), but siGRK4-189_6-8 exhibited slightly stronger activity (IC_{50} = 34 pM). The off-target activity exhibited by siVIM-333 (IC_{50} = 197 pM) was also diminished in siVIM-333_2-5 (IC_{50} = ∞) and slightly enhanced for siVIM-333_6-8 (IC_{50} = 111 pM). The Class III siRNA siVIM-491 exhibited weak RNAi activity (IC_{50} = 490 pM) and almost no off-target activity (IC_{50} = ∞) (Figure 6F, Table 4). Its RNAi activity was significantly diminished by 2′-OMe modifications at positions 2–5 and 2–8 (Student′s *t*-test, $p = 1.3 \times 10^{-7}$ and 5.7×10^{-7}, respectively), but the off-target activity was not (Student′s *t*-test, $p = 0.09$ and 0.07, respectively). However, the RNAi and off-target activities were significantly enhanced by 2′-OMe modifications at positions 6–8 (IC_{50} = 37 pM for RNAi activity, IC_{50} = 1748 for off-target activity) (Student′s *t*-test, $p = 0.003$ and 3.7×10^{-5}, respectively). The results for siGRK4-189, siVIM-333, and siVIM-491 suggest that a high GC-contents at the 5′

terminus seven-nucleotide increases the difficulty of unwinding from the 5′ end of the siRNA, in addition to 2′-OMe modifications at positions 2–5. Thus, the steric hindrance to base-pairing of 2′-OMe-modified nucleotides at positions 2–5 in Class III siRNA might not be rescued, even when nucleotides at positions 6–21 pair with target mRNAs, which is different from Class I siRNAs. Furthermore, siVIM-270 with mismatches at positions 2–5 (siVIM-270_2-5_mm) and 6–8 (siVIM-270_6-8_mm) exhibited little or almost no RNAi and off-target activities (Figure 8), suggesting that the effects of 2′-OMe modifications are not different from those of mismatches, thus base-pairing of 2′-OMe-modified nucleotides on AGO may be deformed.

All of these findings suggest that nucleotides 2–5 and 6–8 may have different functions. 2′-OMe modifications at positions 2–5 function to reduce off-target activity due to steric hindrance. By contrast, 2′-OMe modifications at positions 6–8 slightly enhance RNAi activity and strongly enhance off-target activity.

Effects of 2′-OMe modifications at positions 2–5 and 6–8 in the siRNA seed region on the expression of endogenous genes

To investigate genome-wide off-target effects of siVIM-270 with 2′-OMe modifications at positions 2–5, 6–8, or 2–8, I performed microarray analysis. Unmodified and modified siVIM-270s were transfected into HeLa cells, respectively. Total RNA was purified from cells 1 day later and subjected to microarray analyses. The MA plots (M = intensity ratio, A = average intensity) of the microarray data indicated changes in the expression levels of the annotated transcripts and the cumulative distribution indicated the averaged fold-changes of the transcripts with seed-match (SM) sequences in their 3′ UTRs and non-SM transcripts as control (Figure 9A, B). The expression level of *vimentin* gene with a complete-match (CM) sequence was obviously downregulated by the unmodified siVIM-270, and siVIM-270_2–5, _6–8, or _2–8 exhibited similar levels of RNAi activities as that of the unmodified siVIM-270 (Figure 9C). The difference in the mean $\log_2$ fold-changes of SM or non-SM transcripts of siVIM-270 guide strand was calculated as an indicator of the degree of off-target effects (Figure 9D). The unmodified siVIM-270 exhibited strong off-target effects, but siVIM-270_2-5 exhibited little off-target effects. However, siVIM-270_6-8 exhibited slightly stronger off-target effects compared to those of unmodified siVIM-270. Furthermore, siVIM-270_2-8 exhibited little off-target effects similar to siVIM-270_2-5, suggesting that off-target effects on the endogenous genes are prevented by 2′-OMe modifications at least at positions 2–5.

To confirm the microarray results, the effects of siVIM-270 on its target gene *vimentin* (*VIM*), the off-target genes *vesicle-associated membrane protein-associated protein A* (*VAPA*) and

myotrophin (*MTPN*), and the non-target gene *surfeit 4* (*SURF4*) were examined (Figure 10A). At 24 h after transfection of siVIM-270 into HeLa cells, total RNA was purified from the cells and qRT-PCR was performed. The unmodified siVIM-270 exhibited sufficient RNAi activity with regard to *vimentin* expression (IC_{50} = 312 pM). Furthermore, as shown in the reporter assay (Figure 6A), similar RNAi activity levels were observed for siVIM-270_2-5 (IC_{50} = 1050 pM), siVIM-270_6-8 (IC_{50} = 368 pM), and siVIM-270_2-8 (IC_{50} = 573 pM) (Figure 10B). In addition, siVIM-270 exerted off-target effects on *VAPA* and *MTPN*, which have seed-complementary sequences in their 3′ UTRs. However, siVIM-270_2-5 exerted little off-target effects on either gene, whereas siVIM-270_6-8 exhibited obvious off-target effects (IC_{50} = 3116 pM for *VAPA*, IC_{50} = 8488 pM for *MTPN*), with levels similar to those of unmodified siVIM-270 (IC_{50} = 2730 pM for *VAPA*, IC_{50} = 13,386 pM for *MTPN*). Furthermore, siVIM-270_2-8 exerted little off-target effects on both genes, strongly supporting the result that off-target effects on endogenous genes are also prevented by 2′-OMe modifications at positions 2–5. Almost no repression of the non-target gene *SURF4* was observed. The qRT-PCR results were mostly in consistent with the microarray results (Figure 10C). Thus, these assays confirmed the effects of 2′-OMe modifications on endogenous genes.

Computational simulation of the mechanism for enhancing RNAi/off-target activities by 2′-OMe modifications at positions 6–8

To reveal the mechanism by which 2′-OMe modifications at seed-region positions 6–8 enhance RNAi and off-target activities, 2′-OMe-modified RNA structures on the AGO protein were simulated using density functional theory at the ωB97X-D/6- 31G(d) level (Figure 11). The unmodified 5′-AUU-3′ RNA structure (nucleotides 6−8 [A(6), U(7), and U(8)] of the guide RNA) on the human AGO protein reported by Schirle *et al*. (2014) was used, with side chains of His (H753), Lys (K709), Met (M364), and Ile(I365) residues (PDB: 4W5O). Geometry optimization was achieved by fixing the central carbon atoms (Cαs) of H753 and K709 (Figure 12A). Single-stranded RNA structures in which the sugars of A(6), U(7), U(8), A(6)U(7), A(6)U(8), U(7)U(8), or A(6)U(7)U(8) were modified with 2′-OMe were simulated (Figure 12B–H). In the RNA structure with a 2′-OMe modification in U(7), the hydrophobic side chains of M364 and I365 may support the direction of U(7). This may result in the direction of U(8) is also able to maintain a conformation which is suitable to base-pairing with target/off-target mRNAs (Figure 12C). Similar results were also observed in structures with 2′-OMe modifications in all combinations including U(7) (Figure 12C): A(6)U(7) (Figure 12E), U(7)U(8) (Figure 12G), and A(6)U(7)U(8) (Figure 12H). However, in the RNA structure with 2′-OMe modification at A(6) (Figure 12B), U(8) (Figure 12D), or A(6)U(8) (Figure 12F), U(8) was positioned

orthogonal to U(7). In these cases, base-pairings between U(7)/U(8) nucleotides in the guide RNA and target/off-target mRNAs are considered to be difficult. Thus, 2′-OMe modification at U(7) may have the strongest effect on base-pairing with target/off-target mRNAs.

Furthermore, I also simulated guide RNA and target RNA structures with His (H753), Lys (K709), Met (M364), and Ile(I365) residues (PDB: 4W5O). Optimization was performed using the Cαs of H753 and K709; amino acids are not shown in the figures for simplification. Overlapping structures of unmodified RNA with and without target mRNA revealed differences between the two types (Figure 12I). A similar structural change was also observed in the overlapping structures of 2′-OMe-modified RNA with and without target mRNA (Figure 12J). Thus, nucleotides at positions 6–8 in the guide RNA change the conformation when they base-pair with target mRNAs.

Experimental validation for enhancement of RNAi/off-target activities by 2′-OMe modification at nucleotide 7

Computational validation suggested that 2′-OMe modification of the nucleotide at position 7 produces the largest effect in terms of base-pairing with target/off-target mRNAs. I then validated the result experimentally using siVIM-491, because it exhibited the strongest effects of 2′-OMe modification (Figure 6F). Unmodified siVIM-491 exhibited RNAi activity (IC_{50} = 490 pM) but almost no off-target activity (IC_{50} = ∞) (Figure 13A, Table 4). As expected, siVIM-491_7 exhibited the strongest off-target activity (IC_{50} = 6820 pM) compared to siVIM-491_6 and siVIM-491_8 (IC_{50} = 24,365 and 37,372 pM, respectively), although the RNAi activity of siVIM-491_7 (IC_{50} = 160 pM) was similar to that of siVIM-491_6 (IC_{50} = 158 pM) and slightly stronger compared to that of siVIM-491_8 (IC_{50} = 287 pM). Furthermore, siVIM-491_6-7 and siVIM-491_7-8, both of which had 2′-OMe modification at positions 7, exhibited stronger RNAi (IC_{50} = 46 and 41 pM, respectively) and off-target activities (IC_{50} = 5876 and 1612 pM, respectively) compared to siVIM-491_6+8 (IC_{50} = 103 pM for RNAi activity, IC_{50} = 21,129 pM for off-target activity). Among all modified siRNAs, siVIM-491_6-8 exhibited the strongest RNAi (IC_{50} = 37 pM) and off-target activities (IC_{50} = 1,748 pM), with levels similar to those of siVIM-491_7-8. Results of the RNAi/off-target activities were compared at each concentration of siRNA (Figure 13B-G). When the siRNA concentrations were at 0.05 and 0.5 nM, siVIM-491_6 and siVIM-491_7 significantly increased RNAi activities compared to unmodified siVIM-491, but siVIM-491_8 did not (Figure 13B, C). When two or three 2′-OMe modifications were simultaneously introduced into siRNAs (siVIM-491_6-7, siVIM-491_7-8, siVIM-491_6+8, siVIM-491_6-8), RNAi activities were also significantly enhanced. However, when siRNA concentration was increased to 5 nM, clear differences in RNAi activities in siVIM-491_6, siVIM-491_7, and siVIM-491_8 were not

observed, and siVIM-491_6-7, siVIM-491_7-8, and siVIM-491_6-8 exhibited significant RNAi activities (Figure 13D). As for off-target activity, siRNAs containing 2′-OMes at position 7 (siVIM-491_6-7, siVIM-491_7-8, or siVIM-491_6-8) significantly increased off-target activities at 0.5 nM siRNA (Figure13E), and siVIM-491_7 also additively increased off-target activity at 5 nM siRNA (Figure13F). When siRNA concentration was 50 nM, siVIM-491_6 also increased off-target activity (Figure13G). Thus, these results clearly suggest that 2′-OMe modification at position 7 is the most effective modification for RNAi/off-target activities, and 2′-OMe modification at position 6 contributed to the secondary highest effect, but 2′-OMe modification at position 8 exhibited almost no effect.

I also validated the effects of 2′-OMe modification of siRNA at positions 2–5 (siCLTC-2416_2-5), because the functions of nucleotides at positions 2–5 and 6–8 appear to differ. Although the unmodified siCLTC-2416 exhibited strong RNAi (IC_{50} = 4 pM) and off-target activities (IC_{50} = 285 pM), the RNAi and off-target activities of siCLTC-2416_2-5 were reduced (IC_{50} = 18 pM for RNAi activity, IC_{50} = ∞ for off-target activity) (Figure 14, Table 4). The off-target activities of siCLTC-2416_2-6 and siCLTC-2416_2-5+7 (IC_{50} = 501 and 533 pM, respectively) were stronger than that of siCLTC-2416_2-5+8 (IC_{50} = ∞). Furthermore, the off-target activities of siCLTC-2416_2-7 and siCLTC-2416_2-5+7-8 (IC_{50} = 353 and 382 pM, respectively) were stronger than that of siCLTC-2416_2-5+6+8 (IC_{50} = 2467 pM). The off-target activity of siCLTC-2416_2-8 (IC_{50} = 335 pM) was similar to those of siCLTC-2416_2-7 and siCLTC-2416_2-5+7-8. However, the RNAi activities of these 2′-OMe-modified siRNAs (IC_{50} ranging from 10 to 29 pM) were similar to that of siCLTC-2416_2-5 (IC_{50} = 18 pM), except for siCLTC-2416_2-5+8 (IC_{50} = 107 pM). Thus, these results suggest that the 2′-OMe modification at position 7, in addition to positions 2–5, is the most effective modification for influencing RNAi/off-target activities. In addition, 2′-OMe modification at position 6 produced an effect similar to that from position 7 in the case of siCLTC-2416. A possible explanation is that the functions of nucleotides 6 and 7 may slightly differ according to the siRNA sequence.

Effects of 2′-OMe modifications on AGO loading levels of siRNA guide strands

All classes of siRNAs with 2′-OMe modifications at positions 2–5 exhibited strongly reduced off-target activities. By contrast, the same siRNAs with 2′-OMe modifications at positions 6–8 exhibited same or enhanced off-target activities (Figures 6). Thus, it was possible that guide strands with 2′-OMe modifications at positions 2–5 would be loaded at lower levels on the AGO protein. To investigate the effect of 2′-OMe modifications on AGO loading levels of siRNA guide strands, I performed RNA and protein immunoprecipitation experiments with anti-AGO2 antibody and

quantified the amount of guide strands in the immunoprecipitates (Figure 15A). The AGO2 protein and trinucleotide repeat containing 6A (TNRC6A) proteins, which interact with AGO (Meister *et al*. 2005, Lian *et al*. 2009, Takimoto *et al*. 2009), were detected (Figure 15B). The *Renilla* luciferase protein was clearly observed in the lysate of cells transfected with control siRNA (siCont), siVIM-270_2-5, and siVIM-270_2-8, but luciferase levels were reduced by the transfection of unmodified siVIM-270 and siVIM-270_6-8, consistent with the results of the reporter assay (Figure 15C). Furthermore, I performed qRT-PCR using stem-loop PCR primers specific for the siVIM-270 guide or passenger strand (Figure 15D). The amount of guide strands in the immunoprecipitate was almost similar regardless of 2′-OMe modifications, and the amount of guide strands was higher compared to that of passenger strands (Figure 15E). These results suggest that 2′-OMe modification had almost no effect on AGO loading.

Presumption of region responsible for siRNA off-target effects

In the previous report of my laboratory (Ui-Tei *et al*. 2008a), it was reported that the siRNA off-target effect is correlated with the thermodynamic stability of base-pairing between the siRNA seed region and its target mRNA. However, I found that the siRNA seed region is divided into two functionally different domains, positions 2–5 and 6–8. To identify the exact region responsible for siRNA off-target effects, I used the results of luciferase reporter assays from the previous study (Ui-Tei *et al*. 2008a) (Figure 16A, 17A), and correlations with T_m values in the guide–target duplex were calculated. The results from both 50 nM siRNA (Figure 16B) and 5 nM siRNA (Figure 17B) clearly revealed that the two different regions have correlations with siRNA off-target activities: the 5′ region of the guide strand exhibited a negative correlation with off-target activity, whereas the central region exhibited a positive correlation. To determine the exact start and end positions of each region, a repeated random sampling process was adopted with various combinations of siRNA subgroups from 26 siRNAs. In each sampling cycle, start (x) and end (y) positions of the regions with either the top-ranked or the top 10 most positive or negative correlations were recorded for 13 randomly sampled siRNAs. The random sampling process was repeated 1000 times, generating an x-y list representing the regions with optimal correlations in either direction. The frequencies of occurrence of the optimal x-y positions are shown in Figures 16C and 17C. The most frequent-start and end positions (x-y) with the top-ranked negative correlation were guide positions 2–5, whereas those with top-10 correlations were positions 2–5 and 2–8. By contrast, the most frequently occurring regions with top-ranked and top-10 positive correlations were guide positions 9–14 with 50 nM siRNA (Figure 16C) and 8–14 with 5 nM siRNA (Figure 17C), respectively. Then, absolute correlation coefficients for each of five regions, 2–

5, 2–8, 6–8, 9–14, and 8–14 at 50 nM and 5 nM, were calculated (Figure 16D, 17D). The relationship between luciferase activity and T_m value at positions 2–5 was associated with significantly higher correlation coefficients (r = 0.76 at 50 nM, r = 0.73 at 5 nM) compared to those at positions 2–8 (r = 0.71 at 50 nM, r = 0.67 at 5 nM) based on training data, and the correlation coefficients from validation data were also higher at positions 2–5 (r = 0.77 at 50 nM, r = 0.74 at 5 nM) compared to those at positions 2–8 (r = 0.71 at 50 nM, r = 0.67 at 5 nM). The correlation coefficients associated with thermodynamic stability at positions 6–8 and 9–14 at 50 nM, and 8–14 at 5 nM were also calculated, but the values were low. Therefore, these results suggest that the siRNA off-target effect is correlated with thermodynamic stability at positions 2–5 rather than at positions 2–8.

2.4 Discussion

In RNAi, the siRNA guide strand base-pairs perfectly with its target mRNA. However, off-target effects are also induced on mRNAs with partial complementarity with the seed region of the guide strand (Jackson *et al*. 2003, Scacheri *et al*. 2004, Lewis *et al*. 2005, Lim *et al*. 2005, Lin *et al*. 2005, Birmingham *et al*. 2006, Jackson *et al*. 2006, Grimson *et al*. 2007). RNAi activities of the passenger strands of unmodified siVIM-270 and siCLTC-2416 gradually increased with increasing 2′-OMe modifications from positions 2 through 5 (Figure 5, Table 5), whereas off-target activities of the guide strands decreased with increasing modifications at positions 2–5 but increased with modifications at positions 6–8 (Figure 4, Table 4). The decrease in off-target activity of the guide strand and increase in RNAi activity of the passenger strand with modifications at positions 2–5 may reflect the decrease in the amount of guide strands loaded onto the AGO protein and the increase in that of the passenger strands. Because an RNA strand with weak stability at the 5′ end is easy to load onto AGO as it readily unwinds from its 5′ end (Ui-Tei *et al*. 2004), an increased number of 2′-OMe modifications at the 5′ end of the guide strand may cause difficulty in unwinding from the 5′ end. Furthermore, off-target activity of the guide strand gradually increased with increasing 2′-OMe modifications at positions 6–8 (Figure 4). This supports my finding that 2′-OMe modifications at positions 6–8 enhance the base-pairing stability between the siRNA guide strand and target and off-target mRNAs.

A pioneering structural study revealed that the backbone phosphates of seed nucleotides are ordered on a quasi-helical structure on the surface of the AGO protein; thus, the seed region is able to serve as the entry or nucleation site for mRNA in A-helix form (Schirle and MacRae 2012). Hence, off-target effects are mainly induced by stable base-pairing between the guide-strand seed region and off-target mRNAs on the surface of the AGO protein. In our previous report (Iribe *et al*. 2017), it was revealed that the off-target effect is greatly reduced when the siRNA seed region is modified with 2′-OMe, probably due to steric hindrance of duplex formation on the AGO protein. However, such steric hindrance induced by 2′-OMe modification in the seed region unexpectedly did not affect RNAi activity. In this study, I found that the seed region of the guide strand can be divided into two functionally different regions: nucleotides 2–5 and 6–8 (Figure 6). Although the off-target activities of all classes of siRNAs with 2′-OMe modifications at positions 2–5 were stringently reduced in this study, those with 2′-OMe modifications at positions 6–8 exhibited almost no reduction but rather, a slight enhancement of off-target activities (Figure 6). These results suggest that the reduction of the off-target effect by steric hindrance from 2′-OMe modifications at positions 2–8 is mainly caused by 2′-OMe modifications at positions 2–5, and the 2′-OMe modifications at positions 6–8 caused an

opposite effect to those at positions 2–5. For RNAi activity, 2′-OMe modifications at positions 2–5 in Class Ia and Ib siRNAs resulted in little or no effect (Figure 6A–C), probably because the RNAi activities of Class I siRNAs are inherently strong, and additional activity enhancement is difficult to observe. However, the activities of Class II and III siRNAs were considerably reduced (Figure 6D–F), and the RNAi activities of Class II and III siRNAs with 2′-OMe modifications at positions 2–8 fell to intermediate levels, between those of siRNAs with modifications at positions 2–5 and 6–8 (Figure 6D–F), suggesting that 2′-OMe modifications at positions 2–5 and 6–8 resulted in independent and opposite effects on RNAi activity. The function of nucleotides 6–8 is clearly observed in the Class III siRNA siVIM-491 (Figure 6F). Both the RNAi and off-target activities of siVIM-491_6-8 were enhanced compared to those of unmodified siVIM-491, suggesting that 2′-OMe modifications at positions 6–8 did not cause steric hindrance but instead, enhanced the base-pairing stability between the siRNA guide strand and target/off-target mRNAs. Furthermore, the microarray and qRT-PCR results (Figure 9,10) confirmed that siVIM-270 with 2′-OMe modifications at positions 2–5 strongly reduced off-target effects and siVIM-270 with 2′-OMe modifications at positions 6–8 did not reduce but rather enhanced off-target effects.

The structural analysis revealed that part of the seed region of the single-stranded guide RNA on human AGO protein is organized in a helical conformation, and its base stacking is interrupted by a kink between nucleotides 6 and 7 (Nakanishi *et al* 2012, 2013, Schirle and MacRae 2012, Faehnle *et al*. 2013, Klum *et al*. 2018). This kink is promoted by helix-7 in human AGO2, by inserting helix-7 between nucleotides 6 and 7. Thus, helix-7 creates a steric barrier to base-pairing beyond nucleotide 5, namely, positions 6–8. However, the crystal structures of the guide–target duplex on AGO protein show that helix-7 shifts to dock into the minor groove of the guide–target duplex in stable pairing. Thus, nucleotides 2–5 remain stable on the surface of the AGO protein in both single-stranded and double-stranded form. The 2′-OMe modifications at positions 2–5 disturb the steady loading onto the AGO protein via steric hindrance, resulting in the inhibition of base-pairing with target/off-target mRNAs (Figure 18). By contrast, the conformation of nucleotides 6–8 is changed by the interaction between the guide strand and helix-7; thus, 2′-OMe modifications at positions 6–8 have little or no effect on base-pairing with target/off-target mRNAs structurally but instead enhance the base-pairing stability (Figure 18).

These results revealed that the nucleotides at positions 6–8 function to enhance RNAi/off-target activities. The computational simulation of 2′-OMe modification at each of these nucleotides proposed the possibility that the nucleotide at position 7 exerts the strongest influence on base-pairing with target/off-target mRNA. The methyl group of 2′-OMe of nucleotide 7 creates hydrophobic

interaction with the side chain of M364, which makes the conformation of nucleotide 8 for base pairing to incoming RNA (Figure 12). However, 2′-OMe modification of the nucleotide at position 6 or 8 could not lead such an effect. Thus, due to the 2′-OMe modification of nucleotide 7, it was considered that nucleotide 8 could take a form that easily binds to the target/off-target mRNAs. This speculation was confirmed by reporter assays (Figure 13,14). In the siRNAs (siVIM-491 and siCLTC-2416_2-5 with 2′-OMe modifications at positions 7), the strongest off-target activities were observed compared to either siRNA with 2′-OMe modifications at other positions. These results confirm that 2′-OMe modification at position 7 is the most effective modification for RNAi/off-target activities.

The 2′-OMe modifications in the siRNA guide strand (nucleotides 2–5, 6–8, or 2–8) affect RNAi and off-target activities. It is possible that these activities are affected by the efficiency of AGO loading of 2′-OMe-modified siRNAs. However, the results of the immunoprecipitation experiment clearly revealed that none of the 2′-OMe modifications affected the AGO loading efficiencies of these 2′-OMe-modified siRNAs (Figure 15).

Furthermore, siRNA seed region is suggested to be composed of two functionally different domains. The nucleotides 2–5 are essential for inducing off-target effect and may not contribute significantly to the RNAi effect. The random sampling analysis supported this (Figure 16, 17). By contrast, the nucleotides 6–8, especially nucleotide 7, function to enhance the degree of inhibitory effects on target and off- target genes.

第 3 章については、5 年以内に雑誌などで刊行予定のため、非公開。

Chapter 4 Conclusion

In this study, I firstly investigated the effects of 2′-OMe modifications in the siRNA seed region. I performed reporter assays using siRNAs with 2′-OMe-modified nucleotides from position 2 to 11 sequentially. The results suggested that nucleotides 2–5 and 6–8 in the seed region have different functions. This was also confirmed by the reporter assay and qRT-PCR assay. The 2′-OMe modifications at positions 2–5 function to reduce off-target activity due to steric hindrance; 2′-OMe modifications at positions 6–8 contribute enhancement of RNAi and off-target activities. To investigate mechanism underlying 2′-OMe modification at positions 6–8, computational simulations were performed. It was suggested that 2′-OMe modification at position 7 has the strongest effect on base-pairing with target/off-target mRNAs, and such result was also confirmed by reporter assay. However, its contribution to RNAi and off-target effect was different. Furthermore, one of the possibilities of distinct effects caused by siRNAs with 2′-OMe modifications at positions 2–5 and 6–8 is considered to be the different efficiencies of AGO loading. However, immunoprecipitation experiment clearly revealed that AGO loading efficiencies of these 2′-OMe-modified siRNAs are similar regardless the positions of the modifications. Taken together, it is suggested that siRNA seed region is composed of two functionally different domains, 2–5 and 6–8. The nucleotides 2–5 are essential for inducing off-target effect and may not contribute significantly to the RNAi effect. By contrast, the nucleotides 6-8, especially nucleotide 7, function to enhance the degree of inhibitory effects on target and off- target genes.

5 年以内に雑誌などで刊行予定のため、非公開。

Acknowledgements

First of all, I would like to express my greatest gratitude to my supervisor, Dr. Kumiko Ui-Tei, for the continuous support and advise during my Ph.D. program. I also express my gratitude to Dr. Atsushi Sato and Dr. Yoshimasa Asano.

I am grateful to doctoral student, Daiki Hukuhara, Dr. Dai Akase and Dr. Misako Aida for performing computational simulation.

Finally, I would like to thank my family for financial supporting and being there for me whenever I needed them throughout my studies.

References

1. Adams,D., Gonzalez-Duarte,A., O'Riordan,W.D., Yang,C.C., Ueda,M., Kristen,A.V., Tournev,I., Schmidt,H.H., Coelho,T., Berk,J.L. *et al*. (2018) Patisiran, an RNAi Therapeutic, for Hereditary Transthyretin Amyloidosis. N Engl J Med, 379, 11–21.
2. Balwani,M., Sardh,E., Ventura,P., Peiro',P.A., Rees,D.C., Stolzel,U., Bissell,D.M., Bonkovsky,H.L., Windyga,J., Anderson,K.E. *et al*. (2020) Phase 3 Trial of RNAi Therapeutic Givosiran for Acute Intermittent Porphyria. N Engl J Med, 382, 2289–2301.
3. Bernstein,E., Caudy,A.A., Hammond,S.M. and Hannon,G.J. (2001). Role for a bidentate ribonuclease in the initiation step of RNA interference. Nature, 409, 363–366.
4. Betancur,J.G. and Tomari,Y. (2012) Dicer is dispensable for asymmetric RISC loading in mammals. RNA, 18, 24–30.
5. Birmingham,A., Anderson,E.M., Reynolds,A., Ilsley-Tyree,D., Leake,D., Fedorov,Y., Baskerville,S., Maksimova,E., Robinson,K., Karpilow,J., Marshall,W.S. and Khvorova,A. (2006) 3′ UTR seed matches, but not overall identity, are associated with RNAi off-targets. Nat. Methods, 3, 199–204.
6. Bolstad,B. M., Irizarry,R.A., Gautier,L. and Wu,Z. (2005) Bioinformatics and Computational Biology Solutions Using R and Bioconductor; Gentleman,R., Carey,V., Huber,W., Irizarry,R., Dudoit,S., Eds., Springer: New York, 13−32.
7. Buhrman,G., O′Connor,C., Zerbe,B., Kearney,B.M., Napoleon,R., Kovrigina,E.A., Vajda,S., Kozakov,D., Kovrigin,E.L. and Mattos,C. Analysis of Binding Site Hot Spots on the Surfaceof Ras GTPase. J. Mol. Biol, 413, 773–789
8. Cejas,P., Lopez-Gomez,M., Aguayo,C., Madero,R., de Castro,C.J., Belda-Iniesta,C., Barriuso,J., Moreno,G.V., Larrauri,J., Lopez,R. *et al*. (2009) KRAS mutations in primary colorectal cancer tumors and related metastases: a potential role in prediction of lung metastasis. PLoS One, 4, e8199.
9. Chandradoss,S.D., Schirle,N.T., Szczepaniak,M., MacRae,I.J. and Joo,C. (2015) A Dynamic Search Process Underlies MicroRNA Targeting. Cell, 162, 96–107.
10. Cheloufi,S., Dos Santos,C.O., Chong,M.M. and Hannon,G.J. (2010) A dicer-independent miRNA biogenesis pathway that requires ago catalysis. Nature, 465, 584–589.
11. Chung,W.J., Okamura,K., Martin,R., Lai,E.C. (2008) Endogenous RNA interference provides a somatic defense against Drosophila transposons. Curr. Biol, 18, 795–802.
12. Cifuentes,D., Xue,H., Taylor,D.W., Patnode,H., Mishima,Y., Cheloufi,S., Ma,E., Mane,S.,

Hannon,G.J., Lawson,N.D. *et al*. (2010) A novel miRNA processing pathway independent of Dicer requires Argonaute2 catalytic activity. Science, 328, 1694–1698.

13. Cox,A.D., Fesik,S.W., Kimmelman,A.C., Luo,J. and Der,C.J (2014) Drugging the undruggable RAS: Mission Possible? Nat Rev Drug Discov, 13, 828–851.
14. Czech,B., Malone,C.D., Zhou,R., Stark,A., Schlingeheyde,C., Dus,M., Perrimon,N., Kellis,M., Wohlschlegel,J.A., Sachidanandam,R. *et al*. (2008) An endogenous small interfering RNA pathway in Drosophila. Nature, 453, 798–802.
15. Ding,S.W. and Voinnet,O. (2007) Antiviral immunity directed by small RNAs. Cell, 130, 413–426.
16. Doi,N., Zenno,S., Ueda,R., Ohki-Hamazaki,H., Ui-tei,K. and Saigo,K. (2003) Short-Interfering-RNA-Mediated Gene Silencing in Mammalian Cells Requires Dicer and eIF2C Translation Initiation Factors. Curr. Biol., 13, 41–46.
17. Elbashir,S.M., Lendeckel,W. and Tuschl,T. (2001) RNA interference is mediated by 21-and 22-nucleotide RNAs. Genes Dev., 15, 188–200.
18. Elkayam,E., Kuhn,C.D., Tocilj,A., Haase,A.D., Greene,E.M., Hannon,G.J. and Joshua-Tor,L. (2012) The Structure of Human Argonaute-2 in Complex with miR-20a. Cell, 150, 100–110.
19. Faehnle,C.R., Elkayam,E., Haase,A.D., Hannon,G.J. and Joshua-Tor,L (2013) The making of a slicer: activation of human Argonaute-1. Cell Rep, 3, 1901–1909
20. Fire,A., Xu,S., Montgomery,M.K., Kostas,S.A., Driver,S.E. and Mello,C.C. (1998) Potent and specific genetic interference by double-stranded RNA in Caenorhabditis elegans. Nature, 391, 806–811.
21. Frank,F., Sonenberg,N. and Nagar,B. (2010) Structural basis for 59-nucleotide base-specific recognition of guide RNA by human AGO2. Nature, 465, 818–822.
22. Frank,F., Hauver,J., Sonenberg,N. and Nagar,B. (2012) Arabidopsis Argonaute MID domains use their nucleotide specificity loop to sort small RNAs. EMBO J, 31, 3588–3595.
23. Frisch,M.J., Trucks,G.W., Schlegel,H.B., Scuseria,G.E., Robb,M.A., Cheeseman,J.R., Scalmani,G., Barone,V., Mennucci,B., Petersson,G.A. *et al*. (2009) Gaussian 09, revision E.01; Gaussian, Inc.:Wallingford, CT.
24. Ghildiyal,M., Seitz,H., Horwich,M.D., Li,C., Du,T., Lee,S., Xu,J., Kittler,E.L.W., Zapp,M.L., Weng,Z. *et al*. (2008) Endogenous siRNAs derived from transposons and mRNAs in Drosophila somatic cells. Science, 320, 1077–1081.
25. Grant,B.J, Lukman,S., Hocker,H.J., Sayyah,J., Brown,J.H., McCammon,J.A. and Gorfe,A.A. (2011) Novel Allosteric Sites on Ras for Lead Generation. PLoS One 6, e25711.

26. Grimson,A., Farh,K.K.H., Johnston,W.K., Garrett-Engele,P., Lim,L.P. and Bartel,D.P. (2007) MicroRNA Targeting Specificity in Mammals: Determinants beyond Seed Pairing. Mol. cell, 27, 91–105.
27. Gupta,M., Yates,C.R. and Meibohm,B. (2005) SYBR Green-based real-time PCR allelic discrimination assay for beta2-adrenergic receptor polymorphisms. Anal Biochem, 344, 292–294.
28. Hammond,S.M., Boettcher,S., Caudy,A.A., Kobayashi,R., and Hannon,G.J. (2001) Argonaute2, a Link Between Genetic and Biochemical Analyses of RNAi. Science, 293, 1146–1150.
29. Iribe,H., Miyamoto,K., Takahashi,T., Kobayashi,Y., Leo,J., Aida,M. and Ui-Tei,K. (2017) Chemical Modification of the siRNA Seed Region Suppresses Off-Target Effects by Steric Hindrance to Base-Pairing with Targets. ACS Omega, 2, 2055–2064.
30. Jackson,A.L., Bartz,S.R., Schelter,J., Kobayashi,S.V., Burchard,J., Mao,M., Li,B., Cavet,G. and Linsley,P.S. (2003) Expression profiling reveals off-target gene regulation by RNAi. Nat. Biotech., 21, 635–637.
31. Jackson,A.L., Burchard,J., Schelter,J., Chau,B.N., Cleary,M., Lim,L. and Linsley,P.S. (2006) Widespread siRNA “off-target” transcript silencing mediated by seed region sequence complementarity. RNA, 12, 1179–1187.
32. Kawamata,T., Seitz,H. and Tomari,Y. (2009) Structural determinants of miRNAs for RISC loading and slicer-independent unwinding. Nat. Struct. Mol. Biol, 16, 953–960.
33. Kawamura,Y., Saito,K., Kin,T., Ono,Y., Asai,K., Sunohara,T., Okada,T.N., Siomi,M.C. and Siomi,H. (2008) Drosophila endogenous small RNAs bind to Argonaute 2 in somatic cells. Nature, 453, 793–797.
34. Ketting,R.F., Fischer,S.E.J., Bernstein,E., Sijen,T., Hannon,G.J. and Plasterk,R.H.A. (2001) Dicer functions in RNA interference and in synthesis of small RNA involved in developmental timing in C. elegans. Genes Dev., 15, 2654–2659.
35. Khvorova,A., Reynolds,A. and Jayasena,S.D. (2003) Functional siRNAs and miRNAs exhibit strand bias. Cell, 115, 209–216.
36. Klum,S.M., Chandradoss,S.D., Schirle,N.T., Joo,C. and MacRae,I.J. (2018) Helix-7 in Argonaute2 shapes the microRNA seed region for rapid target recognition. EMBO J, 37, 75–88.
37. Koera,K., Nakamura,K., Nakao,K., Miyoshi,J., Toyoshima,K., Hatta,T., Otani,H., Aiba,A. and Katsuki,M. (1997) K-Ras is essential for the development of the mouse embryo. Oncogene, 15, 1151–1159
38. Lewis,B.P., Burge,C.B. and Bartel,D.P. (2005) Conserved seed pairing, often flanked by adenosines, indicates that thousands of human genes are microRNA targets. Cell, 120, 15–20.

39. Lian,S.L., Li,S., Abadal,G.X., Pauley,B.A., Fritzler,M.J. and Chan,E.K.L. (2009) The C-terminal half of human Ago2 binds to multiple GW-rich regions of GW182 and requires GW182 to mediate silencing. RNA, 15, 804–813.
40. Lièvre,A., Bachet,J.B., Le Corre,D., Boige,V., Landi,B., Emile,J.F., Côté,J.F., Tomasic,G., Penna C., Ducreux,M. *et al*. (2006) KRAS mutation status is predictive of response to cetuximab therapy in colorectal cancer. Cancer Res, 66, 3992–3995.
41. Lim, L.P., Lau,N.C., Garrett-Engele,P., Grimson,A., Schelter,J.M., Castle,J., Bartel,D.P., Linsley,P.S. and Johnson,J.M. (2005) Microarray analysis shows that some microRNAs downregulate large numbers of target mRNAs. Nature, 433, 769–773.
42. Lin,X., Ruan,X., Anderson,M.G, McDowell,J.A., Kroeger,P.E., Resik,S.W. and Shen,Y. (2005) siRNA-mediated off-target gene silencing triggered by a 7 nt complementation. Nucleic Acids Res., 33, 4527–4525.
43. Liu,J., Carmell,M.A., Rivas,F.V., Marsden,C.G, Thomson,J.M., Song,J.J., Hammond,S.M., Joshua-Tor,L. and Hannon,G.J. (2004) Argonaute2 Is the Catalytic Engine of Mammalian RNAi. Science, 305, 1437–1441.
44. Ma,J.B., Yuan,Y.R., Meister,G., Pei,Y., Tuschl,T., Patel,D.J. (2005) Structural basis for 5′-end-specific recognition of guide RNA by the A. fulgidus Piwi protein. Nature, 434, 666–670.
45. Maillard,P.V., Ciaudo,C., Marchais,A., Li,Y., Jay,F., Ding,S.W. and Voinnet,O. (2013) Antiviral RNA interference in mammalian cells. Science, 34, 2235–238.
46. Matranga,C., Tomari,Y., Shin,C., Bartel,D.P. and Zamore,P.D. (2005) Passenger-Strand Cleavage Facilitates Assembly of siRNA into Ago2-Containing RNAi Enzyme Complexes. Cell, 123, 607–620.
47. Meister,G., Landthaler,M., Patkaniowska,A., Dorsett,Y., Teng,G. and Tuschl,T. (2004) Human Argonaute2 Mediates RNA Cleavage Targeted by miRNAs and siRNAs. Mol. cell, 15, 185–197.
48. Meister,G., Landthaler,M., Peters,L., Chen,P.Y., Urlaub,H., Luhrmann,R. and Tuschl,T. (2005) Identification of novel argonaute-associated proteins. Curr. Biol., 15, 2149–2155.
49. Naito,Y., Yoshimura,J., Morishita,S. and Ui-Tei,K. (2009) siDirect 2.0: updated software for designing functional siRNA with reduced seed-dependent off-target effect. BMC Bioinformatics., 10, 392.
50. Nakanishi,K., Weinberg,D.E., Bartel,D.P. and Patel,D.J. (2012) Structure of yeast Argonaute with guide RNA. Nature, 486, 368–374.
51. Nakanishi,K., Ascano,M., Gogakos,T., Ishibe-Murakami,S., Serganov,A.A., Briskin,D., Morozov,P., Tuschl,T. and Patel,D.J. (2013) Eukaryote-specific insertion elements control human

Argonaute slicer activity. Cell Rep, 3, 1893–1900.

52. Noland,C.L., Ma,E. and Doudna,J.A. (2011) siRNA Repositioning for Guide Strand Selection by Human Dicer Complexes. Mol. cell, 43, 110–121.
53. Noland,C.L. and Doudna,J.A. (2013) Multiple sensors ensure guide strand selection in human RNAi pathways. RNA, 19, 639–648.
54. Panjkovich,A. and Melo,F. (2005) Comparison of different melting temperature calculation methods for short DNA sequences. Bioinformatics, 21, 711-722.
55. Park,M.S., Sim,G.Y., Kehling,A.C. and Nakanishia,K. (2020) Human Argonaute2 and Argonaute3 are catalytically activated by different lengths of guide RNA. Proc. Natl. Acad. Sci., USA., 117, 28576–28578.
56. Parker,J.S., Roe,S.M. and Barford,D. (2005) Structural insights into mRNA recognition from a PIWI domain-siRNA guide complex. Nature, 434, 663–666.
57. Pylayeva-Gupta,Y., Grabocka,E. and Bar-Sagi,D. (2011) RAS oncogenes: weaving atumorigenic web. Nat. Rev. Cancer, 11, 761–774.
58. Rand,T.A., Petersen,S., Du,F. and Wang,X. (2005) Argonaute2 Cleaves the Anti-Guide Strand of siRNA during RISC Activation. Cell, 123, 621–629.
59. Rao,D.D., Luo,X., Wang,Z., Jay,C.M., Brunicardi,F.C., Maltese,W., Manning,L., Senzer,N. and Nemunaitis,J. (2018) KRAS mutant allele-specific expression knockdown in pancreatic cancer model with systemically delivered bi-shRNA KRAS lipoplex. PLoS One, 13, e0193644.
60. Réjiba,S., Wack,S., Aprahamian,M. and Hajri,A. (2007) K-ras oncogene silencing strategy reduces tumor growth and enhances gemcitabine chemotherapy efficacy for pancreatic cancer treatment. Cancer Sci, 98, 1128–1136.
61. Rivas,F.V., Tolia,N.H., Song,J.J., Aragon,J.P., Liu,J., Hannon,G.J. and Joshua-Tor,L. (2005) Purified Argonaute2 and an siRNA form recombinant human RISC. Nat. Struct. Mol. Biol, 12, 340–349.
62. Scacheri,P.C., Rozenblatt-Rosen,O., Caplen,N.J., Wolfsberg,T.G., Umayam,L., Lee,J.C., Hughes,C.V., Shanmugam,K.S., Bhattacharjee,A., Meyerson,M. and Collins,F.S. (2004) Short interfering RNAs can induce unexpected and divergent changes in the levels of untargeted proteins in mammalian cells. Proc. Natl. Acad. Sci., USA., 101, 1892–1897.
63. Schirle,N.T. and MacRae,I.J. (2012) The Crystal Structure of Human Argonaute2. Science, 336, 1037–1040.
64. Schirle,N.T., Sheu-Gruttadauria,J. and MacRae,I.J. (2014) Structural basis for microRNA targeting. Science, 346, 608–613.

65. Schirle,N.T., Sheu-Gruttadauria,J., Chandradoss,S.D., Joo,C. and MacRae,I.J. (2015) Water-mediated recognition of t1-adenosine anchors Argonaute2 to microRNA targets. Elife, 4, e07646.
66. Schwarz,D.S., Hutvagner,G., Du,T., Xu,Z., Aronin,N. and Zamore,P.D. (2003) Asymmetry in the assembly of the RNAi enzyme complex. Cell, 115, 199–208.
67. Simanshu,D.K., Nissley,D.V. and McCormick,F. (2017) RAS proteins and theirregulators in human disease. Cell, 170, 17–33.
68. Takimoto,K., Wakiyama,M. and Yokoyama,S. (2009) Mammalian GW182 contains multiple Argonaute-binding sites and functions in microRNA-mediated translational repression. RNA, 15, 1078–1089.
69. Tate,J.G., Bamford,S., Jubb,H.C., Sondka,Z., Bear,D.M., Bindal,N., Boutselakis,H., Cole,C.G., Creatore,C., Dawson,E. *et al*. (2019) COSMIC: the Catalogue Of Somatic Mutations In Cancer. Nucleic Acids Res., 47, D941–D947
70. Tie,J., Lipton,L., Desai,J., Gibbs,P., Jorissen,R.N., Christie,M., Drummond,K.J., Thomson,B.N., Usatoff,V., Evans,P.M. *et al*. (2011) KRAS mutation is associated with lung metastasis in patients with curatively resected colorectal cancer. Clin Cancer Res, 17, 1122–1130.
71. Ui-Tei,K., Naito,Y., Takahashi,F., Haraguchi,T., Ohki-Hamazaki,H., Juni,A., Ueda,R. and Saigo,K. (2004) Guidelines for the selection of highly effective siRNA sequences for mammalian and chick RNA interference. Nucleic Acids Res., 32, 936–948.
72. Ui-Tei,K., Naito,Y., Nishi,K., Juni,A. and Saigo,K. (2008a) Thermodynamic stability and Watson–Crick base pairing in the seed duplex are major determinants of the efficiency of the siRNA-based off-target effect. Nucleic Acids Res., 36, 7100–7109.
73. Ui-Tei,K., Naito,Y., Zenno,S., Nishi,K., Yamato,K., Takahashi,F., Juni,Aya. and Saigo,K. (2008b) Functional dissection of siRNA sequence by systematic DNA substitution: modified siRNA with a DNA seed arm is a powerful tool for mammalian gene silencing with significantly reduced off-target effect. Nucleic Acids Res., 36, 2136–2151.
74. Wang,Y., Sheng,G., Juranek,S., Tuschl,T. and Patel,D.J. (2008a) Structure of the guide-strand-containing argonaute silencing complex. Nature, 456, 209–213.
75. Wang,Y., Juranek,S., Li,H., Sheng,G., Tuschl,T. and Patel,D.J. (2008b) Structure of an argonaute silencing complex with a seed containing guide DNA and target RNA duplex. Nature, 456, 921–926.
76. Xia,T., SantaLucia,J.J., Burkard,M.E., Kierzek,R., Schroeder,S.J., Jiao,X., Cox.C. and Turner,D.H. (1998) Thermodynamic Parameter for an Expanded Nearest-Neighbor Model for Formation of RNA Duplexes with Watson-Crick Base Pairs. Biochemistry, 37, 14719–14735.

77. Yoda,M., Kawamata,T., Paroo,Z., Ye,X., Iwasaki,S., Liu,Q. and Tomari,Y. (2010) ATP-dependent human RISC assembly pathways. Nat. Struct. Mol. Biol, 17, 17–23.
78. Zamore,P.D., Tuschl,T., Sharp,P.A. and Bartel,D.P. (2000) RNAi: Double-Stranded RNA Directs the ATP-Dependent Cleavage of mRNA at 21 to 23 Nucleotide Intervals. Cell, 101, 25–33.

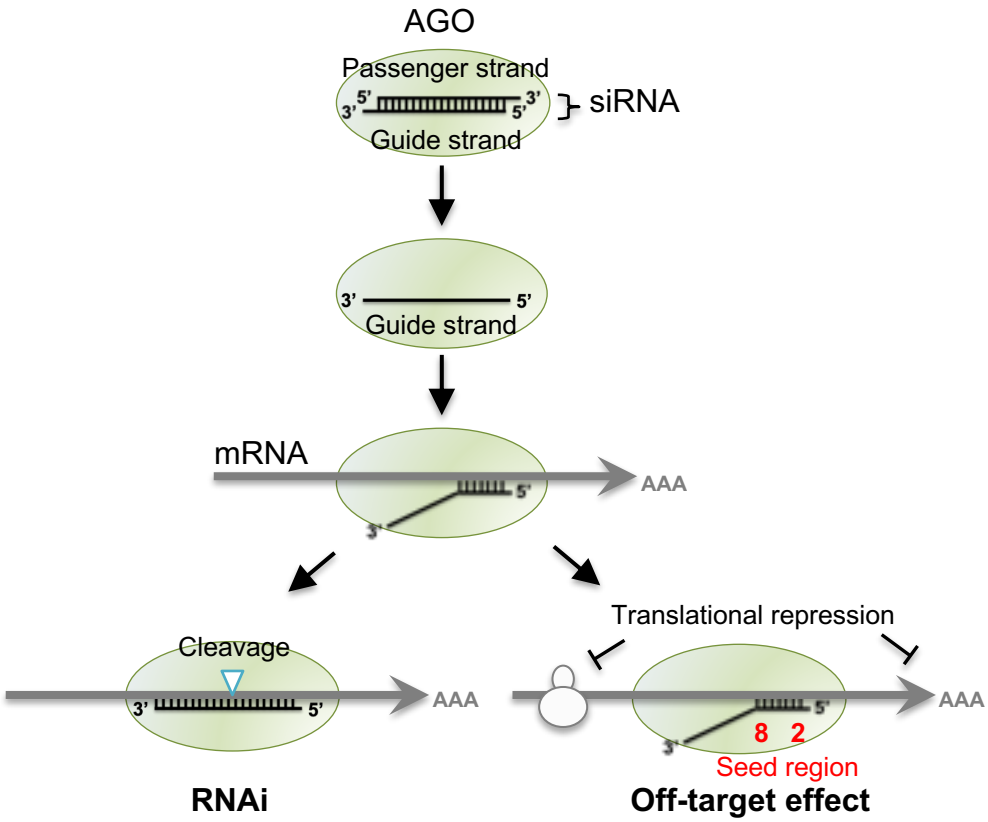

Figure 1. Schematic presentation of siRNA-mediated RNAi and off-target effects.

siRNA is a double-stranded RNA composed of 21-nucleotide guide and passenger strands. siRNA transfected into cells is loaded onto the AGO2 protein, and the passenger strand is removed. The guide strand base-pairs with target and off-target mRNAs through sequence complementarity with the seed region. The guide strand RNA base-pairs with target mRNA with a perfect complementary sequence and cleaves it with AGO2 to repress its expression. On the other hand, off-target mRNAs with sequences complementary to that of the seed region can have their expression reduced through off-target effects via translational repression.

Class	Rule for siRNA sequence	Efficiency
Ia	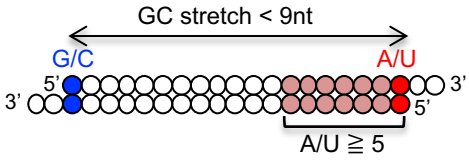	Highly effective
Ib	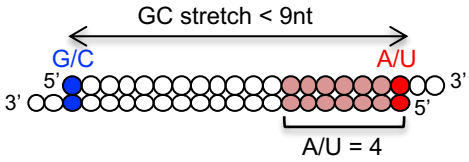	Effective
II	Neither class I nor class Ⅲ	Effective or ineffective
III	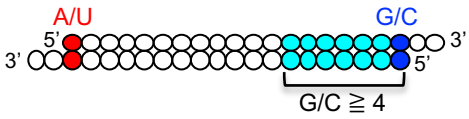	Ineffective

Figure 2. Design rule for functional siRNAs.

In mammalian cells, a limited fraction of siRNAs are functional, thus siRNAs are classified into Classes Ia, Ib, II, and III according to their RNAi efficiency. Class Ia includes highly functional siRNAs, whereas Class Ib includes functional siRNAs. Both have A/U at the 5′ end of the guide strand, G/C at the 5′ end of the passenger strand, and no GC stretch longer than eight nucleotides. However, Class Ia siRNAs have five or more A/Us in the seven-nucleotide 5′ terminus of the guide strand, whereas Class Ib siRNAs have 4 A/Us. Class III siRNAs are nonfunctional and have G/C at the 5′ end of the guide strand, A/U at the 5′ end of the passenger strand, and more than 4 G/Cs within the seven-nucleotide region at the 5′ end of the guide strand. Class II siRNAs are those classified into neither Class I nor Class III.

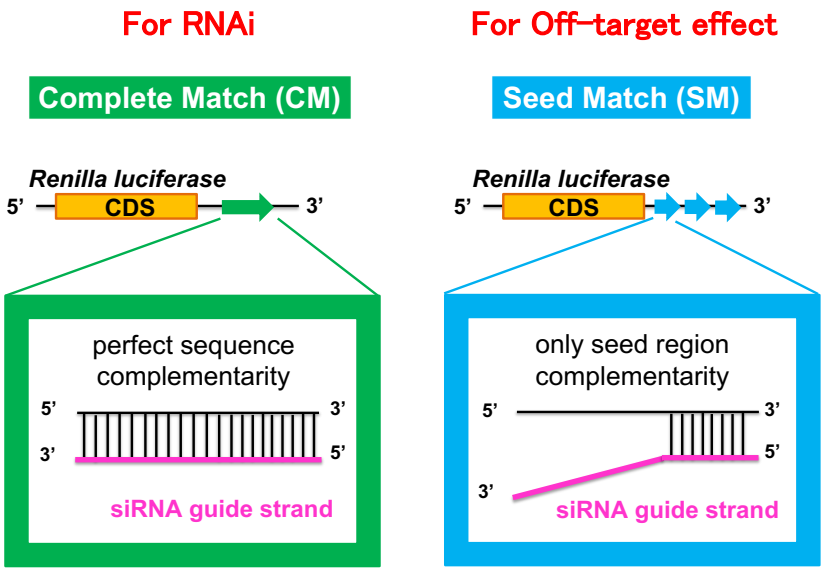

Figure 3. Reporter construct using luciferase reporter assay.

Schematic presentation of RNAi (left) and off-target (right) reporter assays. The psiCHECK-1 plasmids containing complete-matched (CM) or seed-matched (SM) sequences of the siRNA guide strand in the 3′ UTR of the *Renilla luciferase* gene were used for RNAi and off-target activity assays, respectively. I simultaneously transfected each of these constructs, expression construct of firefly *luciferase* gene as an internal control, and each siRNA into HeLa cells, and calculated relative luciferase activity at 1 day after transfection.

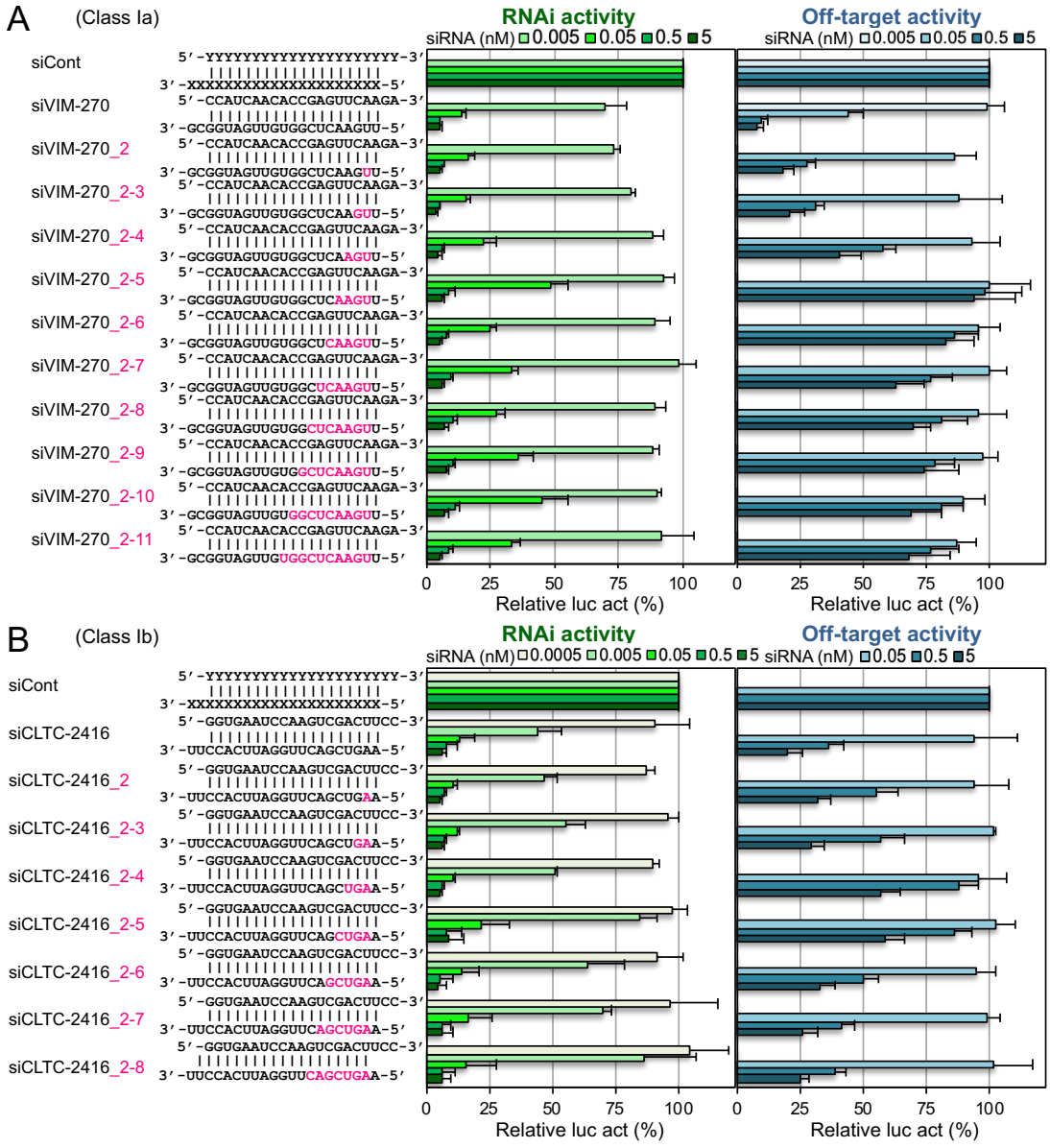

Figure 4. Effects of 2′-OMe modifications of siRNA guide strand on RNAi and off-target activities.

RNAi (left bar graphs) and off-target activities (right bar graphs) of (**B**) siVIM-270 and its modified siRNAs and (**C**) siCLTC-2416 and its modified siRNAs were measured. Each upper sequence indicates the sequence of the passenger strand from 5′ to 3′; the lower sequence indicates the guide strand sequence from 3′ to 5′. Pink indicates positions or nucleotides modified with 2′-OMe. siRNA against green fluorescent protein (GFP) was used as control siRNA (siCont). Each reporter assay was performed at a concentration of 0.0005, 0.005, 0.05, 0.5, or 5 nM siRNA. The horizontal bars indicate relative luciferase activity (Relative luc act). Results are presented as the mean and standard deviation of three independent experiments.

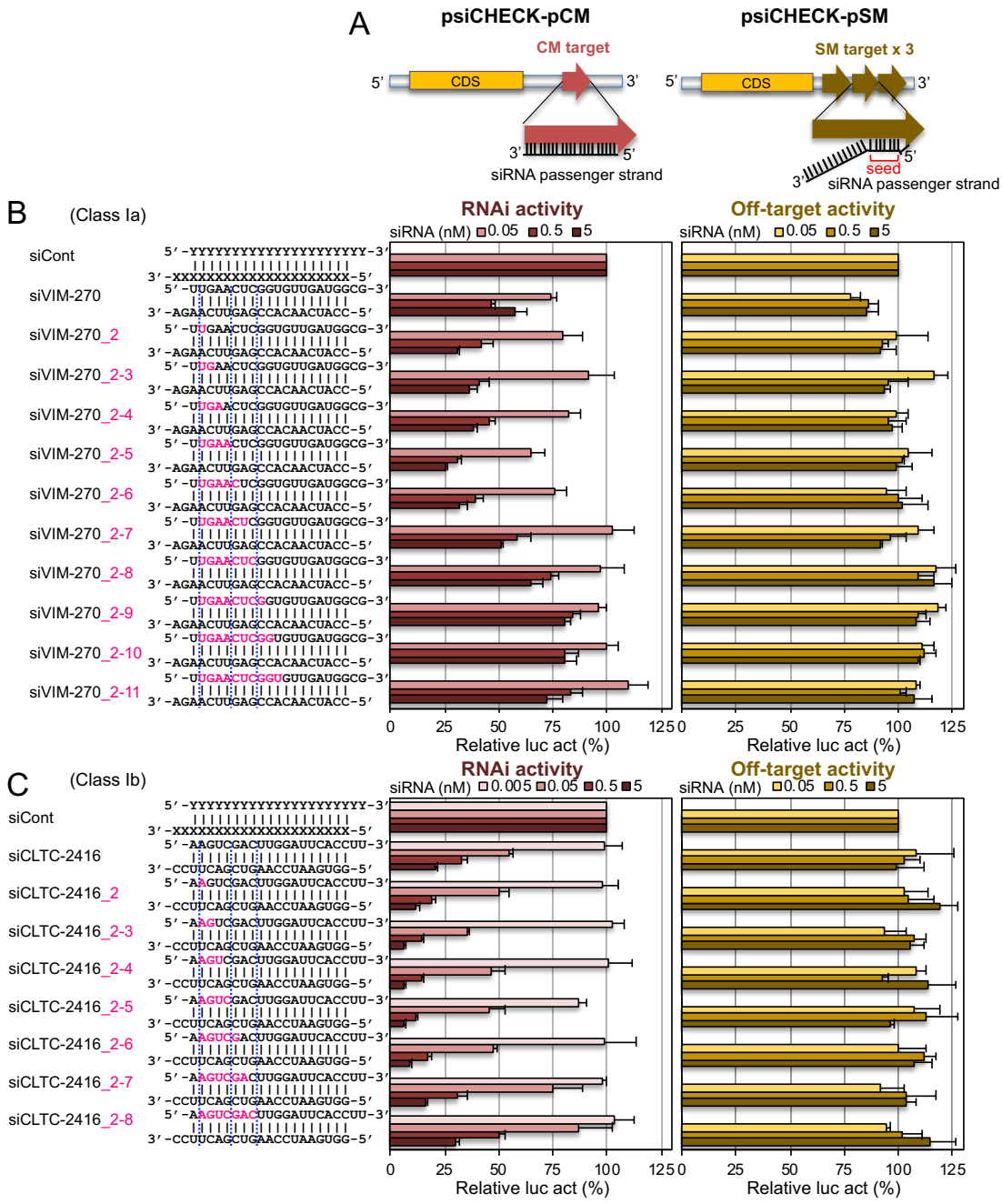

Figure 5. Effects of 2′-OMe modifications of the siRNA guide strand on RNAi and off-target activities of the passenger strand.

(**A**) Schematic presentation of RNAi (left) and off-target (right) reporter assays of the passenger strand. The psiCHECK-1 plasmids containing complete-matched (CM) or seed-matched (SM) sequences of the siRNA passenger strand in the 3′UTR of the *Renilla luciferase* gene were used for RNAi and off-

target activity assays, respectively. The RNAi activities (left bar graphs) and off-target activities (right bar graphs) of (**B**) siVIM-270 and its modified siRNAs and (**C**) siCLTC-2416 and its modified siRNAs. Each upper sequence indicates the sequence of the guide strand from 5′ to 3′; the lower sequence indicates the passenger strand sequence from 3′ to 5′. Pink indicates positions or nucleotides modified with 2′-OMe. siRNA against GFP was used as control siRNA (siCont). Each reporter assay was performed at the indicated concentration. The horizontal bars indicate relative luciferase activity (Relative luc act). Results are presented as the mean and standard deviation of three independent experiments.

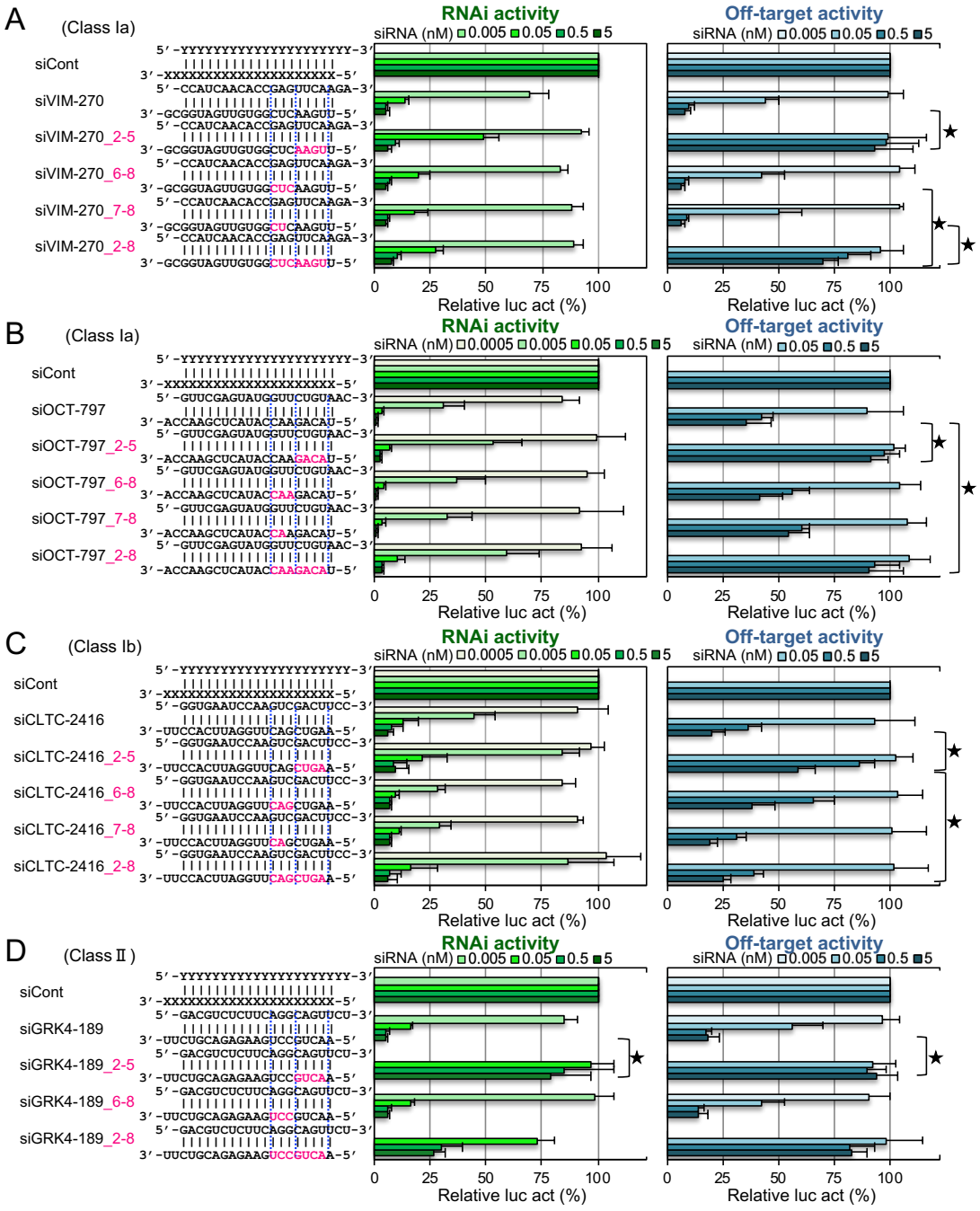
A
(Class Ia)
siCont
siVIM-270
siVIM-270_2-5
siVIM-270_6-8
siVIM-270_7-8
siVIM-270_2-8
RNAi activity
Off-target activity
siRNA (nM) 0.005 0.05 0.5 5
Relative luc act (%)
B
(Class Ia)
siCont
siOCT-797
siOCT-797_2-5
siOCT-797_6-8
siOCT-797_7-8
siOCT-797_2-8
RNAi activity
Off-target activity
siRNA (nM) 0.0005 0.005 0.05 0.5 5
siRNA (nM) 0.05 0.5 5
Relative luc act (%)
C
(Class Ib)
siCont
siCLTC-2416
siCLTC-2416_2-5
siCLTC-2416_6-8
siCLTC-2416_7-8
siCLTC-2416_2-8
RNAi activity
Off-target activity
siRNA (nM) 0.0005 0.005 0.05 0.5 5
siRNA (nM) 0.05 0.5 5
Relative luc act (%)
D
(Class Ⅱ)
siCont
siGRK4-189
siGRK4-189_2-5
siGRK4-189_6-8
siGRK4-189_2-8
RNAi activity
Off-target activity
siRNA (nM) 0.005 0.05 0.5 5
Relative luc act (%)

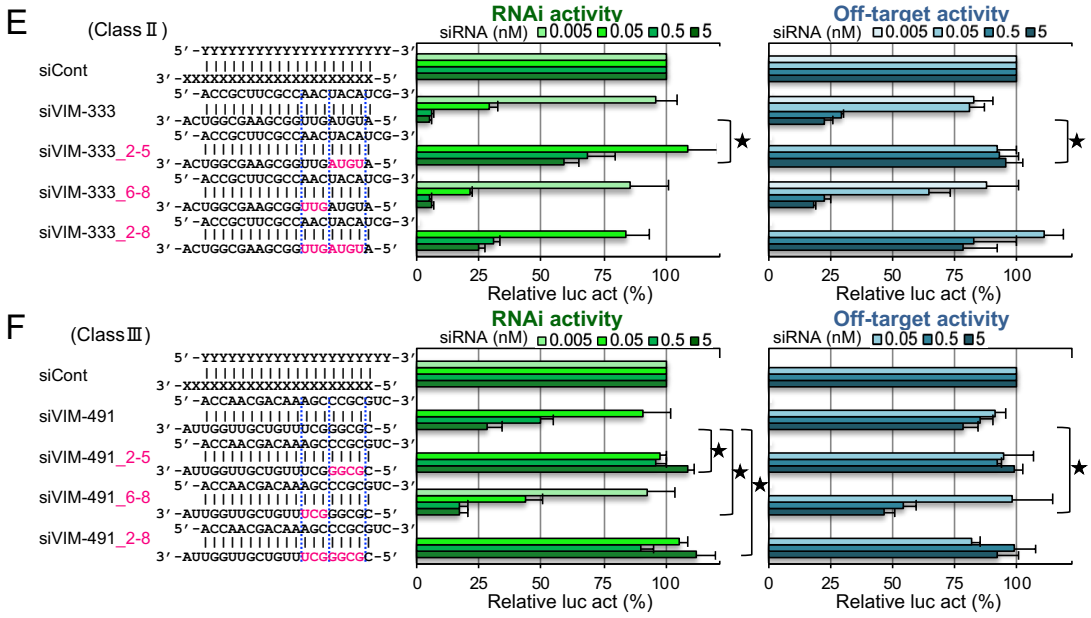

Figure 6. Effects of 2′-OMe modifications at positions 2–5, 6–8 (7–8), or both on RNAi and off-target activities.

RNAi (left bar graphs) and off-target activities (right bar graphs) of (**A**) siVIM-270, (**B**) siOCT-797, (**C**) siCLTC-2416, (**D**) siVIM-333, (**E**) siGRK4-189, and (**F**) siVIM-491 and their modified siRNAs. Each upper sequence indicates the sequence of the passenger strand from 5′ to 3′; the lower sequence indicates the guide strand sequence from 3′ to 5′. Pink indicates positions or nucleotides modified with 2′-OMe. siRNA against GFP was used as control siRNA (siCont). Each reporter assay was performed at a concentration of 0.005, 0.05, 0.5, or 5 nM siRNA. However, reporter assays for the RNAi activity of siOCT-797 and siCLTC-2416 were also performed with 0.0005 nM siRNA, and off-target activity reporter assays for siOCT-797, siCLTC-2416, and siVIM-491 with 0.005 nM siRNA were not performed. The horizontal bars indicate relative luciferase activity (Relative luc act). Results are presented as the mean and standard deviation of three independent experiments. Each *p*-value in RNAi or off-target activity between 2′-OMe-modified siRNA and unmodified siRNA at the concentration of 5 nM was determined by Student's *t*-test (**p* < 0.05). The statistical result indicating no significance compared to the unmodified siRNA at 5 nM concentration was not shown.

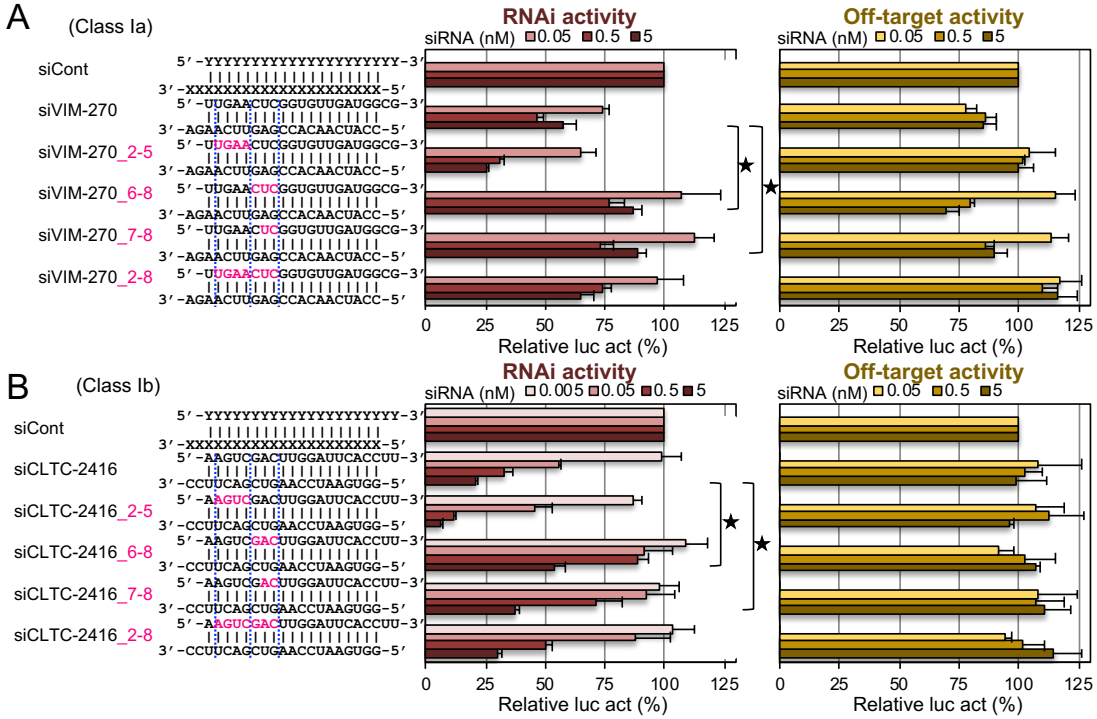

Figure 7. Effects of 2′-OMe modifications at positions 2–5, 6–8 (7–8), or both in the guide strand on RNAi and off-target activities of the passenger strand.

RNAi (left bar graphs) and off-target activities (right bar graphs) by passenger strand of (**A**) siVIM-270 and its modified siRNAs and (**B**) siCLTC-2416 and its modified siRNAs. Each upper sequence indicates the sequence of the guide strand from 5′ to 3′; the lower sequence indicates the passenger strand sequence from 3′ to 5′. Pink indicates positions or nucleotides modified with 2′-OMe. siRNA against GFP was used as control siRNA (siCont). Each reporter assay was performed at the indicated concentration. The horizontal bars indicate relative luciferase activity (Relative luc act). Results are presented as the mean and standard deviation of three independent experiments. Each *p*-value in RNAi or off-target activity between 2′-OMe-modified siRNA and unmodified siRNA at the concentration of 5 nM was determined by Student's *t*-test (*$p < 0.05$). The statistical result indicating no significance compared to the unmodified siRNA at 5 nM concentration was not shown.

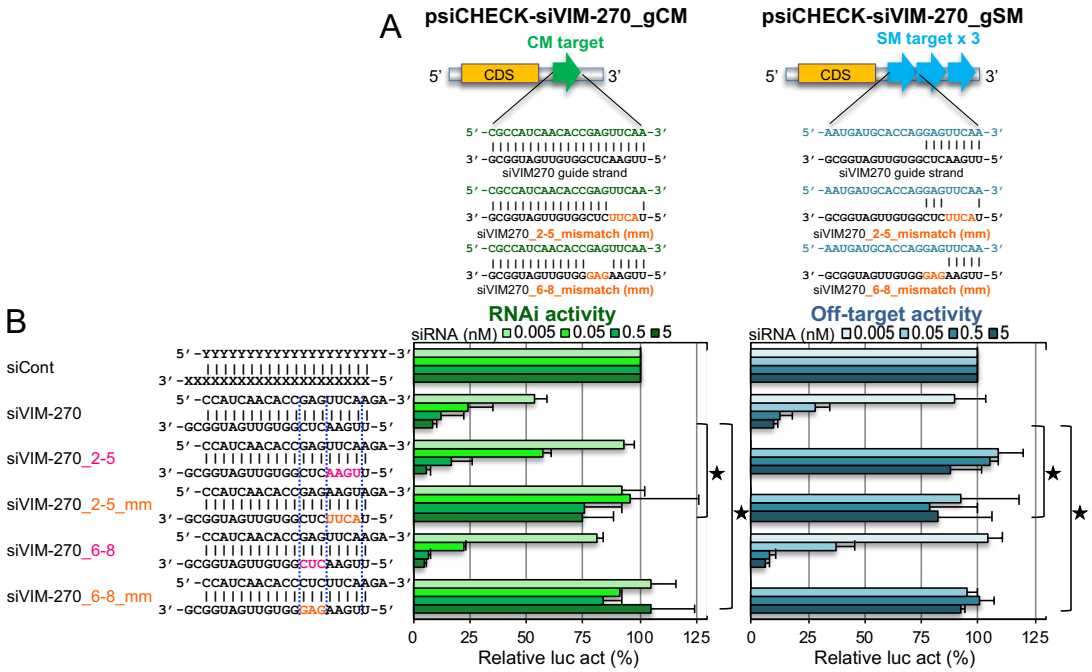

Figure 8. Effects of mismatches between siRNA guide strand and target mRNA on RNAi and off-target activities.

(**A**) Schematic presentation of RNAi (left) and off-target (right) reporter assays by guide strand of the siVIM270 and its modified siRNAs. The psiCHECK-1 plasmids containing complete-matched (CM) and seed-matched (SM) sequences with the guide strands of unmodified or modified siRNAs in the 3′UTR of *Renilla luciferase* gene were used for RNAi and off-target activity assays, respectively. (**B**) RNAi (left graph) and off-target activities (right graph) of the siVIM270 guide strands with or without mismatched nucleotides at positions 2–5 or 6–8 and its modified siRNAs. Each upper sequence indicates the sequence of the passenger strand from 5′ to 3′; the lower sequence indicates the guide strand sequence from 3′ to 5′. Pink indicates positions or nucleotides modified with 2′-OMe. Orange indicates positions or nucleotides mismatched with target or off-target mRNAs. siRNA against GFP was used as control siRNA (siCont). Each reporter assay was performed at the indicated concentration. The horizontal bars indicate relative luciferase activity (Relative luc act). Results are presented as the mean and standard deviation of three independent experiments. Each *p*-value in RNAi or off-target activity between 2′-OMe-modified siRNA and unmodified siRNA at the concentration of 5 nM was determined by Student's *t*-test (*$p < 0.05$). The statistical result indicating no significance compared to the unmodified siRNA at 5 nM concentration was not shown.

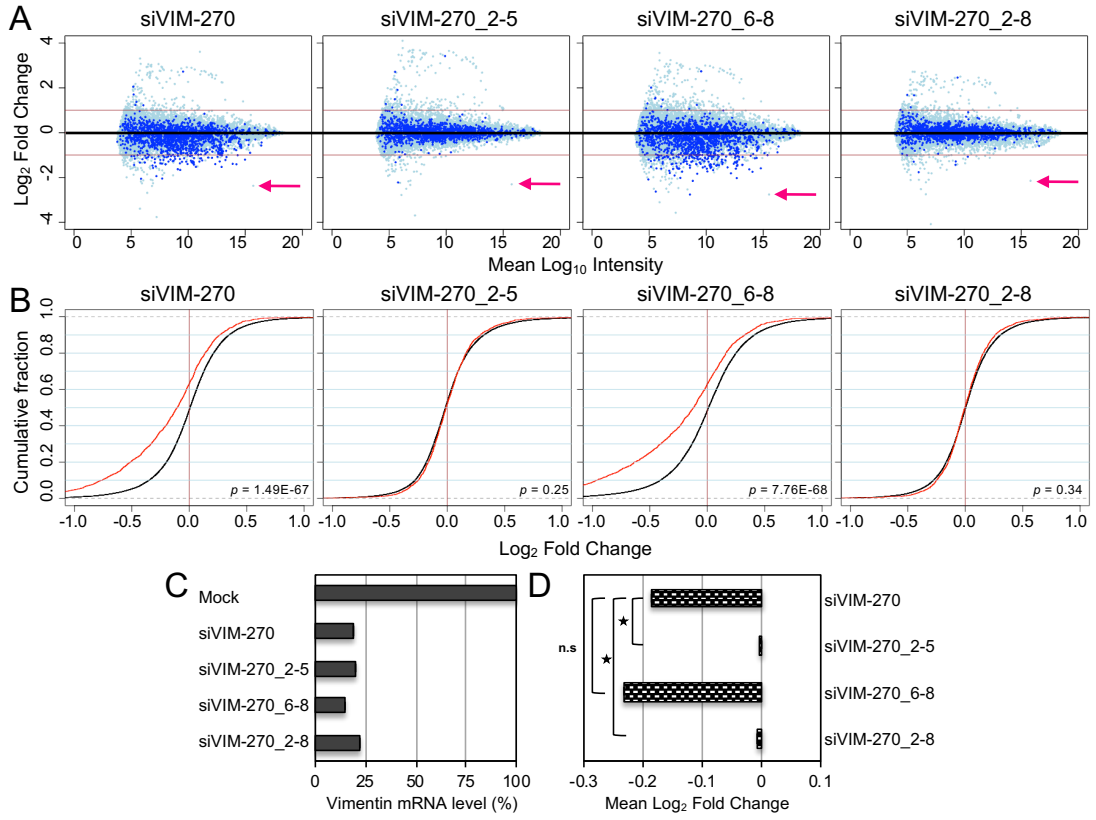

Figure 9. Genome-wide effects of 2′-OMe-modified siRNA on the expression of endogenous target and off-target genes.

Microarray analysis of the expression levels of the target *vimentin* gene and SM off-target genes. (A) MA plots. The vertical bars indicate $\log_2$ fold-changes of signal intensities between each siVIM-270 or its modified siRNA transfection and mock transfection (M value), and the horizontal bars indicate the averaged log 10 signal intensities of mock and each siRNA transfection (A value). The dark blue dots indicate the transcripts with SM sequences, and the light blue dots indicate the other transcripts. The pink arrowhead indicates *vimentin*. (B) Cumulative distributions. The horizontal bars indicate the M values of (A), and the vertical bars indicate the cumulative fractions of transcripts. The red lines indicate the cumulative curves of SM transcripts, and the black lines indicate the cumulative curves of the other non-SM transcripts. The downregulation of SM transcripts is shown by the fold-changes in the expression of SM transcripts compared to that of the other non-SM transcripts. Each *p*-value was determined by Wilcoxon rank sum test. (C) Expression levels of the target *vimentin* gene by the transfection of unmodified siVIM-270 or 2′-OMe-modified siVIM-270s. The horizontal bar indicates signal intensity of *vimentin* gene relative to mock sample. (D) Seed-dependent off-target effects of

unmodified siVIM-270 or 2′-OMe-modified siVIM-270s. The horizontal bar indicates the mean $\log_2$ fold-change of off-target transcripts in the cells transfected with unmodified siVIM-270 or 2′-OMe-modified siVIM-270s. Each *p*-value was determined by Wilcoxon rank sum test (* $p < 0.01$).

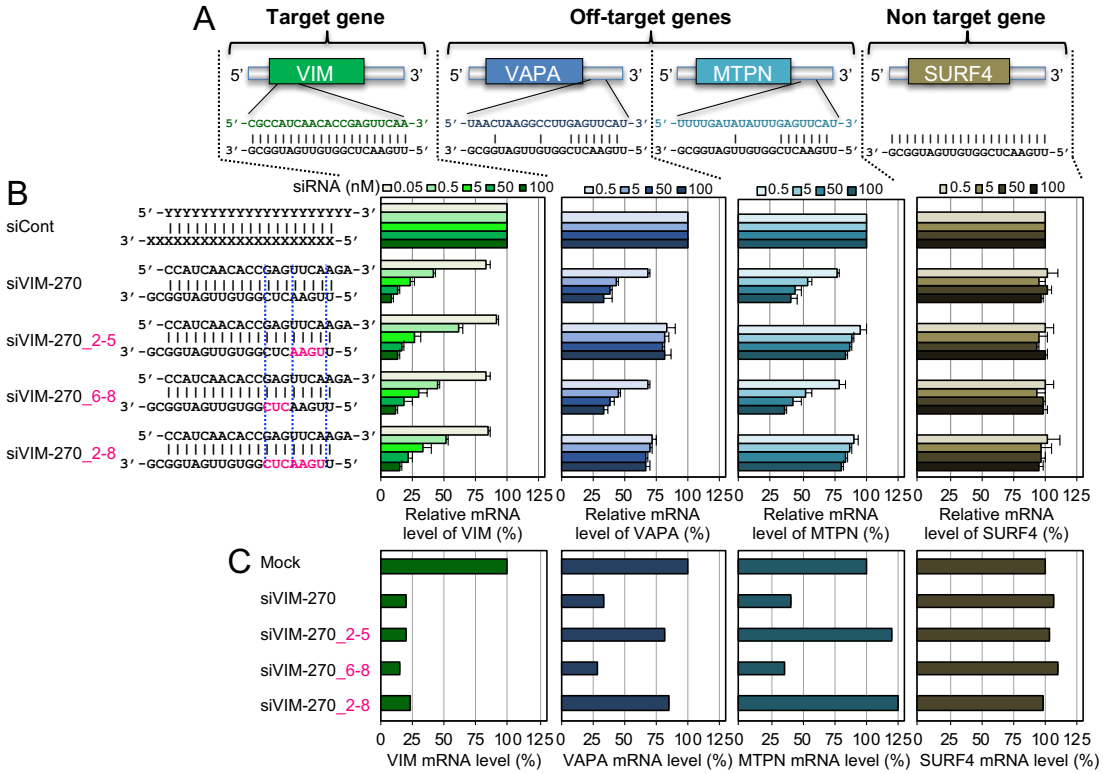

Figure 10. Effects of 2′-OMe-modified siRNA guide strand on the expression of endogenous genes.

RNAi and off-target effects of siVIM-270 against endogenous genes were examined. (**A**) The target gene of siVIM-270 is *VIM*, *VAPA* and *MTPN* are off-target genes, and *SURF4* is a non-target gene. (**B**) The expression levels of these genes were determined using qRT-PCR. Pink indicates positions or nucleotides modified with 2′-OMe. siRNA against GFP was used as control siRNA (siCont). Each qRT-PCR assay was performed at a concentration of 0.05, 0.5, 5, 50, or 100 nM siVIM-270. The horizontal bars indicate relative mRNA level of each gene. Results are presented as the mean and standard deviation of three independent experiments. (**C**) Expression profiles of *VIM*, *VAPA*, *MTPN*, and *SURF4* genes in Microarray analysis (Figure 9). Expression levels of each gene by the transfection of unmodified or 2′-OMe-modified siVIM-270s were shown. The horizontal bars indicate signal intensity of each gene relative to mock sample.

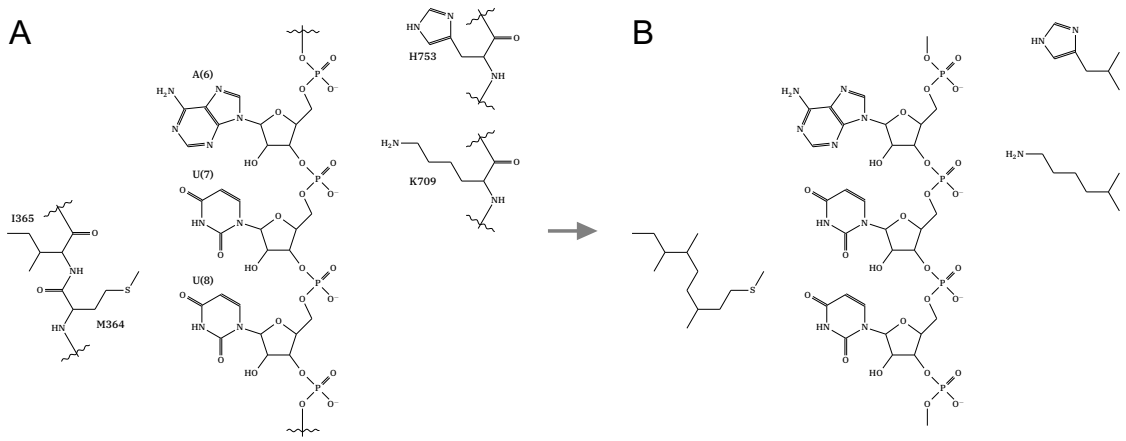

Figure 11. Computational prediction of the structure of modified RNA.

(**A**) Chemical structures of a part of guide RNA (6–8) with neighboring amino acid residues (M364, I365, K709, and H753) of the AGO protein considered in the calculations. (**B**) Chemical structures of a model of the guide RNA (5′-AUU-3′) with amino acid residues used in the geometry optimization. The terminal phosphates of the RNA were capped with methyl groups. The main chain parts of the amino acid residues were replaced with CH2/CH3 groups. This unmodified model was converted into 2′-OMe-modified systems.

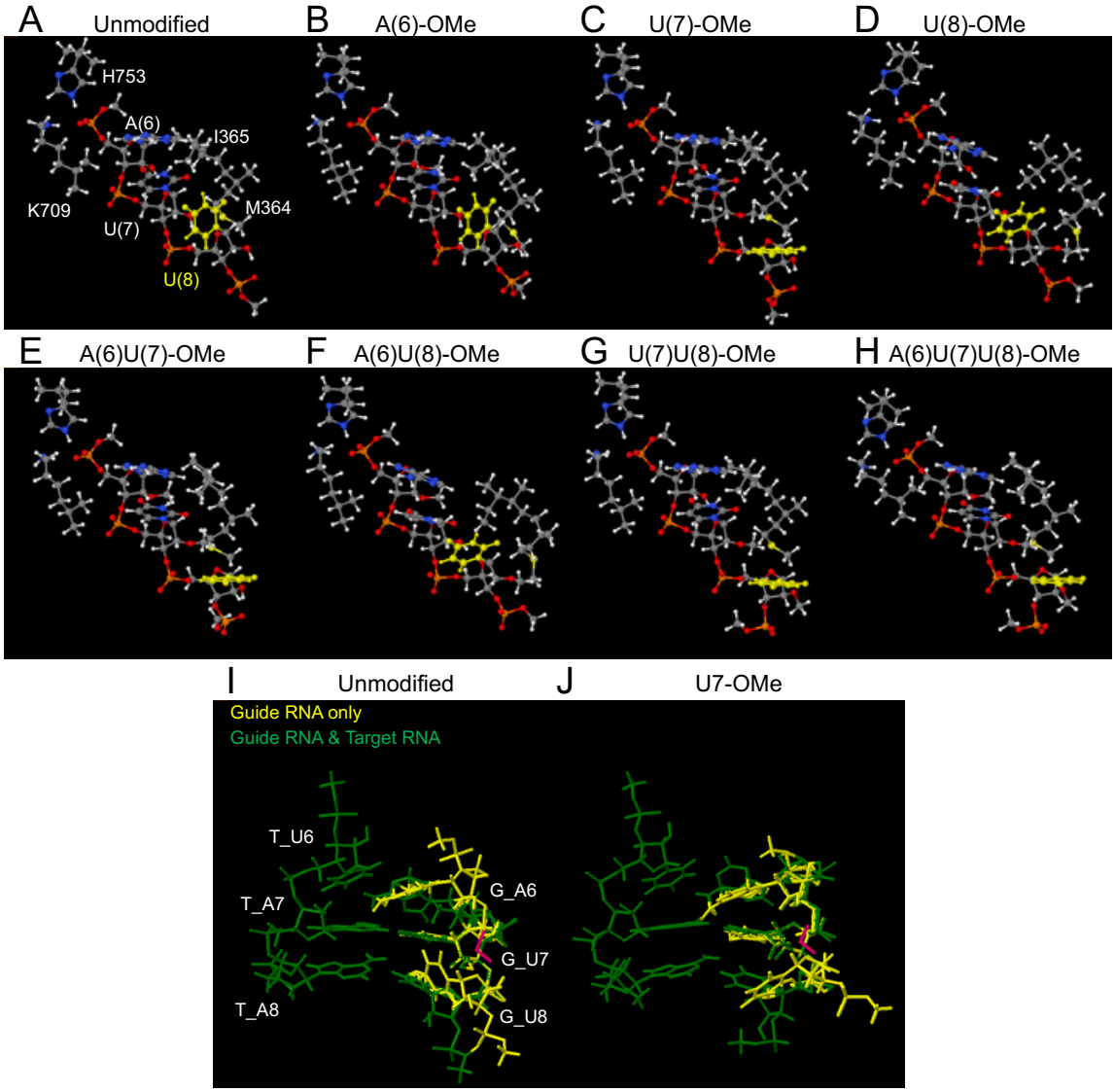

Figure 12. Computational simulation of RNA structures with 2′-OMe modifications in the nucleotides 6-8.

The 5′-AUU-3′ RNA structures of unmodified siRNA (A), siRNAs with 2′-OMe at nucleotide A(6) (B), U(7) (C), U(8) (D), A(6)U(7) (E), A(6)U(8) (F), U(7)U(8) (G), and A(6)U(7)U(8) (H) of the guide RNA with H753, K709, M364, and I365 residues. The geometry optimization was achieved using H753 and K709, by fixing their central carbon atoms (Cαs). The configuration of U(8) base was indicated by yellow. The overlapped structures of guide RNA alone (yellow) and guide-target RNA structure (green) with the His (H753), Lys (K709), Met (M364), and Ile(I365) residues. Unmodified (I) or U(7)-2′-OMe modified guide RNA (J) was used for simulation. The optimization was performed using Cαs of H753 and K709, and amino acids were not shown in the Figures for simplification.

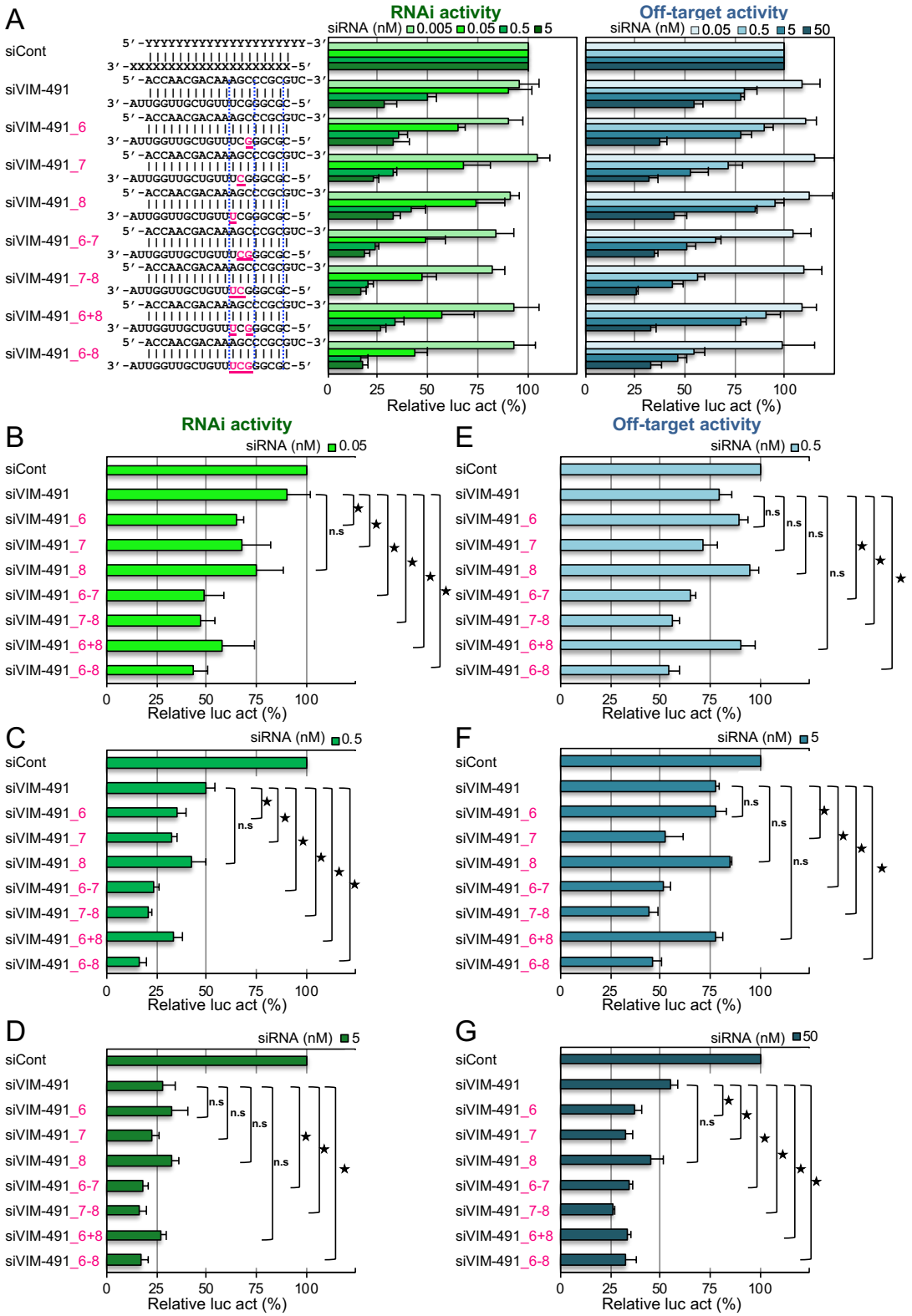
A
RNAi activity
siRNA (nM) 0.005 0.05 0.5 5
Off-target activity
siRNA (nM) 0.05 0.5 5 50
siCont
siVIM-491
siVIM-491_6
siVIM-491_7
siVIM-491_8
siVIM-491_6-7
siVIM-491_7-8
siVIM-491_6+8
siVIM-491_6-8
Relative luc act (%)
B
RNAi activity
siRNA (nM) 0.05
C
siRNA (nM) 0.5
D
siRNA (nM) 5
E
Off-target activity
siRNA (nM) 0.5
F
siRNA (nM) 5
G
siRNA (nM) 50
n.s
Relative luc act (%)

Figure 13. Effects of 2′-OMe modifications of siVIM-491 at positions 6–8 on RNAi and off-target activities.

(**A**) RNAi (left bar graphs) and off-target activities (right bar graphs) of siVIM-491 and its modified siRNAs. In order to obviously show result of Student's *t*-test, reporter assay results of (A) were separately shown per each concentration: (B) 0.05, (C) 0.5, or (D) 5 nM in RNAi activities and (E) 0.5, (F) 5, or (G) 50 nM in off-target activities. Each upper sequence indicates the sequence of the passenger strand from 5′ to 3′; the lower sequence indicates the guide strand sequence from 3′ to 5′. Pink indicates positions or nucleotides modified with 2′-OMe. siRNA against GFP was used as control siRNA (siCont). Each reporter assay was performed at the indicated concentration. The horizontal bars indicate relative luciferase activity (Relative luc act). Results are presented as the mean and standard deviation of three independent experiments. Each *p*-value was determined by Student's *t*-test (*$p < 0.05$). n.s., not significant.

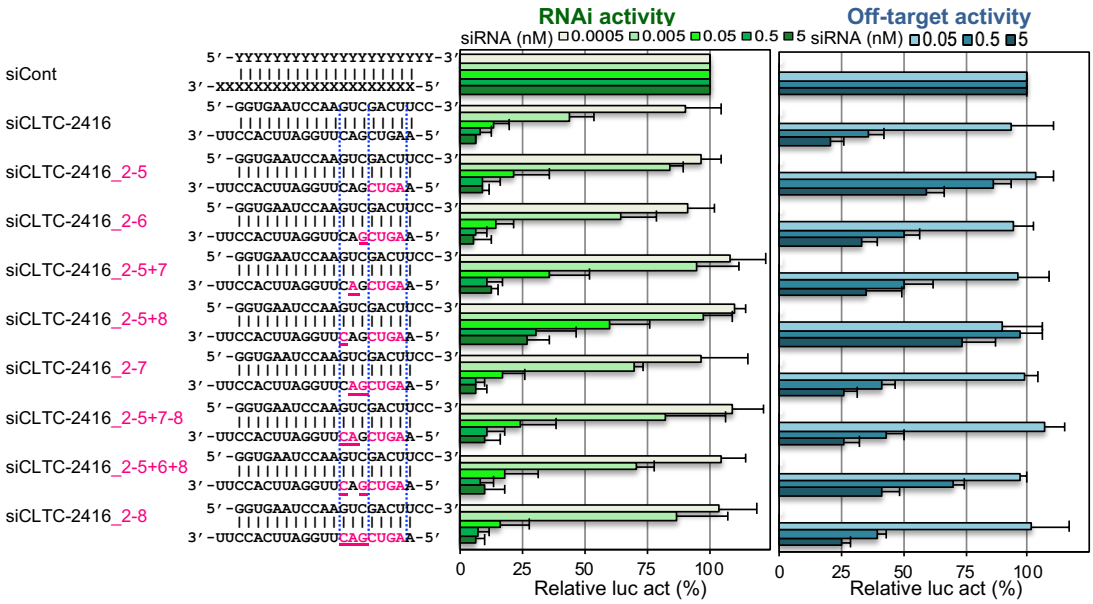

Figure 14. Effects of 2′-OMe modifications of siCLTC-2416 at positions 6–8 on RNAi and off-target activities.

RNAi (left bar graphs) and off-target activities (right bar graphs) of siCLTC-2416 and its modified siRNAs. Each upper sequence indicates the sequence of the passenger strand from 5′ to 3′; the lower sequence indicates the guide strand sequence from 3′ to 5′. Pink indicates positions or nucleotides modified with 2′-OMe. siRNA against GFP was used as control siRNA (siCont). Each reporter assay was performed at the indicated concentration. The horizontal bars indicate relative luciferase activity (Relative luc act). Results are presented as the mean and standard deviation of three independent experiments.

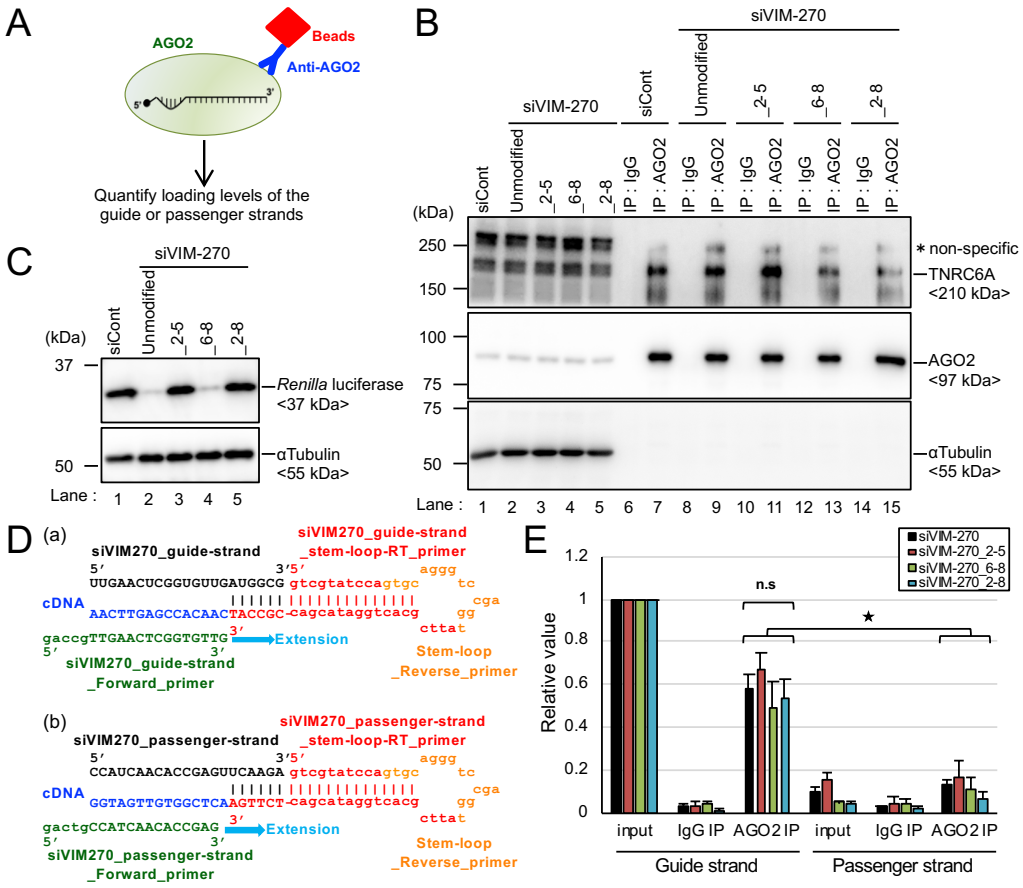

Figure 15. Effects of 2′-OMe modifications of the siRNA guide strand on AGO2 loading of the guide or passenger strand.

(**A**) Schematic presentation of RNA and protein immunoprecipitation experiments. After immunoprecipitation, AGO2 loading levels of guide and passenger strands were quantified. (**B**) Western blot of input samples (lanes 1–5), immunoprecipitates with IgG (IgG-IP; lanes 6, 8, 10, 12, and 14), and immunoprecipitates with anti-AGO2 antibody (AGO2-IP; lanes 7, 9, 11, 13, and 15). Unmodified siVIM-270 or modified siRNAs with 2′-OMe modification at positions 2–5, 6–8, or 2–8 were transfected into HeLa cells with a psiCHECK-VIM270-SM reporter construct and immunoprecipitated with anti-AGO2 antibody or anti-mouse IgG antibody as a negative control. Endogenous TNRC6A, AGO2, and α-tubulin were detected with specific antibodies. (**C**) Western blot of *Renilla* luciferase in input samples (lanes 1–5). α-Tubulin was detected as a control. (**D**) Schematic presentation of stem-loop RT-PCR specific for the (a) siVIM-270 guide strand and (b) passenger strand. Black indicates the sequences of the siVIM-270 guide and passenger strands. Red and orange indicate the sequences of stem-loop reverse-transcription primers specific for the siVIM-270 guide or

passenger strand. Blue indicates cDNA sequences generated by reverse transcription. Green indicates sequences of forward PCR primers specific for the siVIM-270 guide or passenger strand. Orange indicates sequences of reverse primers. Light blue indicates orientations of extension using forward primers. (**E**) Results of quantification of siVIM-270 guide or passenger strands in each fraction. The copy numbers were calculated via an absolute quantification method using standard curves of each synthesized siRNA and normalized to the copy numbers of the guide strands in each input fraction. siRNA against GFP was used as control siRNA (siCont). Results are presented as the mean and standard deviation of three independent experiments. Each *p*-value was determined by Student's *t*-test (*$p < 0.05$). n.s., not significant.

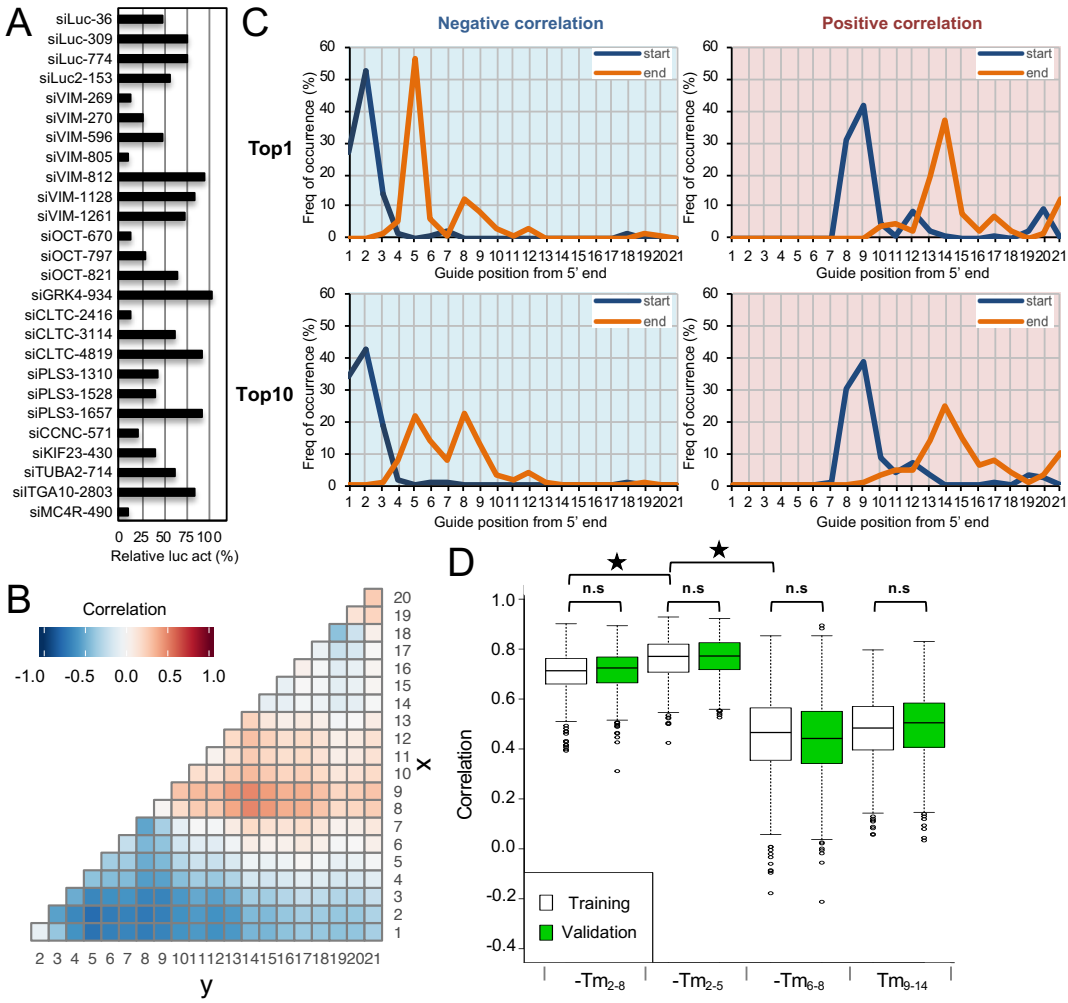

Figure 16. Random sampling analysis to find responsive regions for siRNA off-target effects. (A) Previously reported off-target effects of 26 wild-type siRNAs at 50 nM measured using luc reporter assay (Ui-Tei *et al*. 2008). (B) Heatmap indicates the correlations between Tm values of all possible regions in their siRNAs and relative luciferase activities. Blue indicates negative correlation; red, positive correlation. x = start position; y = end position. (C) Start and end positions of each responsive region significantly correlated with relative luciferase activities. Upper panels indicate top-ranked positions with the most negative (left) and positive (right) correlations; the lower panels indicate top 10 positions with the most negative (left) and positive (right) correlations. Sampling was repeated 1000 times for the calculation of each region. (D) Mean values of correlation coefficients between Tm values of positions 2–8, 2–5, 6–8, or 9–14 and relative luc activities were calculated using random sampling procedure. Left boxes in each region indicate training data using randomly selected 13 samples, and right boxes in each region indicate validation data using randomly selected 13 samples.

The horizontal lines in the boxes indicate middle values. The correlation coefficients at positions 2–8, 2–5, 6–8, or 9–14 in the training data were as follows: r = 0.71, 0.76, 0.46, or 0.48. The correlation coefficients at positions 2–8, 2–5, 6–8, or 9–14 in the validation data were as follows: r = 0.71, 0.77, 0.44, 0.49. Each *p*-value was determined by Student's *t*-test (*$p < 0.01$). n.s., not significant.

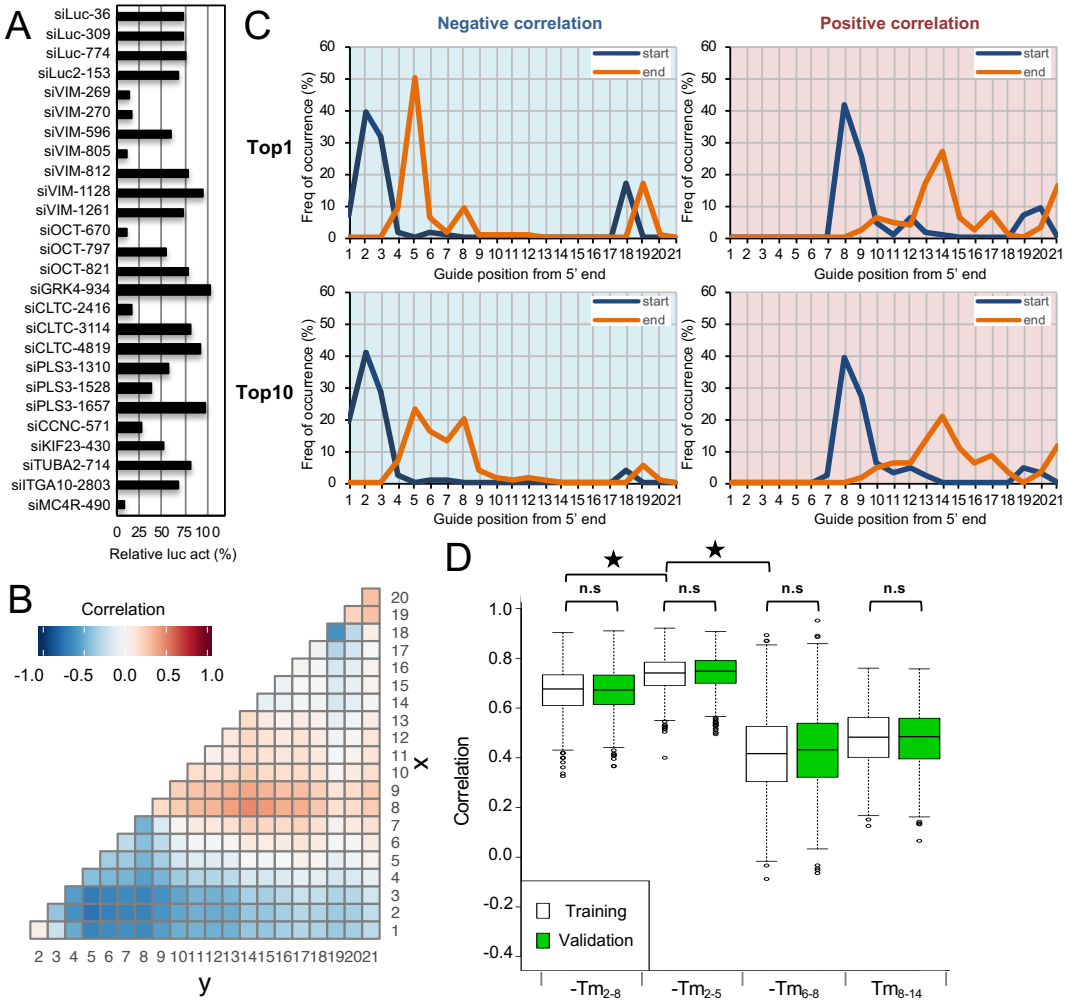

Figure 17. Random sampling analysis to find responsive regions for siRNA off-target effects. (A) Previously reported off-target effects of 26 wild-type siRNAs at 5 nM measured using luc reporter assay (Ui-Tei *et al*. 2008). (B) Heatmap indicates the correlations between Tm values of all possible regions in their siRNAs and relative luciferase activities. Blue indicates negative correlation; red, positive correlation. x = start position; y = end position. (C) Start and end positions of each responsive region significantly correlated with relative luciferase activities. Upper panels indicate top-ranked positions with the most negative (left) and positive (right) correlations; the lower panels indicate top 10 positions with the most negative (left) and positive (right) correlations. Sampling was repeated 1000 times for the calculation of each region. (D) Mean values of correlation coefficients between Tm values of positions 2–8, 2–5, 6–8, or 8–14 and relative luc activities were calculated using random sampling procedure. Left boxes in each region indicate training data using randomly selected 13 samples, and right boxes in each region indicate validation data using randomly selected 13 samples.

The horizontal lines in the boxes indicate middle values. The correlation coefficients at positions 2–8, 2–5, 6–8, or 8–14 in the training data were as follows: r = 0.67, 0.73, 0.42, or 0.48. The correlation coefficients at positions 2–8, 2–5, 6–8, or 8–14 in the validation data were as follows: r = 0.67, 0.74, 0.43, 0.47. Each *p*-value was determined by Student's *t*-test (*$p < 0.01$). n.s., not significant.

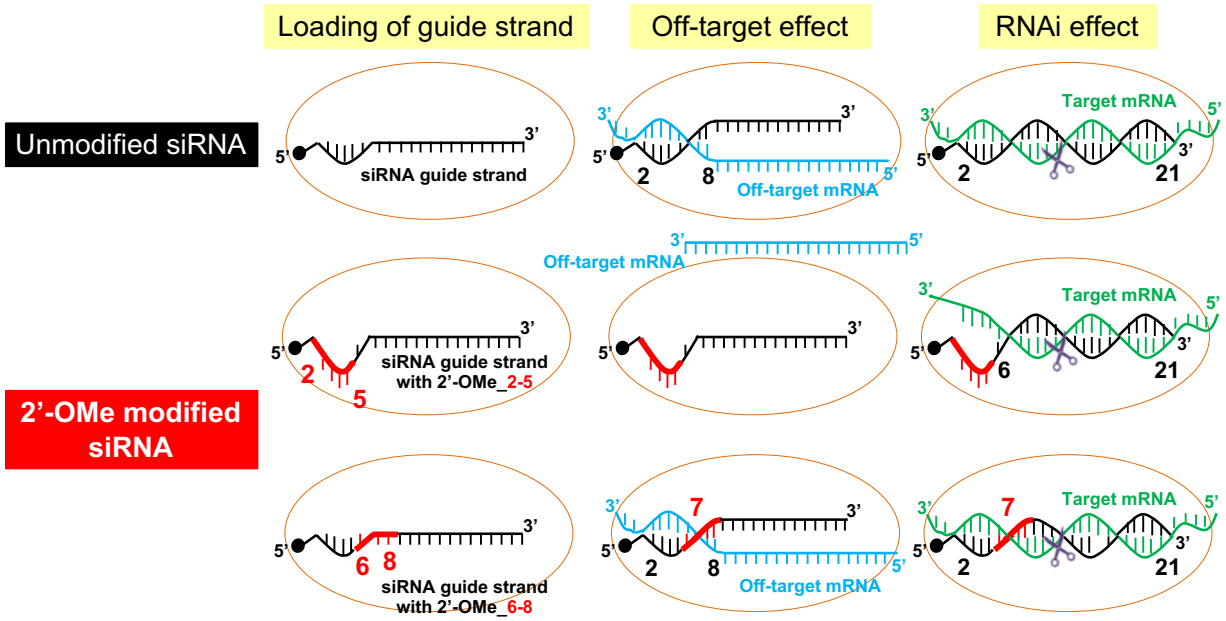

Figure 18. Possible machinery of siRNA guide strand with 2′-OMe at positions 2–5 or 6–8.

In the case of unmodified siRNA, siRNA guide strand is stably loaded onto AGO protein and induces off-target effect for off-target mRNAs with seed complementarities and RNAi effect for a target mRNA with perfect sequence complementarity.

The siRNA guide strand with 2′-OMe at positions 2–5 is also successfully loaded on AGO. However, the base-pairing at positions 2–5 between guide RNA and off-target mRNA induces steric hindrance which shows different effect compared to mismatch, resulting in prevention of off-target effect. Also, it is considered that RNAi is induced via base-pairing between siRNA nucleotides at least positions 6–21 without 2–5 and target mRNA.

On the other hand, the siRNA guide strand with 2′-OMe at positions 6–8 is also successfully loaded on AGO. The base-pairing at positions 6–8 between guide RNA and off-target mRNA doesn't induce steric hindrance. Therefore, RNAi and off-target effects are induced with the same mechanism as unmodified siRNA. Furthermore, 2′-OMe modifications in nucleotides 7 enhance silencing effects for both target and off-target mRNAs

Table 1. SiRNA sequences used for reporter assay or RT-PCRs.

siRNA	Passenger strand (5'→3')	Guide strand (5'→3')
siCont	GCCACAACGUCUAUAUCAUGG	AUGAUAUAGACGUUGUGGCUG
siVIM-270	CCAUCAACACCGAGUUCAAGA	UUGAACUCGGUGUUGAUGGCG
siVIM-270_2	CCAUCAACACCGAGUUCAAGA	UUGAACUCGGUGUUGAUGGCG
siVIM-270_2-3	CCAUCAACACCGAGUUCAAGA	UUGAACUCGGUGUUGAUGGCG
siVIM-270_2-4	CCAUCAACACCGAGUUCAAGA	UUGAACUCGGUGUUGAUGGCG
siVIM-270_2-5	CCAUCAACACCGAGUUCAAGA	UUGAACUCGGUGUUGAUGGCG
siVIM-270_2-6	CCAUCAACACCGAGUUCAAGA	UUGAACUCGGUGUUGAUGGCG
siVIM-270_2-7	CCAUCAACACCGAGUUCAAGA	UUGAACUCGGUGUUGAUGGCG
siVIM-270_2-8	CCAUCAACACCGAGUUCAAGA	UUGAACUCGGUGUUGAUGGCG
siVIM-270_2-9	CCAUCAACACCGAGUUCAAGA	UUGAACUCGGUGUUGAUGGCG
siVIM-270_2-10	CCAUCAACACCGAGUUCAAGA	UUGAACUCGGUGUUGAUGGCG
siVIM-270_2-11	CCAUCAACACCGAGUUCAAGA	UUGAACUCGGUGUUGAUGGCG
siVIM-270_6-8	CCAUCAACACCGAGUUCAAGA	UUGAACUCGGUGUUGAUGGCG
siVIM-270_7-8	CCAUCAACACCGAGUUCAAGA	UUGAACUCGGUGUUGAUGGCG
siVIM-270_2-5_mismatch	CCAUCAACACCGAGAAGUAGA	UACUUCUCGGUGUUGAUGGCG
siVIM-270_6-8_mismatch	CCAUCAACACCCUCUUCAAGA	UUGAAGAGGGUGUUGAUGGCG
siCLTC-2416	GGUGAAUCCAAGUCGACUUCC	AAGUCGACUUGGAUUCACCUU
siCLTC-2416_2	GGUGAAUCCAAGUCGACUUCC	AAGUCGACUUGGAUUCACCUU
siCLTC-2416_2-3	GGUGAAUCCAAGUCGACUUCC	AAGUCGACUUGGAUUCACCUU
siCLTC-2416_2-4	GGUGAAUCCAAGUCGACUUCC	AAGUCGACUUGGAUUCACCUU
siCLTC-2416_2-5	GGUGAAUCCAAGUCGACUUCC	AAGUCGACUUGGAUUCACCUU
siCLTC-2416_2-6	GGUGAAUCCAAGUCGACUUCC	AAGUCGACUUGGAUUCACCUU
siCLTC-2416_2-7	GGUGAAUCCAAGUCGACUUCC	AAGUCGACUUGGAUUCACCUU
siCLTC-2416_2-8	GGUGAAUCCAAGUCGACUUCC	AAGUCGACUUGGAUUCACCUU
siCLTC-2416_6-8	GGUGAAUCCAAGUCGACUUCC	AAGUCGACUUGGAUUCACCUU
siCLTC-2416_7-8	GGUGAAUCCAAGUCGACUUCC	AAGUCGACUUGGAUUCACCUU
siCLTC-2416_2-5+7	GGUGAAUCCAAGUCGACUUCC	AAGUCGACUUGGAUUCACCUU
siCLTC-2416_2-5+8	GGUGAAUCCAAGUCGACUUCC	AAGUCGACUUGGAUUCACCUU
siCLTC-2416_2-5+7-8	GGUGAAUCCAAGUCGACUUCC	AAGUCGACUUGGAUUCACCUU
siCLTC-2416_2-5+6+8	GGUGAAUCCAAGUCGACUUCC	AAGUCGACUUGGAUUCACCUU
siOCT-797	GUUCGAGUAUGGUUCUGUAAC	UACAGAACCAUACUCGAACCA
siOCT-797_2-5	GUUCGAGUAUGGUUCUGUAAC	UACAGAACCAUACUCGAACCA

siOCT-797_6-8	GUUCGAGUAUGGUUCUGUAAC	UACAGAACCAUACUCGAACCA
siOCT-797_7-8	GUUCGAGUAUGGUUCUGUAAC	UACAGAACCAUACUCGAACCA
siOCT-797_2-8	GUUCGAGUAUGGUUCUGUAAC	UACAGAACCAUACUCGAACCA
siVIM-333	ACCGCUUCGCCAACUACAUCG	AUGUAGUUGGCGAAGCGGUCA
siVIM-333_2-5	ACCGCUUCGCCAACUACAUCG	AUGUAGUUGGCGAAGCGGUCA
siVIM-333_6-8	ACCGCUUCGCCAACUACAUCG	AUGUAGUUGGCGAAGCGGUCA
siVIM-333_2-8	ACCGCUUCGCCAACUACAUCG	AUGUAGUUGGCGAAGCGGUCA
siGRK4-189	GACGUCUCUUCAGGCAGUUCU	AACUGCCUGAAGAGACGUCUU
siGRK4-189_2-5	GACGUCUCUUCAGGCAGUUCU	AACUGCCUGAAGAGACGUCUU
siGRK4-189_6-8	GACGUCUCUUCAGGCAGUUCU	AACUGCCUGAAGAGACGUCUU
siGRK4-189_2-8	GACGUCUCUUCAGGCAGUUCU	AACUGCCUGAAGAGACGUCUU
siVIM-491	ACCAACGACAAAGCCCGCGUC	CGCGGGCUUUGUCGUUGGUUA
siVIM-491_2-5	ACCAACGACAAAGCCCGCAUC	CGCGGGCUUUGUCGUUGGCUA
siVIM-491_6-8	ACCAACGACAAAGCCCGCAUC	CGCGGGCUUUGUCGUUGGCUA
siVIM-491_2-8	ACCAACGACAAAGCCCGCAUC	CGCGGGCUUUGUCGUUGGCUA
siVIM-491_6	ACCAACGACAAAGCCCGCGUC	CGCGGGCUUUGUCGUUGGUUA
siVIM-491_7	ACCAACGACAAAGCCCGCGUC	CGCGGGCUUUGUCGUUGGUUA
siVIM-491_8	ACCAACGACAAAGCCCGCGUC	CGCGGGCUUUGUCGUUGGUUA
siVIM-491_6-7	ACCAACGACAAAGCCCGCGUC	CGCGGGCUUUGUCGUUGGUUA
siVIM-491_7-8	ACCAACGACAAAGCCCGCGUC	CGCGGGCUUUGUCGUUGGUUA
siVIM-491_6+8	ACCAACGACAAAGCCCGCGUC	CGCGGGCUUUGUCGUUGGUUA

5 年以内に雑誌などで刊行予定のため、非公開。

5 年以内に雑誌などで刊行予定のため、非公開。

siCont = control siRNA

underline = 2'-OMe modification

Table 2. Inserted oligonucleotide sequences in psiCHECK-CM-reporters.

Oligonucleotide name	Sequence (5'→3')
siVIM-270_gCM_s	tcgagCGCCATCAACACCGAGTTCAAGAg
siVIM-270_gCM_as	aattcTCTTGAACTCGGTGTTGATGGCGc
siCLTC-2416_gCM_s	tcgagAAGGTGAATCCAAGTCGACTTCCg
siCLTC-2416_gCM_as	aattcGGAAGTCGACTTGGATTCACCTTc
siOCT-797_gCM_s	tcgagTGGTTCGAGTATGGTTCTGTAACg
siOCT-797_gCM_as	aattcGTTACAGAACCATACTCGAACCAc
siVIM-333_gCM_s	tcgagTGACCGCTTCGCCAACTACATCGg
siVIM-333_gCM_as	aattcCGATGTAGTTGGCGAAGCGGTCAc
siGRK4-189_gCM_s	tcgagAAGACGTCTCTTCAGGCAGTTCTg
siGRK4-189_gCM_as	aattcAGAACTGCCTGAAGAGACGTCTTc
siVIM-491_gCM_s	tcgagTAACCAACGACAAAGCCCGCGTCg
siVIM-491_gCM_as	aattcGACGCGGGCTTTGTCGTTGGTTAc
siVIM-270_pCM_s	tcgagTCTTGAACTCGGTGTTGATGGAAg
siVIM-270_pCM_as	aattcTTCCATCAACACCGAGTTCAAGAc
siCLTC-2416_pCM_s	tcgagGGAAGTCGACTTGGATTCACCTTg
siCLTC-2416_pCM_as	aattcAAGGTGAATCCAAGTCGACTTCCc

5 年以内に雑誌などで刊行予定のため、非公開。

5 年以内に雑誌などで刊行予定のため、非公開。

_s =sense strand; _as =antisense strand

lower case =sequence of restriction enzyme site

underline = single-nucleotide mutation site

Table 3. Inserted oligonucleotide sequences in psiCHECK-SM-reporters.

Oligonucleotide name	Sequence (5'→3')
siVIM-270_gSM_s	tcgagAATGATGCACCAGGAGTTCAAGAAATGATGCACCAGGAGTTCAAGAAATGATGCACCAGGAGTTCAAGAg
siVIM-270_gSM_as	aattcTCTTGAACTCCTGGTGCATCATTTCTTGAACTCCTGGTGCATCATTTCTTGAACTCCTGGTGCATCATTc
siCLTC-2416_gSM_s	tcgagCCGAGCAAGTGGTGTCGACTTCCCCGAGCAAGTGGTGTCGACTTCCCCGAGCAAGTGGTGTCGACTTCCg
siCLTC-2416_gSM_as	aattcGGAAGTCGACACCACTTGCTCGGGGAAGTCGACACCACTTGCTCGGGGAAGTCGACACCACTTGCTCGGc
siOCT-797_gSM_s	tcgagGCTGAAGCTAGTAGTTCTGTAACGCTGAAGCTAGTAGTTCTGTAACGCTGAAGCTAGTAGTTCTGTAACg
siOCT-797_gSM_as	aattcGTTACAGAACTACTAGCTTCAGCGTTACAGAACTACTAGCTTCAGCGTTACAGAACTACTAGCTTCAGCc
siVIM-333_gSM_s	tcgagACTGAACTTGCGGAACTACATGAACTGAACTTGCGGAACTACATGAACTGAACTTGCGGAACTACATGAg
siVIM-333_gSM_as	aattcTCATGTAGTTCCGCAAGTTCAGTTCATGTAGTTCCGCAAGTTCAGTTCATGTAGTTCCGCAAGTTCAGTc
siGRK4-189_gSM_s	tcgagAATTTTTGTAAGAAGGCAGTAACAATTTTTGTAAGAAGGCAGTAACAATTTTTGTAAGAAGGCAGTAACg
siGRK4-189_gSM_as	aattCGTTACTGCCTTCTTACAAAAATTGTTACTGCCTTCTTACAAAAATTGTTACTGCCTTCTTACAAAAATTc
siVIM-491_gSM_s	tcgagAATGATGCACGTTAGCCCGCGAGAATGATGCACGTTAGCCCGCGAGAATGATGCACGTTAGCCCGCGAGC
siVIM-491_gSM_as	aattGCTCGCGGGCTAACGTGCATCATTCTCGCGGGCTAACGTGCATCATTCTCGCGGGCTAACGTGCATCATTc
siVIM-270_pSM_s	tcgagCTATGCGACTTGAGTTGATGGCGCTATGCGACTTGAGTTGATGGCGCTATGCGACTTGAGTTGATGGCGg
siVIM-270_pSM_as	aattcCGCCATCAACTCAAGTCGCATAGCGCCATCAACTCAAGTCGCATAGCGCCATCAACTCAAGTCGCATAGc
siCLTC-2416_pSM_s	tcgagCCGATTCGCTGGTGATTCACCTTCCGATTCGCTGGTGATTCACCTTCCGATTCGCTGGTGATTCACCTTg
siCLTC-2416_pSM_as	aattcAAGGTGAATCACCAGCGAATCGGAAGGTGAATCACCAGCGAATCGGAAGGTGAATCACCAGCGAATCGGc

_s =sense strand; _a =antisense strand

underline = complementary sequence with seed region of the siRNA guide or passenger strand

lower case =sequence of restriction enzyme site

Table 4. IC_{50} of reporter assay using each unmodified or 2'-OMe modified siRNA (The results are shown in Figures 4, 6, and 12).

siRNA	siVIM-270		siOCT-797		siCLTC-2416		siGRK4-189		siVIM-333		siVIM-491	
	RNAi (pM)	OTE* (pM)	RNAi (pM)	OTE* (pM)	RNAi (pM)	OTE* (pM)	RNAi (pM)	OTE* (pM)	RNAi (pM)	OTE* (pM)	RNAi (pM)	OTE* (pM)
Unmodified	11	39	2	348	4	285	16	72	24	197	490	∞
_2	13	206	-	-	4	815	-	-	-	-	-	-
_2-3	14	234	-	-	7	873	-	-	-	-	-	-
_2-4	19	1,408	-	-	5	∞	-	-	-	-	-	-
_2-5	46	∞	6	∞	18	∞	∞	∞	∞	∞	∞	∞
_2-6	20	∞	-	-	10	501	-	-	-	-	-	-
_2-7	28	∞	-	-	12	353	-	-	-	-	-	-
_2-8	21	∞	8	∞	17	335	170	∞	219	∞	∞	∞
_2-9	27	∞	-	-	-	-	-	-	-	-	-	-
_2-10	39	∞	-	-	-	-	-	-	-	-	-	-
_2-11	26	∞	-	-	-	-	-	-	-	-	-	-
_6-8	17	38	3	1,333	2	1,819	20	34	18	111	37	1,748
_7-8	18	51	3	∞	2	265	-	-	-	-	41	1,612
_2-5+7	-	-	-	-	29	533	-	-	-	-	-	-
_2-5+8	-	-	-	-	107	∞	-	-	-	-	-	-
_2-5+7-8	-	-	-	-	18	382	-	-	-	-	-	-
_2-5+6+8	-	-	-	-	12	2,467	-	-	-	-	-	-
_6	-	-	-	-	-	-	-	-	-	-	158	24,365
_7	-	-	-	-	-	-	-	-	-	-	160	6,820
_8	-	-	-	-	-	-	-	-	-	-	287	37,372
_6-7	-	-	-	-	-	-	-	-	-	-	46	5,876
_6+8	-	-	-	-	-	-	-	-	-	-	103	21,129

*OTE = Off-target effect

Table 5. IC_{50} of reporter assay using each siRNA passenger strand (The results are shown in Figures 5 and 7).

siRNA	siVIM-270		siCLTC-2416	
	RNAi (pM)	OTE* (pM)	RNAi (pM)	OTE* (pM)
Unmodified	370	∞	85	∞
_2	302	∞	52	∞
_2-3	332	∞	31	∞
_2-4	371	∞	42	∞
_2-5	139	∞	39	∞
_2-6	253	∞	44	∞
_2-7	∞	∞	184	∞
_2-8	∞	∞	520	∞
_2-9	∞	∞	-	-
_2-10	∞	∞	-	-
_2-11	∞	∞	-	-
_6-8	∞	∞	∞	∞
_7-8	∞	∞	2110	∞

*OTE = Off-target effect

Table 6. Primer sequences used for qRT-PCRs.

Primer name	Sequence (5'→3')
Vimentin_F	CAGGACTCGGTGGACTTCTC
Vimentin_R	GTCGATGTAGTTGGCGAAGC
VAPA_F	TTCAGGAAATGCCAAGAGGT
VAPA_R	TCAACAACTGCCTCACAAGG
MTPN_F	TAGGTGCAGTGTGTGGAAGC
MTPN_R	TGCATGGAAGAAAACAGCAG
SURF4_F	GTCAAGGTTGGTTGGCTGAT
SURF4_R	GCCAGGAGAAACAGGAACAC
GAPDH_F	TGCACCACCAACTGCTTAG
GAPDH_R	AGAGGCAGGGATGATGTTC
siVIM270_guide-strand_stem-loop-RT	GTCGTATCCAGTGCAGGGTCCGAGGTATTCGCACTGGATACGACCGCCAT
siVIM270_passenger-strand_stem-loop-RT	GTCGTATCCAGTGCAGGGTCCGAGGTATTCGCACTGGATACGACTCTTGA
siVIM270_guide-strand_F	GACCGTTGAACTCGGTGTTG
siVIM270_passenger-strand_F	GACTGCCATCAACACCGAG
stem-loop_R	GTGCAGGGTCCGAGGT

5 年以内に雑誌などで刊行予定のため、非公開。

_F =forward primer; _R =reverse primer

Table 7. IC_{50} of qRT-PCR against endogenous gene of unmodified or 2'-OMe modified siVIM-270 (The results are shown in Figure 9).

siVIM-270	Target gene	Off-target genes		Non target gene
	VIM (pM)	VAPA (pM)	MTPN (pM)	SURF4 (pM)
Unmodified	312	2,730	13,386	∞
_2-5	1,050	∞	∞	∞
_6-8	368	3,116	8,488	∞
_2-8	573	∞	∞	∞

8 Appendix

Total energies and Cartesian coordinates of optimized structures of unmodified and 2′-OMe-modified 5′-AUU-3′ models (All the calculation is performed at the ωB97X-D/6-31G(d) level of theory).

Total energies of optimized structures of unmodified and 2′-OMe-modified 5′-AUU-3′ models

Model		Total energy (a.u.)
Unmodified	Figure 5A	-6604.204924
A(6)-OMe	Figure 5B	-6643.485055
U(7)-OMe	Figure 5C	-6643.479683
U(8)-OMe	Figure 5D	-6643.472217
A(6)U(7)-OMe	Figure 5E	-6682.765654
A(6)U(8)-OMe	Figure 5F	-6682.758450
U(7)U(8)-OMe	Figure 5G	-6682.768148
A(6)U(7)U(8)-OMe	Figure 5H	-6722.053169

Cartesian coordinates of optimized structures of unmodified and 2′-OMe modified 5′-AUU-3′ models

Unmodified	Figure 5A		
C57H94N12O26P4S			
Charge = − 4			
C	5.041777	6.455714	0.716336
C	4.765040	5.535238	-0.476435
C	3.364907	5.775548	-1.068710
C	5.019022	4.070353	-0.088583
C	4.885923	3.037549	-1.207771
S	5.883589	3.374585	-2.705970
C	7.536355	3.568549	-1.981004
C	2.213149	5.618648	-0.065523
C	0.872023	5.206760	-0.693400
C	0.452255	6.213664	-1.771590
H	-0.458026	5.901128	-2.290914
C	-0.237831	5.018026	0.369957
C	0.205257	4.162752	1.576083
C	-1.525485	4.445439	-0.239810
C	0.764046	2.784153	1.231089
C	-4.455722	-5.683010	-1.204147
C	-5.500145	-4.602915	-0.908947
C	-5.268666	-4.020350	0.487950
H	-5.955504	-3.200634	0.717395
C	-6.921759	-5.154951	-1.089484
C	-8.025054	-4.101165	-1.031068
C	-9.423226	-4.673751	-1.260565
C	-10.531180	-3.611232	-1.270649
N	-10.443214	-2.616537	-2.339249
C	-14.109796	4.030220	-2.513938
C	-13.114471	4.547204	-1.471630
C	-11.790737	4.945409	-2.126568
C	-12.898020	3.520862	-0.336342

C	-12.217171	2.254257	-0.756469
N	-12.885869	1.242359	-1.414883
C	-10.891958	1.920876	-0.609116
C	-11.959825	0.326111	-1.649932
N	-10.746791	0.692195	-1.185467
H	7.776426	2.724371	-1.331045
H	7.623009	4.503447	-1.417465
H	8.253208	3.588105	-2.806111
H	3.855055	2.973868	-1.572417
H	5.151933	2.049420	-0.827755
H	4.344201	3.754646	0.717223
H	6.020398	3.985355	0.350327
H	5.483714	5.787751	-1.268283
H	4.873839	7.509590	0.456177
H	6.077999	6.347856	1.057963
H	4.390681	6.211521	1.564081
H	2.073874	6.555941	0.495250
H	2.497012	4.865612	0.673829
H	1.234173	6.334079	-2.528863
H	0.265107	7.199582	-1.322051
H	1.027170	4.235944	-1.187182
H	-0.472724	6.022729	0.763323
H	-1.953895	5.106406	-1.000859
H	-2.287455	4.314785	0.537568
H	-1.355686	3.464644	-0.698944
H	1.663960	2.844219	0.607009
H	0.029667	2.182363	0.690999
H	1.029729	2.242808	2.142010
H	0.945364	4.720044	2.165459
H	-0.661609	4.018854	2.233613
H	3.220354	5.079259	-1.904551
H	3.339445	6.781035	-1.512350
H	-4.586227	-6.102260	-2.210983
H	-4.547399	-6.508126	-0.481227
H	-3.450620	-5.256512	-1.130054
H	-5.353998	-3.791082	-1.635658
H	-5.401538	-4.801268	1.252048
H	-4.240166	-3.650786	0.557158
H	-6.979434	-5.677271	-2.058800
H	-7.102403	-5.924773	-0.319656
H	-10.512396	-3.063352	-0.321092
H	-11.510230	-4.112184	-1.334387
H	-10.189793	-3.084880	-3.208007
H	-9.665456	-1.988249	-2.116699
H	-7.819521	-3.328781	-1.782727
H	-8.011134	-3.579525	-0.068186
H	-9.450843	-5.221602	-2.218783
H	-9.647506	-5.417747	-0.479962
H	-13.874469	3.281363	0.106921
H	-12.299723	4.000212	0.450387
H	-13.546902	5.449388	-1.008985
H	-14.252983	4.763439	-3.319195
H	-15.085745	3.828020	-2.055916
H	-13.753731	3.089125	-2.943822
H	-11.080025	5.327914	-1.384148
H	-11.943576	5.722884	-2.886083
H	-11.324723	4.078783	-2.606480

H	-12.098389	-0.632878	-2.133747
H	-9.856898	0.155000	-1.245847
H	-10.052751	2.418998	-0.146961
C	-7.052724	1.418575	1.489191
O	-7.721061	0.979957	0.317078
P	-7.615091	-0.620910	-0.055769
O	-8.405839	-0.721209	-1.344835
O	-7.894382	-1.468001	1.135685
O	-6.018885	-0.789419	-0.397100
C	-5.484424	-0.110943	-1.520299
C	-4.075136	0.365551	-1.235378
O	-4.089926	1.216412	-0.077508
C	-3.017427	-0.699932	-0.936899
O	-2.523809	-1.251807	-2.120751
C	-2.001000	0.126259	-0.130667
O	-1.223842	0.948129	-0.966695
C	-2.934389	1.022696	0.689870
N	-3.265335	0.437443	1.990303
C	-4.140845	-0.585484	2.297875
N	-4.034157	-1.013551	3.531607
C	-3.020792	-0.244178	4.063563
C	-2.354897	-0.267019	5.296049
N	-2.695074	-1.161087	6.283273
N	-1.357880	0.599659	5.521750
C	-1.024295	1.446549	4.532021
N	-1.540717	1.541933	3.314111
C	-2.532917	0.661757	3.125540
P	-1.666299	-2.683722	-2.038842
O	-1.621694	-3.207727	-3.428186
O	-2.103849	-3.431435	-0.818563
O	-0.162503	-2.114694	-1.604109
C	0.617614	-1.332674	-2.471897
C	1.799506	-0.791415	-1.681120
O	1.291287	-0.105202	-0.518338
C	2.793811	-1.826657	-1.142426
O	3.795247	-2.030447	-2.107491
C	3.278639	-1.168586	0.163442
O	4.284722	-0.217985	-0.076884
C	2.070776	-0.353014	0.628962
N	1.255617	-1.001819	1.672122
C	1.388075	-0.552125	2.974651
O	2.087264	0.398315	3.310711
N	0.639707	-1.247581	3.892389
C	-0.231464	-2.323578	3.681915
O	-0.789440	-2.845598	4.639170
C	-0.357909	-2.671626	2.285364
C	0.386681	-2.026840	1.363233
P	5.076963	-3.057816	-1.793382
O	5.522233	-3.605827	-3.101324
O	4.784976	-3.828434	-0.552223
O	6.197831	-1.886442	-1.312078
C	6.808111	-1.090615	-2.307362
C	7.747257	-0.104425	-1.632115
O	7.002997	0.645797	-0.668766
C	8.949684	-0.708517	-0.889292
O	10.086405	-0.607133	-1.717973
C	9.036180	0.142727	0.410001

O	9.814729	1.294543	0.240834
C	7.599726	0.637981	0.606704
N	6.785507	-0.111914	1.564501
C	5.792205	0.610128	2.235834
O	5.713377	1.826126	2.200919
N	4.938699	-0.157199	2.999017
C	4.876513	-1.553171	3.072909
O	4.011060	-2.097132	3.743924
C	5.892148	-2.219437	2.284411
C	6.749423	-1.488890	1.550598
P	11.536494	-1.133257	-1.134170
O	11.473242	-2.557115	-0.696398
O	12.088829	-0.067100	-0.211122
O	12.299907	-0.984794	-2.596630
C	13.692101	-0.826679	-2.528561
H	14.183149	-1.716017	-2.104074
H	13.966916	0.043391	-1.918631
H	14.059939	-0.685735	-3.552495
H	-0.200317	2.121643	4.751878
H	-4.852953	-0.948224	1.564788
H	5.853798	-3.294130	2.180613
H	7.453341	-1.967533	0.885689
H	-1.057822	-3.433529	1.970269
H	0.288403	-2.256107	0.305239
H	-6.110167	0.751601	-1.776221
H	-5.453086	-0.787614	-2.382314
H	-3.728268	0.944171	-2.102815
H	-3.435644	-1.483637	-0.294417
H	-1.376731	-0.497694	0.511910
H	-2.453547	1.978454	0.908467
H	-3.111599	-1.998211	5.891563
H	-1.893932	-1.388175	6.858637
H	0.021258	-0.501818	-2.871737
H	0.997523	-1.927120	-3.312058
H	2.360723	-0.075230	-2.292956
H	2.285782	-2.769384	-0.909452
H	3.583625	-1.921133	0.895661
H	5.040636	-0.673355	-0.495643
H	2.413581	0.584765	1.062791
H	0.717440	-0.911458	4.843234
H	6.044632	-0.531894	-2.865220
H	7.368138	-1.715853	-3.012020
H	8.134401	0.591118	-2.386946
H	8.770555	-1.763495	-0.648759
H	9.387880	-0.459828	1.260020
H	10.732702	0.968706	0.059980
H	7.617633	1.657906	0.985136
H	4.110834	0.326548	3.345321
H	-5.992171	1.588295	1.279050
H	-7.153808	0.682171	2.294254
H	-7.520488	2.359531	1.799481
H	-0.301735	0.652725	-0.864993
A(6)-OMe	Figure 5B		
C58H96N12O26P4S			
Charge = − 4			
C	7.512622	4.848249	0.589800
C	6.880142	4.665936	-0.794188

C	5.515457	5.375208	-0.908989
C	6.790011	3.173234	-1.133748
C	6.611277	2.840454	-2.612756
S	8.011050	3.303046	-3.699772
C	9.394276	2.469477	-2.864270
C	4.564342	5.120056	0.267073
C	3.082903	5.432521	-0.008903
C	2.911640	6.795227	-0.693193
H	1.859629	7.010814	-0.904320
C	2.233649	5.366411	1.286090
C	2.527779	4.137085	2.164376
C	0.728559	5.454796	0.990631
C	2.175165	2.787369	1.546148
C	-4.923877	-5.753271	-1.407632
C	-6.173764	-4.915771	-1.689785
C	-5.778009	-3.474844	-2.023083
H	-6.640844	-2.887245	-2.357729
C	-7.154044	-4.980553	-0.506925
C	-8.341422	-4.026625	-0.630424
C	-9.451409	-4.269034	0.392796
C	-10.447324	-3.100195	0.491538
N	-10.944710	-2.576667	-0.786324
C	-14.692966	3.685334	-3.091090
C	-13.429866	4.478466	-2.745136
C	-12.370429	4.324369	-3.837964
C	-12.870629	4.079080	-1.359665
C	-12.292296	2.697881	-1.273829
N	-13.080525	1.564774	-1.264377
C	-10.965512	2.343907	-1.206506
C	-12.222144	0.559534	-1.191169
N	-10.940262	0.979726	-1.157673
H	9.166310	1.427240	-2.628030
H	9.668159	2.973312	-1.935053
H	10.243320	2.498100	-3.552925
H	5.746212	3.355269	-3.045820
H	6.431693	1.767913	-2.713144
H	5.955660	2.708167	-0.593453
H	7.687066	2.657611	-0.774900
H	7.549828	5.129542	-1.532718
H	7.547674	5.906952	0.881215
H	8.534704	4.453414	0.595615
H	6.949933	4.301316	1.354860
H	4.896149	5.716130	1.130639
H	4.647237	4.072369	0.575445
H	3.451198	6.840670	-1.644404
H	3.298322	7.598358	-0.049732
H	2.707808	4.663074	-0.700581
H	2.511714	6.252754	1.882755
H	0.432624	6.441990	0.618541
H	0.141954	5.247618	1.892638
H	0.431057	4.711269	0.242912
H	2.745029	2.591011	0.630841
H	1.105737	2.705483	1.321619
H	2.420531	1.993226	2.253063
H	3.582610	4.124612	2.458882
H	1.960454	4.259117	3.098213
H	5.031671	5.057394	-1.843582

H	5.684463	6.456455	-1.012827
H	-5.185512	-6.792714	-1.159014
H	-4.357242	-5.314144	-0.579737
H	-4.247211	-5.749720	-2.268320
H	-6.690696	-5.341054	-2.567952
H	-5.353962	-2.988751	-1.137971
H	-5.004898	-3.455716	-2.797521
H	-7.513448	-6.017468	-0.394492
H	-6.607036	-4.740666	0.416031
H	-9.950864	-2.268408	1.002195
H	-11.304261	-3.405949	1.111842
H	-11.089265	-3.348546	-1.435431
H	-10.189507	-2.007510	-1.176989
H	-8.761777	-4.096197	-1.645024
H	-7.988097	-2.998101	-0.525395
H	-9.983889	-5.202967	0.141560
H	-9.005527	-4.424681	1.385082
H	-13.675256	4.186369	-0.618345
H	-12.089219	4.800229	-1.084344
H	-13.702214	5.544560	-2.684285
H	-15.074555	3.961117	-4.083537
H	-15.484801	3.872727	-2.355180
H	-14.480923	2.611872	-3.070451
H	-11.459537	4.882254	-3.590017
H	-12.743999	4.689453	-4.803578
H	-12.088106	3.272696	-3.950481
H	-12.456534	-0.496559	-1.132211
H	-10.085936	0.385269	-1.099510
H	-10.052810	2.919206	-1.164331
C	-7.203454	2.085225	1.174161
O	-7.914744	1.422539	0.142827
P	-7.820892	-0.223801	0.102042
O	-8.672084	-0.578291	-1.100351
O	-8.047481	-0.816117	1.447572
O	-6.233883	-0.458691	-0.259141
C	-5.747394	0.009183	-1.503977
C	-4.320986	0.498044	-1.393472
O	-4.251161	1.562230	-0.426240
C	-3.227763	-0.485583	-0.958489
O	-2.856049	-1.330462	-2.002137
C	-2.148887	0.507623	-0.497186
O	-1.582211	1.106690	-1.641137
C	-3.026022	1.520941	0.249769
N	-3.219343	1.140134	1.649753
C	-4.168295	0.305636	2.208118
N	-3.995448	0.102109	3.489557
C	-2.862226	0.826619	3.792443
C	-2.119701	0.991076	4.969084
N	-2.469187	0.364188	6.140331
N	-1.032459	1.774416	4.956291
C	-0.676462	2.342779	3.793140
N	-1.267468	2.246386	2.606793
C	-2.361982	1.473873	2.663444
P	-2.273291	-2.860020	-1.636559
O	-2.355742	-3.620103	-2.913817
O	-2.841389	-3.289758	-0.320671
O	-0.693018	-2.510171	-1.268844

C	0.155777	-1.802958	-2.139868
C	1.345592	-1.302227	-1.338193
O	0.853522	-0.526005	-0.237239
C	2.264116	-2.362042	-0.714997
O	3.249872	-2.701202	-1.661221
C	2.781752	-1.631949	0.538748
O	3.814141	-0.735383	0.213113
C	1.611621	-0.721689	0.921125
N	0.729721	-1.211276	2.003341
C	0.942510	-0.712431	3.273447
O	1.811775	0.099668	3.566104
N	0.069776	-1.192394	4.222760
C	-1.041828	-2.028659	4.049236
O	-1.723673	-2.329628	5.023965
C	-1.231069	-2.424848	2.674834
C	-0.352731	-2.019622	1.731765
P	4.520347	-3.713680	-1.281182
O	4.907986	-4.409119	-2.536749
O	4.274204	-4.341353	0.046947
O	5.681552	-2.516764	-0.978322
C	6.218835	-1.825107	-2.083204
C	7.157415	-0.737491	-1.582157
O	6.451819	0.107521	-0.675304
C	8.435665	-1.204402	-0.866762
O	9.505819	-1.134167	-1.781923
C	8.555483	-0.227414	0.338000
O	9.291283	0.924412	0.026887
C	7.113589	0.241918	0.561721
N	6.382349	-0.426737	1.635694
C	5.416484	0.337218	2.301929
O	5.306010	1.544377	2.157741
N	4.643066	-0.371016	3.194789
C	4.624139	-1.756268	3.404397
O	3.837071	-2.249275	4.198165
C	5.593458	-2.475363	2.603895
C	6.382276	-1.799593	1.752070
P	11.044805	-1.533653	-1.283230
O	11.101354	-2.911824	-0.734644
O	11.564845	-0.336364	-0.514401
O	11.725369	-1.534350	-2.780060
C	11.710462	-0.324274	-3.499523
H	11.964023	0.524391	-2.852037
H	10.724460	-0.145278	-3.947271
H	12.455911	-0.402788	-4.300670
C	-0.518632	1.992810	-1.372840
H	0.229388	1.530247	-0.722117
H	-0.864578	2.933503	-0.916023
H	-0.060687	2.225960	-2.338420
H	0.231141	2.940365	3.825116
H	-4.973534	-0.104273	1.608144
H	5.578203	-3.555504	2.605890
H	7.054229	-2.324400	1.088986
H	-2.083134	-3.024484	2.384077
H	-0.484536	-2.289817	0.686804
H	-6.371382	0.834497	-1.866647
H	-5.773613	-0.796927	-2.244589
H	-4.033714	0.892154	-2.377969

H	-3.560083	-1.074533	-0.094917
H	-1.375498	0.066035	0.137432
H	-2.581415	2.519198	0.276817
H	-2.864767	-0.557128	5.977857
H	-1.695742	0.334740	6.792094
H	-0.376210	-0.948127	-2.574367
H	0.521336	-2.450320	-2.947707
H	1.968331	-0.660640	-1.974732
H	1.689933	-3.246961	-0.416232
H	3.065004	-2.330276	1.332573
H	4.537459	-1.235087	-0.209507
H	2.014296	0.223003	1.279199
H	0.219657	-0.814239	5.147713
H	5.410781	-1.357850	-2.662834
H	6.765926	-2.508833	-2.743182
H	7.472820	-0.138103	-2.447085
H	8.333778	-2.237600	-0.512990
H	8.967785	-0.733676	1.222287
H	10.210503	0.608829	-0.181792
H	7.118340	1.292825	0.838841
H	3.821103	0.117197	3.546081
H	-6.145367	2.180849	0.907964
H	-7.294346	1.543675	2.122385
H	-7.643252	3.082673	1.285818

U(7)-OMe Figure 5C

C58H96N12O26P4S

Charge = − 4

C	5.176517	6.103030	1.065973
C	4.782388	5.283140	-0.166677
C	3.348401	5.593847	-0.627570
C	5.046680	3.789185	0.081438
C	4.777402	2.838264	-1.088365
S	5.493313	3.342023	-2.693695
C	7.229628	3.628265	-2.248572
C	2.266868	5.440476	0.448948
C	0.852093	5.210894	-0.109980
C	0.489493	6.296385	-1.131722
H	-0.498520	6.128491	-1.569381
C	-0.221869	5.119453	1.002760
C	0.197116	4.248643	2.203710
C	-1.570353	4.640440	0.446063
C	0.569489	2.807754	1.867377
C	-4.409915	-5.577343	-2.125239
C	-5.672806	-4.722786	-2.252603
C	-5.320323	-3.239363	-2.131042
H	-6.192475	-2.601674	-2.308532
C	-6.742263	-5.149906	-1.231589
C	-7.931459	-4.190888	-1.163646
C	-9.190059	-4.760905	-0.513969
C	-10.278249	-3.693926	-0.310313
N	-10.637379	-2.926348	-1.507176
C	-14.921926	3.030741	-3.375644
C	-13.813043	3.958908	-2.872702
C	-12.706640	4.109118	-3.918517
C	-13.243315	3.482725	-1.516361
C	-12.498780	2.181334	-1.553186
N	-13.143207	0.967660	-1.679793

C	-11.140791	1.982289	-1.475753
C	-12.172044	0.068478	-1.675408
N	-10.950982	0.632341	-1.559054
H	7.687398	2.763850	-1.764377
H	7.341618	4.508314	-1.606490
H	7.767703	3.805697	-3.183063
H	3.703928	2.744348	-1.281748
H	5.144292	1.840879	-0.835441
H	4.448266	3.432696	0.931874
H	6.094610	3.670698	0.388050
H	5.437788	5.588681	-0.992533
H	5.004681	7.174554	0.900199
H	6.236962	5.960646	1.305150
H	4.595575	5.803672	1.946671
H	2.258970	6.330079	1.097820
H	2.530042	4.598420	1.096706
H	1.208202	6.327884	-1.956464
H	0.483770	7.285712	-0.652108
H	0.865429	4.246356	-0.639218
H	-0.362047	6.142861	1.392527
H	-1.991263	5.341335	-0.282622
H	-2.301896	4.538556	1.256341
H	-1.477749	3.662977	-0.041223
H	1.414568	2.754545	1.170172
H	-0.265428	2.274388	1.408161
H	0.845944	2.266954	2.776388
H	1.034103	4.730093	2.726858
H	-0.636956	4.225550	2.917026
H	3.112571	4.945978	-1.481227
H	3.330827	6.619312	-1.021990
H	-4.638256	-6.649399	-2.219350
H	-3.930598	-5.398503	-1.156346
H	-3.670470	-5.297854	-2.882046
H	-6.105115	-4.884841	-3.255288
H	-4.937887	-3.021422	-1.128640
H	-4.529373	-2.975499	-2.839830
H	-7.087767	-6.167032	-1.482333
H	-6.278727	-5.219078	-0.236898
H	-9.924152	-2.971472	0.432985
H	-11.184148	-4.172858	0.093360
H	-10.630794	-3.543346	-2.318066
H	-9.893477	-2.239707	-1.663958
H	-8.180915	-3.853000	-2.178782
H	-7.640166	-3.293120	-0.610920
H	-9.585538	-5.584791	-1.133848
H	-8.941214	-5.201885	0.462387
H	-14.073746	3.406650	-0.800465
H	-12.567268	4.260476	-1.135687
H	-14.255166	4.953888	-2.702099
H	-15.322969	3.380348	-4.336741
H	-15.747717	2.983999	-2.655293
H	-14.539049	2.012392	-3.491777
H	-11.923687	4.793877	-3.570878
H	-13.106170	4.498526	-4.863856
H	-12.232543	3.141720	-4.113668
H	-12.278439	-1.008840	-1.725549
H	-10.036386	0.135879	-1.518786

H	-10.309649	2.658911	-1.345137
C	-7.544094	1.652595	1.299732
O	-8.088376	1.122052	0.102901
P	-7.858329	-0.486818	-0.173458
O	-8.534281	-0.704688	-1.511151
O	-8.186374	-1.300045	1.030271
O	-6.226419	-0.561368	-0.344192
C	-5.599040	0.151024	-1.394137
C	-4.212794	0.593076	-0.978513
O	-4.321086	1.449565	0.173675
C	-3.204334	-0.486794	-0.572743
O	-2.617921	-1.073424	-1.696516
C	-2.246343	0.343408	0.298482
O	-1.402719	1.157404	-0.480206
C	-3.235290	1.252449	1.033822
N	-3.676889	0.669657	2.302852
C	-4.635731	-0.294684	2.542602
N	-4.620668	-0.752763	3.770397
C	-3.581775	-0.070761	4.367484
C	-2.973982	-0.177275	5.625028
N	-3.424140	-1.068285	6.569621
N	-1.923404	0.602805	5.916340
C	-1.483626	1.445765	4.965415
N	-1.936762	1.611790	3.729635
C	-2.985420	0.816261	3.475384
P	-1.891386	-2.573403	-1.544423
O	-1.867684	-3.143207	-2.918640
O	-2.415929	-3.241473	-0.313889
O	-0.350826	-2.121986	-1.096495
C	0.474896	-1.323260	-1.903157
C	1.593276	-0.767324	-1.033621
O	0.996001	-0.080078	0.086551
C	2.568081	-1.773702	-0.408447
O	3.590082	-2.036994	-1.317644
C	2.978329	-1.060791	0.889478
O	3.972871	-0.110693	0.592160
C	1.696204	-0.310498	1.283366
N	0.833224	-1.005150	2.261973
C	0.951851	-0.621756	3.587918
O	1.717246	0.245698	3.985876
N	0.130901	-1.315071	4.451240
C	-0.819194	-2.304331	4.156923
O	-1.458427	-2.812178	5.070616
C	-0.903462	-2.593042	2.745097
C	-0.084312	-1.958943	1.878865
P	4.866107	-3.047355	-0.905583
O	4.997672	-4.049544	-1.995370
O	4.780661	-3.371006	0.553570
O	6.111820	-1.946918	-1.014820
C	6.178915	-0.977385	-2.024446
C	7.334418	-0.035887	-1.747112
O	7.162361	0.566942	-0.444687
C	8.751847	-0.617471	-1.727952
O	9.239585	-0.663255	-3.048039
C	9.478109	0.376250	-0.790850
O	9.774042	1.587195	-1.427833
C	8.378804	0.676294	0.228552

N	8.404329	-0.239972	1.402648
C	9.278291	0.090423	2.420933
O	9.993318	1.081704	2.413757
N	9.279226	-0.803406	3.473770
C	8.522940	-1.979471	3.633527
O	8.678930	-2.653327	4.643344
C	7.630112	-2.213986	2.524602
C	7.606387	-1.357390	1.478192
P	10.853639	-0.883344	-3.301755
O	11.365360	-2.135576	-2.671974
O	11.551695	0.436722	-3.052115
O	10.673200	-1.085293	-4.934121
C	11.848891	-1.460535	-5.601340
H	12.265818	-2.387594	-5.185100
H	12.616690	-0.674236	-5.538358
H	11.597070	-1.621521	-6.656429
H	-0.618424	2.046504	5.237848
H	-5.327968	-0.600052	1.765061
H	6.961786	-3.065128	2.520538
H	6.931441	-1.513141	0.637626
H	-1.634596	-3.293631	2.364281
H	-0.148493	-2.147865	0.809830
H	-6.190110	1.036426	-1.657795
H	-5.506437	-0.486380	-2.280396
H	-3.773820	1.163431	-1.808698
H	-3.686988	-1.248760	0.050069
H	-1.675162	-0.274145	0.994848
H	-2.767690	2.205922	1.288223
H	-3.898760	-1.852649	6.137006
H	-2.666056	-1.383500	7.161596
H	-0.102576	-0.494614	-2.334117
H	0.920204	-1.904660	-2.720002
H	2.183720	-0.046836	-1.613269
H	2.030984	-2.692569	-0.137890
H	3.324020	-1.770342	1.645839
H	1.945276	0.638557	1.749943
H	0.149424	-0.987792	5.408502
H	5.246411	-0.400584	-2.053006
H	6.339734	-1.435935	-3.010050
H	7.314051	0.756727	-2.504352
H	8.754966	-1.621523	-1.284830
H	10.365812	-0.066851	-0.322173
H	10.458979	1.356635	-2.108915
H	8.505526	1.683503	0.628938
H	9.922654	-0.580600	4.219925
H	-6.462722	1.796340	1.198392
H	-7.746607	0.988767	2.147975
H	-8.025265	2.621092	1.474431
H	-0.500997	0.810930	-0.361835
C	4.686670	0.294457	1.736262
H	5.465481	0.978999	1.394518
H	5.157457	-0.569764	2.222277
H	4.038845	0.799924	2.469041
U(8)-OMe	Figure 5D		
C58H96N12O26P4S			
Charge = − 4			
C	8.964641	5.361218	0.865521

C	8.106061	5.005764	-0.353348
C	6.712096	5.657832	-0.263910
C	8.071113	3.483482	-0.535044
C	7.438675	2.983032	-1.832367
S	8.414466	3.318452	-3.341528
C	9.764364	2.116832	-3.117325
C	5.859643	5.231115	0.937138
C	4.391632	5.689506	0.877020
C	4.294553	7.211540	0.711048
H	3.257595	7.541868	0.600018
C	3.593071	5.201658	2.111701
C	3.681916	3.677754	2.336602
C	2.121610	5.641073	2.053884
C	3.207227	2.814183	1.168721
C	-5.750709	-5.289194	0.641870
C	-6.664716	-4.061985	0.603555
C	-6.266456	-3.071541	1.701002
H	-6.853957	-2.149469	1.662847
C	-8.138125	-4.486003	0.693463
C	-9.148016	-3.366880	0.450658
C	-10.598149	-3.848574	0.492116
C	-11.629875	-2.751202	0.196013
N	-11.576755	-2.176939	-1.148021
C	-14.599868	4.358189	-3.639193
C	-13.462184	5.075074	-2.907375
C	-12.166612	5.016964	-3.719128
C	-13.262310	4.516137	-1.480146
C	-12.762729	3.104655	-1.419141
N	-13.593824	2.021465	-1.621932
C	-11.475727	2.673205	-1.202862
C	-12.799518	0.967145	-1.524891
N	-11.518213	1.310843	-1.277091
H	9.392623	1.148152	-2.775604
H	10.503162	2.470988	-2.392917
H	10.253570	1.986861	-4.085691
H	6.455421	3.432428	-2.003111
H	7.289907	1.903715	-1.780953
H	7.544643	3.024736	0.311720
H	9.093291	3.094314	-0.478043
H	8.594767	5.427623	-1.243317
H	8.978826	6.444818	1.042949
H	9.998503	5.025445	0.723094
H	8.582886	4.875946	1.771288
H	6.308171	5.615092	1.865932
H	5.880988	4.140381	1.020217
H	4.838537	7.553967	-0.175100
H	4.721138	7.722424	1.586118
H	3.936746	5.230553	-0.013422
H	4.047296	5.683389	2.994402
H	2.003864	6.721991	2.187579
H	1.542175	5.147241	2.841766
H	1.662515	5.370381	1.096059
H	3.863888	2.897333	0.295478
H	2.187388	3.073081	0.855082
H	3.186542	1.766229	1.472894
H	4.705945	3.386922	2.595031
H	3.075490	3.435589	3.220190

H	6.155556	5.448131	-1.187764
H	6.860030	6.746720	-0.246007
H	-6.011465	-6.003666	-0.150579
H	-5.848968	-5.807892	1.608131
H	-4.709827	-4.981687	0.501868
H	-6.510273	-3.562381	-0.363282
H	-6.406346	-3.525330	2.693820
H	-5.207594	-2.816416	1.590529
H	-8.317530	-5.289915	-0.039509
H	-8.315673	-4.936406	1.685277
H	-11.490066	-1.925709	0.904045
H	-12.640828	-3.154154	0.367060
H	-11.457282	-2.929506	-1.824396
H	-10.731048	-1.601991	-1.209157
H	-8.944051	-2.905517	-0.523269
H	-9.020448	-2.563773	1.184798
H	-10.738709	-4.669280	-0.232777
H	-10.810691	-4.280731	1.482970
H	-14.218374	4.586958	-0.943275
H	-12.551303	5.166783	-0.953196
H	-13.743922	6.134936	-2.797964
H	-14.728549	4.758043	-4.654064
H	-15.548460	4.477146	-3.101342
H	-14.396008	3.284719	-3.699243
H	-11.350004	5.534997	-3.202043
H	-12.297636	5.482828	-4.704266
H	-11.852381	3.978592	-3.865549
H	-13.083371	-0.074524	-1.607505
H	-10.702289	0.675690	-1.154880
H	-10.548700	3.187451	-0.997383
C	-7.571144	2.573176	0.756789
O	-8.342968	1.809187	-0.154105
P	-8.402741	0.179369	0.098375
O	-9.314222	-0.298082	-1.013136
O	-8.641367	-0.127045	1.534891
O	-6.864923	-0.279780	-0.235797
C	-6.351751	-0.071157	-1.539643
C	-4.886489	0.314045	-1.489723
O	-4.722407	1.448801	-0.617536
C	-3.885656	-0.718922	-0.967385
O	-3.572432	-1.673479	-1.936385
C	-2.724603	0.204045	-0.567690
O	-2.019289	0.671096	-1.688437
C	-3.499315	1.366418	0.059469
N	-3.701049	1.128530	1.494202
C	-4.696229	0.412970	2.131219
N	-4.387077	0.059416	3.354361
C	-3.102374	0.536532	3.524818
C	-2.136308	0.319662	4.517673
N	-2.390522	-0.451031	5.624880
N	-0.914500	0.850325	4.366754
C	-0.647725	1.510394	3.230090
N	-1.439471	1.716975	2.182449
C	-2.659717	1.199996	2.384739
P	-2.842174	-3.093731	-1.430920
O	-2.988707	-4.042967	-2.564270
O	-3.232121	-3.341561	-0.007003

O	-1.255344	-2.606158	-1.295093
C	-0.532470	-2.140394	-2.405670
C	0.718085	-1.420062	-1.920333
O	0.334979	-0.486738	-0.874798
C	1.854403	-2.230631	-1.290628
O	2.679761	-2.783193	-2.279752
C	2.525087	-1.149617	-0.427557
O	3.210203	-0.202483	-1.208973
C	1.304637	-0.424594	0.132592
N	0.814871	-1.042234	1.392095
C	1.605215	-0.821818	2.502087
O	2.606678	-0.116430	2.470986
N	1.196193	-1.462585	3.644626
C	-0.003648	-2.148359	3.850607
O	-0.294466	-2.541757	4.978125
C	-0.770943	-2.320322	2.639067
C	-0.327569	-1.798944	1.473148
P	3.927793	-3.783408	-1.800712
O	4.288618	-4.596790	-2.991791
O	3.660174	-4.283466	-0.419542
O	5.134540	-2.642719	-1.551028
C	5.680285	-1.919724	-2.620177
C	6.680038	-0.928887	-2.040416
O	6.008123	-0.160022	-1.024853
C	7.919116	-1.536369	-1.366921
O	8.956552	-1.574599	-2.310532
C	8.161998	-0.614857	-0.150415
O	9.028457	0.432194	-0.505676
C	6.777796	-0.007179	0.140451
N	6.085843	-0.551717	1.313925
C	6.001461	0.270889	2.427246
O	6.446425	1.412100	2.471500
N	5.407164	-0.318322	3.518067
C	4.767134	-1.564149	3.594072
O	4.195481	-1.881634	4.628283
C	4.906668	-2.343899	2.383478
C	5.536023	-1.817803	1.313982
P	10.473859	-2.094128	-1.882597
O	10.967137	-3.078831	-2.887913
O	10.511888	-2.353753	-0.404112
O	11.231986	-0.629770	-2.184521
C	12.622782	-0.664314	-2.027994
H	13.085760	-1.401702	-2.699628
H	12.905200	-0.914110	-0.993160
H	13.014770	0.333142	-2.266739
H	0.366281	1.898810	3.144428
H	-5.628440	0.185909	1.627021
H	4.431880	-3.312384	2.299027
H	5.580917	-2.348702	0.365527
H	-1.688942	-2.892139	2.650529
H	-0.842680	-1.975821	0.533075
H	-6.913751	0.723030	-2.044045
H	-6.443811	-0.991992	-2.127453
H	-4.577019	0.593962	-2.506658
H	-4.284590	-1.204979	-0.069021
H	-2.055377	-0.263997	0.154734
H	-2.946915	2.304324	-0.033802

H	-3.205549	-1.038354	5.493355
H	-1.574536	-0.994996	5.894598
H	-1.150008	-1.443468	-2.985705
H	-0.225761	-2.966976	-3.059367
H	1.146801	-0.847210	-2.751420
H	1.452658	-3.015939	-0.638800
H	3.152121	-1.579455	0.353559
H	4.163085	-0.350574	-1.112442
H	1.565996	0.610635	0.346432
H	1.819476	-1.355120	4.436969
H	4.887465	-1.377398	-3.153483
H	6.196023	-2.577682	-3.331062
H	7.020320	-0.243321	-2.827307
H	7.685940	-2.542314	-0.998356
H	8.559348	-1.181212	0.694120
H	6.896408	1.050156	0.364218
H	5.237306	0.307170	4.293312
H	-6.502413	2.424733	0.571515
H	-7.806420	2.300477	1.791805
H	-7.822500	3.626694	0.590764
H	-1.085427	0.483249	-1.497622
C	10.048997	0.677313	0.430256
H	10.725859	1.402624	-0.031034
H	10.599027	-0.249179	0.632567
H	9.640234	1.104652	1.360927
A(6)U(7)-OMe	Figure 5E		
C59H98N12O26P4S			
Charge = − 4			
C	-5.607991	-5.877501	-1.239978
C	-4.826168	-4.726426	-1.880732
C	-3.315379	-5.017924	-1.938849
C	-5.157798	-3.394414	-1.189295
C	-4.708388	-2.125623	-1.917157
S	-5.240203	-2.004062	-3.664991
C	-6.998081	-2.447720	-3.555385
C	-2.699862	-5.452739	-0.603802
C	-1.182751	-5.233738	-0.490223
C	-0.444387	-5.920884	-1.644338
H	0.626466	-5.699129	-1.634374
C	-0.646236	-5.689480	0.888204
C	-1.437826	-5.088012	2.069634
C	0.849903	-5.397058	1.064229
C	-1.579705	-3.566429	2.036660
C	4.438579	5.886243	-0.240110
C	5.710733	5.139716	-0.647019
C	5.372437	3.711805	-1.079382
H	6.253474	3.191782	-1.470594
C	6.756291	5.168899	0.482110
C	7.954863	4.256295	0.221648
C	9.186703	4.543555	1.077146
C	10.278360	3.473497	0.910493
N	10.668817	3.185973	-0.474104
C	15.111545	-1.736216	-4.069303
C	13.975936	-2.761059	-4.006055
C	12.931298	-2.492443	-5.090941
C	13.328129	-2.809740	-2.602995
C	12.569026	-1.578975	-2.205553

N	13.202257	-0.398196	-1.875608
C	11.206964	-1.419131	-2.113010
C	12.220909	0.443049	-1.591429
N	11.003608	-0.125356	-1.724981
H	-7.542009	-1.854864	-2.816478
H	-7.132596	-3.512527	-3.336182
H	-7.434985	-2.237142	-4.535027
H	-3.616738	-2.050702	-1.955419
H	-5.068399	-1.251775	-1.370743
H	-4.715997	-3.365384	-0.183232
H	-6.242787	-3.332535	-1.035197
H	-5.161832	-4.636119	-2.921316
H	-5.362292	-6.837169	-1.713453
H	-6.687032	-5.714344	-1.343022
H	-5.389445	-5.967666	-0.169207
H	-2.920586	-6.515901	-0.421516
H	-3.194428	-4.901914	0.201956
H	-0.831486	-5.590138	-2.613035
H	-0.567433	-7.011881	-1.586128
H	-1.001892	-4.153531	-0.579065
H	-0.780382	-6.784047	0.934843
H	1.464389	-5.903938	0.313302
H	1.191220	-5.735236	2.049542
H	1.057317	-4.323514	1.014803
H	-2.196949	-3.235720	1.192774
H	-0.605667	-3.073985	1.945820
H	-2.048746	-3.184442	2.947686
H	-2.433539	-5.546641	2.121751
H	-0.927562	-5.378963	2.998189
H	-2.799191	-4.121300	-2.306413
H	-3.140791	-5.794860	-2.695531
H	4.660951	6.917779	0.071185
H	3.943253	5.361661	0.584330
H	3.714376	5.905159	-1.060481
H	6.159311	5.656652	-1.513283
H	4.986148	3.140043	-0.229727
H	4.587255	3.719835	-1.841885
H	7.094710	6.208595	0.627470
H	6.273646	4.866834	1.422567
H	9.913374	2.533239	1.337747
H	11.172351	3.775011	1.478635
H	10.672447	4.053116	-1.009348
H	9.931364	2.603970	-0.882192
H	8.235722	4.324219	-0.838337
H	7.658752	3.217061	0.388799
H	9.593568	5.536963	0.818512
H	8.901372	4.593614	2.138031
H	14.117978	-3.006577	-1.864406
H	12.642663	-3.667568	-2.570124
H	14.408267	-3.757634	-4.192098
H	15.558859	-1.703515	-5.072005
H	15.901086	-1.985009	-3.349631
H	14.737969	-0.741968	-3.806536
H	12.126765	-3.236969	-5.058668
H	13.383980	-2.520831	-6.090467
H	12.473054	-1.508815	-4.945397
H	12.314964	1.469703	-1.257276

H	10.082696	0.324471	-1.542253
H	10.380263	-2.098455	-2.256808
C	7.553217	-2.094111	0.512406
O	8.095089	-1.176575	-0.421171
P	7.878710	0.428222	-0.105961
O	8.564109	1.101535	-1.275807
O	8.203661	0.753244	1.309966
O	6.246073	0.572373	-0.241641
C	5.618860	0.283499	-1.475899
C	4.237173	-0.295862	-1.266460
O	4.332777	-1.494915	-0.468872
C	3.173265	0.549337	-0.553580
O	2.634386	1.514950	-1.398765
C	2.204813	-0.562796	-0.121712
O	1.524265	-1.018456	-1.266680
C	3.216352	-1.608283	0.364630
N	3.584324	-1.376393	1.765673
C	4.635688	-0.644413	2.283561
N	4.617668	-0.559181	3.590424
C	3.486475	-1.256191	3.954260
C	2.855995	-1.454534	5.188423
N	3.371933	-0.941694	6.354538
N	1.715849	-2.157409	5.236099
C	1.207457	-2.609673	4.079714
N	1.677264	-2.453858	2.845724
C	2.826963	-1.764508	2.837905
P	1.937738	2.879797	-0.709050
O	1.887981	3.883082	-1.805717
O	2.534933	3.081832	0.648303
O	0.416903	2.310529	-0.367026
C	-0.428402	1.742012	-1.337288
C	-1.550601	1.007275	-0.623314
O	-0.972354	0.059839	0.292925
C	-2.515169	1.841047	0.230123
O	-3.500678	2.388560	-0.589710
C	-2.981682	0.807155	1.264521
O	-3.955191	-0.018680	0.668839
C	-1.704864	-0.019976	1.477487
N	-0.866130	0.419682	2.622522
C	-1.148875	-0.149821	3.848340
O	-2.060868	-0.943008	4.040549
N	-0.308826	0.250790	4.865472
C	0.812944	1.088616	4.795102
O	1.470312	1.292858	5.811268
C	1.036694	1.611264	3.469605
C	0.203791	1.268566	2.461169
P	-4.772908	3.272044	0.052292
O	-4.845002	4.549342	-0.704838
O	-4.753402	3.155494	1.544299
O	-6.030957	2.284881	-0.421350
C	-6.083340	1.710601	-1.697426
C	-7.244350	0.739304	-1.772551
O	-7.117126	-0.252544	-0.728544
C	-8.666614	1.290041	-1.624164
O	-9.096393	1.770264	-2.873535
C	-9.415051	0.044772	-1.093896
O	-9.650550	-0.900106	-2.099905

C	-8.357385	-0.560577	-0.171289
N	-8.439689	-0.051524	1.226807
C	-9.362835	-0.666300	2.050980
O	-10.078499	-1.594383	1.703267
N	-9.413780	-0.142489	3.327777
C	-8.657905	0.907633	3.882437
O	-8.858974	1.234139	5.044778
C	-7.710371	1.456966	2.943709
C	-7.639011	0.968344	1.684613
P	-10.707487	2.039639	-3.185461
O	-11.284023	3.068566	-2.283265
O	-11.350217	0.678252	-3.360672
O	-10.485596	2.705476	-4.672173
C	-9.897510	1.891078	-5.659173
H	-10.400800	0.918083	-5.720849
H	-8.833363	1.724844	-5.450418
H	-9.995770	2.412080	-6.619377
C	0.645322	-2.092900	-1.043778
H	0.144293	-2.011394	-0.073599
H	1.162308	-3.064006	-1.106826
H	-0.116464	-2.055888	-1.828527
H	0.267347	-3.150737	4.164624
H	5.379275	-0.197994	1.632831
H	-7.037342	2.252150	3.236476
H	-6.921510	1.363961	0.966614
H	1.871888	2.267487	3.263289
H	0.352121	1.651284	1.454057
H	6.218656	-0.436940	-2.045159
H	5.515145	1.197980	-2.069970
H	3.838229	-0.559094	-2.255029
H	3.590953	1.020367	0.344281
H	1.496535	-0.266564	0.657884
H	2.825841	-2.629409	0.321885
H	3.985855	-0.156976	6.166676
H	2.627935	-0.668414	6.985457
H	0.134771	1.031693	-1.953981
H	-0.867950	2.514358	-1.980986
H	-2.149131	0.463117	-1.366271
H	-1.955854	2.625083	0.758852
H	-3.365672	1.278253	2.172621
H	-1.955081	-1.058018	1.691131
H	-0.451238	-0.228678	5.743590
H	-5.151192	1.171476	-1.906471
H	-6.226558	2.473875	-2.475421
H	-7.193755	0.232798	-2.743394
H	-8.698120	2.093423	-0.876669
H	-10.334471	0.305762	-0.554732
H	-10.311474	-0.463310	-2.702166
H	-8.490124	-1.641848	-0.108043
H	-10.091875	-0.575793	3.938310
H	6.474853	-2.209785	0.356036
H	7.738909	-1.761235	1.539911
H	8.048965	-3.057580	0.349794
C	-4.730580	-0.715459	1.613150
H	-5.512598	-1.235112	1.054253
H	-5.199803	-0.018919	2.319567
H	-4.132260	-1.440624	2.185608

A(6)U(8)-OMe Figure 5F

C59H98N12O26P4S

Charge = − 4

C	-4.793938	-6.415227	0.044951
C	-4.481342	-5.407376	-1.065301
C	-3.093458	-5.649587	-1.684257
C	-4.678960	-3.968823	-0.559657
C	-4.529659	-2.858626	-1.604407
S	-5.494382	-3.089880	-3.139837
C	-7.154123	-3.334257	-2.444403
C	-1.938566	-5.684388	-0.672931
C	-0.580228	-5.236881	-1.236397
C	-0.213384	-6.056635	-2.479771
H	0.708904	-5.698084	-2.945093
C	0.544939	-5.297819	-0.173383
C	0.146299	-4.688819	1.186918
C	1.842565	-4.653797	-0.681399
C	-0.355920	-3.248171	1.138215
C	4.356426	5.874384	-1.010374
C	5.655840	5.121836	-1.306499
C	5.365019	3.634096	-1.512419
H	6.261084	3.084837	-1.820962
C	6.699354	5.362831	-0.200952
C	7.922272	4.450819	-0.301801
C	9.133590	4.905513	0.509032
C	10.249367	3.848150	0.548781
N	10.678884	3.334209	-0.756189
C	15.155696	-2.148264	-3.548473
C	14.010078	-3.136515	-3.312788
C	12.953985	-3.024491	-4.413948
C	13.381580	-2.954977	-1.911593
C	12.634477	-1.670647	-1.706355
N	13.273831	-0.453521	-1.586023
C	11.274189	-1.492835	-1.619418
C	12.297107	0.426225	-1.430637
N	11.077907	-0.152452	-1.447857
H	-7.326771	-2.615053	-1.641261
H	-7.290451	-4.353712	-2.067870
H	-7.885548	-3.137547	-3.230950
H	-3.490147	-2.766709	-1.935382
H	-4.798620	-1.897609	-1.157904
H	-3.973197	-3.744636	0.252511
H	-5.677671	-3.893077	-0.109760
H	-5.211050	-5.561505	-1.870985
H	-4.668999	-7.446037	-0.311399
H	-5.825381	-6.299164	0.398316
H	-4.131815	-6.277980	0.908024
H	-1.838808	-6.697105	-0.252876
H	-2.193203	-5.036691	0.170522
H	-1.000770	-6.006119	-3.238633
H	-0.070368	-7.113895	-2.214425
H	-0.687743	-4.187118	-1.548338
H	0.749308	-6.367473	0.007892
H	2.245811	-5.166176	-1.561259
H	2.614309	-4.693418	0.096103
H	1.692734	-3.599853	-0.942181
H	-1.264182	-3.147059	0.531370

H	0.394178	-2.576601	0.715223
H	-0.585871	-2.892515	2.145834
H	-0.611773	-5.324755	1.663470
H	1.023770	-4.716274	1.845764
H	-2.909189	-4.867891	-2.431997
H	-3.122545	-6.593147	-2.246695
H	4.540024	6.947867	-0.855217
H	3.879570	5.460127	-0.115244
H	3.633218	5.745027	-1.821808
H	6.083365	5.515632	-2.244847
H	4.998381	3.187669	-0.582543
H	4.581254	3.499485	-2.264404
H	7.010115	6.420857	-0.230068
H	6.221603	5.209695	0.777622
H	9.893193	2.987474	1.124859
H	11.123255	4.264904	1.073659
H	10.686581	4.095890	-1.433084
H	9.961541	2.675689	-1.074023
H	8.216849	4.350506	-1.355450
H	7.648535	3.445949	0.031351
H	9.526776	5.848730	0.090165
H	8.827490	5.130099	1.541241
H	14.180672	-3.038630	-1.161336
H	12.690818	-3.790132	-1.732593
H	14.428659	-4.155328	-3.346810
H	15.592985	-2.281560	-4.547323
H	15.950089	-2.288085	-2.804900
H	14.795056	-1.120585	-3.444269
H	12.143927	-3.747813	-4.261157
H	13.393979	-3.207297	-5.402848
H	12.505327	-2.025943	-4.413328
H	12.398835	1.493557	-1.274724
H	10.157601	0.322342	-1.338268
H	10.443824	-2.182767	-1.635022
C	7.644998	-1.747728	1.070239
O	8.206512	-0.990294	0.011769
P	7.926848	0.633904	0.022841
O	8.635656	1.112630	-1.227156
O	8.184818	1.224708	1.364876
O	6.299495	0.690373	-0.192647
C	5.729833	0.165557	-1.376730
C	4.348818	-0.385314	-1.095308
O	4.457088	-1.442549	-0.124153
C	3.303183	0.574171	-0.516522
O	2.718495	1.349483	-1.520448
C	2.351848	-0.426848	0.159126
O	1.540767	-1.089060	-0.781215
C	3.348274	-1.440520	0.728675
N	3.746913	-1.107994	2.098797
C	4.663033	-0.177793	2.549286
N	4.619445	0.014334	3.844884
C	3.606849	-0.818461	4.270889
C	2.989166	-1.003888	5.514523
N	3.396067	-0.314395	6.631128
N	1.971659	-1.870416	5.621124
C	1.574632	-2.513345	4.508971
N	2.040982	-2.397501	3.272591

C	3.054269	-1.522800	3.204638
P	1.933554	2.765576	-1.096945
O	1.892995	3.582182	-2.340109
O	2.425383	3.208129	0.243827
O	0.408967	2.179792	-0.759049
C	-0.399003	1.554043	-1.721115
C	-1.515032	0.815983	-0.994689
O	-0.912621	-0.074213	-0.028996
C	-2.508468	1.662893	-0.188566
O	-3.538412	2.085714	-1.028921
C	-2.906328	0.704196	0.944096
O	-3.892980	-0.182568	0.476790
C	-1.619750	-0.098349	1.186238
N	-0.771580	0.392684	2.291513
C	-0.890429	-0.257791	3.509403
O	-1.636371	-1.206164	3.710537
N	-0.094210	0.262941	4.506741
C	0.820635	1.324209	4.437176
O	1.431808	1.655735	5.445803
C	0.906483	1.900905	3.116415
C	0.115802	1.433909	2.126372
P	-4.881433	2.884575	-0.417686
O	-5.203762	3.968018	-1.385086
O	-4.726653	3.051928	1.060285
O	-6.015750	1.676754	-0.577598
C	-6.140613	0.958520	-1.775847
C	-7.402817	0.124698	-1.730397
O	-7.384993	-0.714538	-0.548577
C	-8.732394	0.873727	-1.645809
O	-9.121898	1.297667	-2.916189
C	-9.633727	-0.188431	-0.991903
O	-9.979956	-1.235771	-1.873360
C	-8.662671	-0.814462	0.011119
N	-8.693139	-0.155171	1.342244
C	-9.628001	-0.628233	2.243766
O	-10.400390	-1.546557	2.010161
N	-9.617347	0.025540	3.459815
C	-8.808925	1.098425	3.877484
O	-8.961623	1.556947	5.001392
C	-7.871196	1.509399	2.860165
C	-7.851195	0.884652	1.661422
P	-10.387873	2.403919	-3.044388
O	-11.011955	2.511872	-1.684034
O	-11.147539	2.028235	-4.272496
O	-9.535058	3.760042	-3.399852
C	-8.611317	4.231442	-2.432094
H	-9.064387	4.252774	-1.433562
H	-8.325948	5.248968	-2.716636
H	-7.699040	3.624938	-2.398327
H	0.737916	-3.196621	4.637604
H	5.348467	0.309354	1.864066
H	-7.174369	2.314510	3.051426
H	-7.141474	1.172028	0.886709
H	1.616320	2.688057	2.900144
H	0.179821	1.843435	1.120944
H	6.360031	-0.637809	-1.776961
H	5.640365	0.952502	-2.133779

H	3.945619	-0.798728	-2.030013
H	3.756063	1.215069	0.248179
H	1.755540	0.032848	0.949420
H	2.899554	-2.434952	0.782435
H	3.836910	0.563365	6.380263
H	2.624832	-0.166041	7.269470
H	0.194160	0.841761	-2.310220
H	-0.847258	2.285763	-2.404796
H	-2.088978	0.216416	-1.711956
H	-1.988737	2.520552	0.258370
H	-3.252209	1.251166	1.824361
H	-1.869094	-1.123661	1.450460
H	-0.111421	-0.253372	5.376938
H	-5.267414	0.307214	-1.909737
H	-6.210155	1.630794	-2.642052
H	-7.429789	-0.520870	-2.616953
H	-8.639335	1.716039	-0.948437
H	-10.521123	0.252763	-0.527564
H	-8.920545	-1.859698	0.187799
H	-10.302447	-0.302779	4.125530
H	6.575514	-1.911916	0.899065
H	7.786904	-1.240655	2.031361
H	8.162869	-2.712797	1.090556
H	0.630093	-0.786275	-0.619672
C	-4.735467	-0.640195	1.509426
H	-5.513613	-1.244899	1.039308
H	-5.207174	0.210130	2.016949
H	-4.180266	-1.240360	2.247345
C	-11.141957	-0.999367	-2.643683
H	-11.384081	-1.954547	-3.123761
H	-10.998996	-0.225847	-3.403564
H	-11.981481	-0.700445	-1.998128

U(7)U(8)-OMe Figure 5G

C59H98N12O26P4S

Charge = − 4

C	9.320338	5.055524	0.972230
C	8.568041	4.779108	-0.333643
C	7.227194	5.534858	-0.374519
C	8.427266	3.262779	-0.530462
C	7.715212	2.807270	-1.802873
S	8.659568	3.058721	-3.346289
C	9.845765	1.684054	-3.205990
C	6.208071	5.111020	0.695544
C	4.745630	5.353487	0.289866
C	4.494868	6.847336	0.047519
H	3.500076	7.034503	-0.367647
C	3.745792	4.756038	1.308132
C	4.027721	3.275127	1.638740
C	2.292010	4.926373	0.843614
C	4.155087	2.344102	0.435196
C	-5.596268	-5.537272	0.317450
C	-6.847157	-4.748007	-0.076145
C	-6.457051	-3.492572	-0.860235
H	-7.337994	-2.987175	-1.273222
C	-7.696055	-4.408950	1.160333
C	-8.865131	-3.470289	0.865257
C	-9.904003	-3.386001	1.982935

C	-10.911946	-2.240978	1.789399
N	-11.521216	-2.149236	0.457667
C	-15.699961	2.871847	-3.353543
C	-14.470263	3.781784	-3.415009
C	-13.495145	3.313009	-4.496574
C	-13.773001	3.891545	-2.039139
C	-13.118707	2.632497	-1.553872
N	-13.844657	1.563478	-1.069651
C	-11.776617	2.335426	-1.526848
C	-12.935816	0.651221	-0.762508
N	-11.679451	1.069940	-1.023140
H	9.347270	0.729823	-3.025337
H	10.559496	1.844767	-2.395196
H	10.390596	1.628793	-4.152049
H	6.759018	3.321621	-1.940242
H	7.491756	1.741130	-1.737267
H	7.906026	2.828830	0.332520
H	9.424644	2.811201	-0.512875
H	9.175607	5.163337	-1.165625
H	9.458222	6.132705	1.134540
H	10.309208	4.581941	0.960801
H	8.772680	4.650190	1.831171
H	6.411604	5.633924	1.642048
H	6.338404	4.048030	0.910729
H	5.224551	7.263604	-0.655885
H	4.579150	7.406912	0.989788
H	4.585913	4.831105	-0.666005
H	3.860821	5.323936	2.246802
H	1.994839	5.978457	0.774419
H	1.604056	4.438634	1.541946
H	2.133918	4.468598	-0.139955
H	5.078714	2.515136	-0.131436
H	3.317755	2.435773	-0.263739
H	4.153004	1.307079	0.772994
H	4.936420	3.188613	2.244952
H	3.213964	2.901381	2.271757
H	6.778207	5.399378	-1.367814
H	7.436249	6.611063	-0.291623
H	-5.857453	-6.441892	0.886845
H	-4.929565	-4.910023	0.918904
H	-5.019435	-5.824077	-0.567732
H	-7.469559	-5.380892	-0.733323
H	-5.933650	-2.788452	-0.204970
H	-5.768484	-3.741696	-1.673535
H	-8.069447	-5.346149	1.606482
H	-7.048260	-3.942303	1.915933
H	-10.396912	-1.291123	1.967583
H	-11.709290	-2.331307	2.543509
H	-11.696862	-3.087116	0.100338
H	-10.815441	-1.733273	-0.155721
H	-9.360498	-3.788817	-0.063696
H	-8.478903	-2.467440	0.666667
H	-10.437131	-4.350080	2.057166
H	-9.396336	-3.239980	2.946782
H	-14.515552	4.226124	-1.301138
H	-13.010463	4.679731	-2.102041
H	-14.810705	4.795323	-3.682419

H	-16.179589	2.788989	-4.338193
H	-16.439409	3.261369	-2.642909
H	-15.414516	1.874313	-3.005817
H	-12.619182	3.970604	-4.552374
H	-13.976163	3.299111	-5.483072
H	-13.132225	2.304552	-4.273464
H	-13.109366	-0.325188	-0.325921
H	-10.796880	0.536767	-0.869669
H	-10.895219	2.900006	-1.791990
C	-7.678321	2.845140	0.415382
O	-8.460350	1.902861	-0.297452
P	-8.409254	0.341225	0.235347
O	-9.356801	-0.370127	-0.708056
O	-8.546251	0.272278	1.715538
O	-6.859906	-0.081540	-0.111659
C	-6.417703	-0.028391	-1.455582
C	-4.963495	0.380907	-1.544141
O	-4.780152	1.650119	-0.881092
C	-3.887241	-0.522162	-0.928753
O	-3.617280	-1.638643	-1.715800
C	-2.738203	0.488381	-0.809771
O	-2.224705	0.744585	-2.094931
C	-3.517584	1.698832	-0.281823
N	-3.617103	1.625099	1.180496
C	-4.606233	1.059316	1.961962
N	-4.249308	0.884682	3.209690
C	-2.943235	1.327215	3.249065
C	-1.943298	1.227838	4.227213
N	-2.182229	0.661185	5.452103
N	-0.710814	1.674603	3.946367
C	-0.473999	2.143657	2.713066
N	-1.305292	2.226184	1.677976
C	-2.531320	1.789477	2.003208
P	-2.935137	-2.981200	-0.962694
O	-3.124835	-4.095449	-1.931729
O	-3.353338	-2.979415	0.473689
O	-1.340423	-2.526745	-0.898089
C	-0.627304	-2.175331	-2.059429
C	0.640014	-1.433343	-1.664993
O	0.298244	-0.400657	-0.714760
C	1.775184	-2.200653	-0.980766
O	2.557317	-2.893344	-1.915511
C	2.498770	-1.042735	-0.275037
O	3.184275	-0.234463	-1.202490
C	1.305468	-0.234174	0.232465
N	0.849376	-0.702902	1.571317
C	1.675082	-0.378598	2.629279
O	2.690683	0.295942	2.497861
N	1.277079	-0.876535	3.845603
C	0.050452	-1.464296	4.157231
O	-0.235820	-1.686595	5.333418
C	-0.758932	-1.743043	2.994792
C	-0.330078	-1.376190	1.765496
P	3.779329	-3.877357	-1.350739
O	4.080532	-4.838912	-2.443355
O	3.530161	-4.203757	0.085650
O	5.034697	-2.766186	-1.254328

C	5.540748	-2.121294	-2.390114
C	6.593704	-1.127933	-1.915084
O	5.997732	-0.291128	-0.905310
C	7.848413	-1.743104	-1.278547
O	8.846728	-1.820998	-2.261627
C	8.168056	-0.807060	-0.089033
O	9.110076	0.163626	-0.465761
C	6.831872	-0.099518	0.206472
N	6.159445	-0.517414	1.442805
C	6.219989	0.361945	2.511318
O	6.827537	1.427012	2.490553
N	5.559437	-0.073079	3.635358
C	4.775180	-1.224770	3.795481
O	4.183141	-1.399640	4.852620
C	4.808856	-2.093975	2.640689
C	5.472252	-1.710905	1.531052
P	10.349342	-2.422769	-1.886502
O	10.758252	-3.423102	-2.914818
O	10.413623	-2.697698	-0.412506
O	11.178532	-1.003031	-2.209268
C	12.566543	-1.153273	-2.313606
H	12.837128	-1.858720	-3.110818
H	13.007198	-1.515354	-1.370786
H	12.995064	-0.167744	-2.539356
H	0.550110	2.465355	2.529973
H	-5.565301	0.786317	1.537208
H	4.236344	-3.012132	2.625504
H	5.447368	-2.308079	0.621266
H	-1.706706	-2.253156	3.099624
H	-0.888791	-1.614161	0.864106
H	-7.018428	0.694344	-2.020413
H	-6.522556	-1.011353	-1.927061
H	-4.724289	0.500513	-2.609561
H	-4.183242	-0.835663	0.079770
H	-1.938630	0.172724	-0.135592
H	-3.033700	2.652144	-0.511966
H	-3.022603	0.095779	5.451203
H	-1.379889	0.145903	5.805382
H	-1.242743	-1.520159	-2.686894
H	-0.345618	-3.065685	-2.636788
H	1.059401	-0.959081	-2.562048
H	1.373484	-2.889419	-0.227882
H	3.146095	-1.390229	0.529421
H	4.135099	-0.318996	-1.033632
H	1.550398	0.824524	0.338251
H	1.928817	-0.716148	4.605484
H	4.734275	-1.591450	-2.914298
H	6.006601	-2.832264	-3.085114
H	6.909424	-0.490942	-2.751160
H	7.610005	-2.735847	-0.880298
H	8.527043	-1.383963	0.765937
H	7.019901	0.961979	0.347626
H	5.504451	0.604267	4.382987
H	-6.616790	2.726963	0.171565
H	-7.820208	2.728582	1.495740
H	-8.011857	3.843184	0.109883
C	10.140086	0.348535	0.474487

H	10.855975	1.040521	0.020992
H	10.640473	-0.606974	0.669607
H	9.751212	0.790574	1.406407
C	-1.207677	1.721509	-2.130493
H	-0.482571	1.418709	-2.891426
H	-0.688288	1.804732	-1.171141
H	-1.620397	2.706007	-2.403530

A(6)U(7)U(8)-OMe Figure 5H
C60H100N12O26P4S
Charge = − 4

C	5.381046	6.169165	0.840539
C	4.596748	5.277918	-0.127223
C	3.084287	5.553582	-0.067877
C	4.959816	3.800046	0.088206
C	4.405154	2.806485	-0.935250
S	4.706499	3.247189	-2.685316
C	6.485978	3.610664	-2.647696
C	2.472954	5.465442	1.335526
C	0.965993	5.163644	1.360889
C	0.187170	6.196781	0.539302
H	-0.870760	5.934736	0.449680
C	0.432567	5.060630	2.809678
C	1.256544	4.090526	3.683825
C	-1.052547	4.679149	2.867916
C	1.453022	2.698418	3.083506
C	-4.749799	-5.489294	0.436779
C	-5.792457	-4.385153	0.247817
C	-5.689854	-3.366591	1.384950
H	-6.402046	-2.544399	1.273384
C	-7.203476	-4.974155	0.105467
C	-8.263893	-3.965267	-0.331245
C	-9.643316	-4.585075	-0.548944
C	-10.697176	-3.585999	-1.046890
N	-10.446627	-3.001706	-2.364435
C	-14.062978	3.233662	-4.678681
C	-13.367906	3.995039	-3.547421
C	-11.935083	4.365595	-3.935059
C	-13.409224	3.202334	-2.220469
C	-12.644869	1.913707	-2.234708
N	-13.185230	0.749207	-2.741030
C	-11.353051	1.689568	-1.821517
C	-12.218364	-0.147286	-2.624856
N	-11.099167	0.373288	-2.079306
H	7.027734	2.845733	-2.089397
H	6.690175	4.593904	-2.210028
H	6.845848	3.597187	-3.679036
H	3.318145	2.707065	-0.851231
H	4.826805	1.817513	-0.743222
H	4.629793	3.462398	1.081083
H	6.053598	3.706597	0.096615
H	4.912434	5.536471	-1.145918
H	5.140936	7.229391	0.686997
H	6.460177	6.040533	0.696546
H	5.156498	5.923701	1.885588
H	2.659547	6.402298	1.883110
H	2.995200	4.682683	1.893736
H	0.585341	6.275479	-0.476982

H	0.254013	7.190309	1.005284
H	0.822714	4.184855	0.881333
H	0.536468	6.064231	3.257481
H	-1.688791	5.402362	2.347662
H	-1.392274	4.632274	3.909058
H	-1.230463	3.687628	2.439690
H	2.092101	2.723496	2.193046
H	0.498464	2.249814	2.787844
H	1.928135	2.020161	3.799372
H	2.236047	4.532322	3.907024
H	0.745791	3.992536	4.651450
H	2.575732	4.846839	-0.736348
H	2.898102	6.549892	-0.491491
H	-4.808914	-6.236060	-0.366637
H	-4.906727	-6.010582	1.393481
H	-3.748486	-5.049214	0.422201
H	-5.543762	-3.860178	-0.684503
H	-5.880209	-3.848696	2.355309
H	-4.678586	-2.948813	1.402999
H	-7.171216	-5.796263	-0.628478
H	-7.499555	-5.433636	1.063833
H	-10.766068	-2.754022	-0.336046
H	-11.681551	-4.079851	-1.062088
H	-10.099865	-3.726548	-2.990571
H	-9.690627	-2.319776	-2.262329
H	-7.930944	-3.481088	-1.258019
H	-8.355720	-3.159209	0.404461
H	-9.572046	-5.414886	-1.273723
H	-9.996004	-5.034310	0.392756
H	-14.458791	2.993054	-1.973370
H	-13.014019	3.847719	-1.424065
H	-13.922862	4.931878	-3.376872
H	-14.025031	3.801286	-5.617986
H	-15.114830	3.041283	-4.435035
H	-13.585346	2.261030	-4.831724
H	-11.440266	4.927805	-3.133837
H	-11.918310	4.980014	-4.844325
H	-11.341548	3.463757	-4.116234
H	-12.261155	-1.193606	-2.899552
H	-10.198557	-0.110754	-1.887705
H	-10.602924	2.320454	-1.368209
C	-7.799704	2.087459	0.739381
O	-8.266072	1.333462	-0.366112
P	-8.056017	-0.303312	-0.293507
O	-8.661650	-0.785421	-1.592546
O	-8.458215	-0.826180	1.040636
O	-6.422230	-0.435913	-0.375678
C	-5.745069	0.084568	-1.503772
C	-4.387500	0.637684	-1.120286
O	-4.524249	1.575796	-0.032504
C	-3.305847	-0.338023	-0.647217
O	-2.738301	-1.018938	-1.719399
C	-2.373074	0.638418	0.086587
O	-1.711310	1.422860	-0.877292
C	-3.426515	1.475211	0.828119
N	-3.807841	0.825455	2.089094
C	-4.898757	0.022237	2.360911

N	-4.850000	-0.542291	3.541545
C	-3.656747	-0.103800	4.071674
C	-2.953724	-0.460975	5.229190
N	-3.436226	-1.392309	6.115472
N	-1.761484	0.103239	5.468274
C	-1.266388	0.942041	4.547925
N	-1.791101	1.303473	3.380558
C	-2.994007	0.744384	3.188311
P	-2.020137	-2.506630	-1.421278
O	-1.884463	-3.155333	-2.749164
O	-2.660981	-3.098365	-0.204584
O	-0.538030	-2.013781	-0.857319
C	0.317828	-1.202496	-1.625162
C	1.461928	-0.737607	-0.741581
O	0.911441	-0.136109	0.449683
C	2.446689	-1.796938	-0.226763
O	3.405958	-2.062274	-1.205342
C	2.945829	-1.134526	1.063042
O	3.879081	-0.133961	0.727745
C	1.678975	-0.439963	1.573103
N	0.884416	-1.250506	2.534034
C	1.287777	-1.193691	3.854138
O	2.234527	-0.526834	4.250245
N	0.529269	-1.962830	4.711002
C	-0.640088	-2.679568	4.430950
O	-1.229352	-3.245810	5.349047
C	-0.996650	-2.648282	3.034565
C	-0.233330	-1.954983	2.158103
P	4.825647	-2.887196	-0.877870
O	5.056154	-3.807297	-2.024565
O	4.868015	-3.277864	0.565596
O	5.902857	-1.618883	-0.996312
C	5.841015	-0.757088	-2.101745
C	7.060403	0.136026	-2.123696
O	7.162031	0.855542	-0.867758
C	8.425768	-0.528413	-2.294505
O	8.662614	-0.800795	-3.641551
C	9.349553	0.526461	-1.659755
O	9.500461	1.678193	-2.462821
C	8.497113	0.978574	-0.472600
N	8.752320	0.180429	0.754417
C	9.771014	0.623360	1.577014
O	10.431097	1.630872	1.367578
N	9.987548	-0.172772	2.683939
C	9.333974	-1.361476	3.054541
O	9.682410	-1.940263	4.074683
C	8.293073	-1.730792	2.125666
C	8.048520	-0.967038	1.037136
P	9.953276	-1.810799	-4.039001
O	10.731129	-2.040509	-2.776467
O	10.553757	-1.252314	-5.285876
O	9.124023	-3.160558	-4.463812
C	8.327500	-3.785809	-3.470244
H	8.887955	-3.911594	-2.535891
H	8.040196	-4.770514	-3.851411
H	7.408540	-3.226628	-3.261315
H	-0.288088	1.359174	4.777891

H	-5.685905	-0.114769	1.629929
H	7.698574	-2.617321	2.301053
H	7.254418	-1.218940	0.334375
H	-1.871797	-3.174693	2.677634
H	-0.469128	-1.926574	1.096346
H	-6.338207	0.885729	-1.959710
H	-5.591089	-0.703096	-2.250578
H	-3.988881	1.165966	-1.996130
H	-3.718122	-1.047839	0.080270
H	-1.656511	0.157492	0.759882
H	-3.073541	2.477657	1.087210
H	-4.167181	-1.955655	5.695896
H	-2.682085	-1.974219	6.469503
H	-0.231401	-0.329572	-1.997980
H	0.733887	-1.756628	-2.475864
H	2.044890	0.019202	-1.283055
H	1.897234	-2.710137	0.041514
H	3.369126	-1.858691	1.760930
H	1.945875	0.469522	2.107012
H	0.764052	-1.862926	5.688519
H	4.933249	-0.142477	-2.044027
H	5.818187	-1.317078	-3.046740
H	6.937448	0.864563	-2.934233
H	8.477153	-1.439547	-1.685342
H	10.319201	0.108015	-1.371653
H	8.722969	2.012990	-0.210505
H	10.736006	0.133473	3.289200
H	-6.706811	2.164999	0.719459
H	-8.116172	1.629552	1.683364
H	-8.235612	3.089231	0.655498
C	4.884194	0.022280	1.702104
H	5.607723	0.735085	1.297430
H	5.385193	-0.935839	1.879730
H	4.470345	0.399930	2.649885
C	10.558938	1.613079	-3.397688
H	10.635198	2.614085	-3.837325
H	10.388528	0.873524	-4.185202
H	11.507427	1.373756	-2.892651
C	-0.787364	2.345213	-0.352047
H	-0.169456	2.682757	-1.189753
H	-0.140149	1.879293	0.398595
H	-1.282729	3.226282	0.086436